QUANTITATIVE DNA PLOIDY ANALYSIS AND ITS CORRELATION WITH THE BIOLOGICAL BEHAVIOR OF RENAL CELL CARCINOMA

THESIS

SUBMITTED IN PARTIAL FULFILLMENT FOR THE DEGREE OF

MASTER OF PHILOSOPHY

BY

TONG HUNG MAN, JOANNA

DIVISION OF ANATOMICAL AND CELLULAR PATHOLOGY

THE CHINESE UNIVERSITY OF HONG KONG

OCTOBER, 1997

UL


香港中文大學
圖書館系統
22 MAY 1998
UNIVERSITY
LIBRARY SYSTEM
THE CHINESE UNIVERSITY OF HONG KONG

Abstract

The prognostic value of DNA ploidy in renal cell carcinoma (RCC) is controversial. Results of the ploidy status showed great variations in the literature.

A comprehensive study of 46 renal tumors using flow cytometry (COULTER EPICS XL flow cytometry) and static image cytometry (CAS 200 image analyzer) was performed. Both disaggregated nuclear suspension for cytospin preparations and tissue sections were subject to static image analysis.

Intratumoral heterogeneity was found in up to 32.6%. This implies that sampling error may lead to incorrect assignment of ploidy class. Multiple sampling is mandatory in order to properly evaluate the potential role of ploidy status in RCC.

Significant role of DNA ploidy analysis performed on tissue sections was demonstrated in this study. Despite the inherent limitation of measuring cut nuclei, high concordant rate was found between ICM analysis using cytospin and tissue section, indicating routinely processed paraffin sections can also applicable in quantitative DNA content analysis.

Comparison among three methods have found high concordant rate, with some discrepancies. Reasons for discrepancies are described in detail. Although image cytometry (ICM) was more sensitive in detecting aneuploidy and tetraploidy (54.6%) than flow cytometry (FCM) did (33%), results showed no additional prognostic significance in our study. However, further study is warranted.

In order to assess the relationship between the ploidy status and the proliferation activity, immunohistochemical study were carried out using two cell cycle-related antibodies: Ki 67 (MIB-1) and $p27^{kip1}$.

Correlation among different clinical - pathological data and the survival analysis were performed. DNA ploidy profiles measured by all three methods showed correlations with nuclear grade, nuclear area, and significantly associated with event free survival in high stage

stage (stage III, IV) patients. However, significant correlation with Ki 67 (MIB-1) and $p27^{kip1}$ has not been demonstrated .

The results from univariate survival analysis indicated that the expression of cell cycle-related antigen {Ki 67 (MIB-1) and $p27^{kip1}$}, tumor grade and stage carried prognostic information. The most powerful prognostic parameters for event free survival were Ki 67 (MIB-1) expression and tumor stage by multivariate analysis.

Acknowledgments

I am extremely grateful to Dr. To Ka Fai, who has taken time from his busy life to supervise me during the last two years. He also gave me opportunities to expose to many fields besides this particular project, i.e. molecular biology. Without his patient instruction this work would not have been possible.

Special thanks will also give to Dr. Tsoi Wai Tsiu of the department of Hematology, Prince of Wales hospital, who taught me how to perform of flow cytometric DNA analysis and introduced me into the family of Hong Kong Society of Flow Cytometry (HKSFC).

I would like to express my warmest thanks to Dr. Terrence C W Poon for his steady guidance and inspiration along the way and Mr. Lo Kwok Wai for his invaluable advises.

My thanks is convey to David SY Lo, Hardy CW Ko and KF Mak, the experienced histological technicians in the department of Anatomical and Cellular Pathology, for their guidance in immunohistochemistry.

Many other people of the department of Anatomical and Cellular Pathology freely made available the resources. To these kind and cooperative people, I express my sincere thanks.

Finally, my parents and brother have always been the sources of encouragement and love, words can not express my gratitude for their support and understanding.

Contents

Chapter 1

Introduction

Renal cell carcinoma (RCC) is the most common renal malignancy in adult. It results in significant morbidity and mortality. However, the biological behavior of RCC is notoriously unpredictable. There are reports that a third of all patients with RCC have evidence of metastasis at diagnosis (Skinner *et al.*, 1971; Montie *et al.*, 1977; Middleton, 1978). The 5-year survival rates after radical nephrectomy for stage I tumors range from 60% to 75%; for stage II, from 40% to 65%; for stage III, from 15% to 30%; and for stage IV, a dismal 10% to 20% (Brodsky and Garnick, 1994).

Deciding on an optimum plan for patient management and therapy in the treatment of tumor requires an accurate and precise characterization of the lesion. It is generally agreed that tumor stage and histopathological grade are the most important predictors of prognosis. However, these still cannot allow an accurate prediction of clinical behavior in individual cases (Currin, Lee and Walther, 1990). Attempts in searching for useful biological markers were explored. These include tumor ploidy status, cell cycle-related markers, oncogenes and tumor suppressor genes (Hall, 1990).

Many authors have focused on DNA ploidy analysis. Studies have suggested that abnormalities in cellular DNA content correlate with the biological behavior of malignancies, such as breast, colorectal, ovarian and endometrial cancer (Mellin, 1990; Koss *et al.*, 1989; Aziz and Peter, 1991). Tumors with diploid DNA content generally have a more favorable prognosis and run a less aggressive course than aneuploid tumor. The assessment of DNA ploidy in these tumors has prognostic value and may predict the treatment responses. However, in RCC, the prognostic value of DNA ploidy is still controversial due to conflicting results from different studies. Some studies have demonstrated a worse prognosis for aneuploid tumor (deKernion *et al.*, 1989; Otto, Baisch and Kloppel, 1984; Baisch *et al.*, 1982; Kloppel *et al.*, 1986) both across the range of grades and in well differentiated RCCs (Rainwater, 1987). Others have failed to demonstrate the prognostic value of ploidy status when considered independently of grade and stage (Currin, Lee and Walther, 1990; Grignon *et al.*, 1989; Ekfors *et al.*, 1987), or have found only a weak correlation (Chin, Pontes and Frankfurt, 1985).

Most of the previous DNA ploidy studies were using flow cytometry (FCM). The frequency of aneuploidy showed great variations, ranging from 29% to 77%. Few studies have been focused on whether these variations were related to technical discrepancies or intratumoral heterogeneity. Flow cytometric measurement is based on analysis of large number of nuclei from whole cell preparations. This technique is well established. It is generally agree that the assessment is reproducible and rapid. However, several limitations have been described. "Rare events" (that is, a small specific cell clone) can be hidden amongst the data (Saith, Parkinson and Leong, 1996). Ambiguous histograms may be difficult to interpret. FCM DNA analysis also subjected to lack of morphological correlation.

Static image cytometry (ICM) has been introduced into the field of quantitative analysis in recent years. Nuclei in tissue sections or cytological preparations can be measured using a light microscope and image analyzer. It has the advantage of combining analysis with morphological assessment. A specific cellular population can be selected for analysis (Carey, 1994). The combination of flow and static image cytometry will no doubt provide a more comprehensive approach to quantitative DNA analysis.

For ICM, most investigators used single cell preparations (smear, cytospin, imprint etc.). Thus, the whole intact nuclei can be measured. Recently, ploidy study performed on tissue sections has been advocated with the advantage of preservation of tissue architecture. It is also feasible for small biopsy specimen and applicable to microscopic lesions, for example in-situ lesions. Furthermore, in archival tissue, disaggregation of solid tumor into cell suspension is time consuming and the techniques are potentially subject to loss of specific cellular population (Danque, 1993). However, the major inherent problem is the "cut effect". In the section, most often the partially cut nuclei rather than whole intact nuclei were measured. Appropriate corrections are required. Despite this limitation, some authors claimed that this method can also provided useful information (Williams *et al.*, 1991; Mellin *et al.*, 1990).

No study has been done to correlate the ploidy status analysis using FCM, ICM on cytological preparations and tissue sections in the same specimen. In our study, the ploidy profiles were assessed using both FCM and ICM. For ICM, both cytospin preparations and tissue sections were used. One of the principal purposes was to see whether by combining FCM and ICM in DNA content assessment, an accurate and reliable DNA status could be drawn up. Those factors that might lead to any discrepancies could be established.

There is considerable evidence that assessment of cellular proliferation in a variety of tumors, including RCC, provides useful information in the understanding of the patho-biology and may be of prognostic importance (Piffko *et al.*, 1996; Hall and Levison, 1990; Brugal, 1994). Cell cycle-related markers were frequently employed. Along this line, cell cycle related markers were used to assess the proliferation activity in our study. Their potential relationship between ploidy status and other clinicopathological data could be explored.

Two cell cycle-related monoclonal antibodies were used including Ki 67 (MIB-1) and $p27^{kip1}$. Ki 67 (MIB-1) reacts with a nuclear non-histone protein present in all active parts of cell cycle but not in G_0 phase (Gerdes *et al.*, 1983; 1984; 1991). Expression of Ki 67 have been suggested to be of prognostic significance in the patients with RCC (Jochum *et al.*, 1996; Tannapfel *et al.*, 1996). $p27^{kip1}$ is one of the cyclin-dependent kinase inhibitors that can inhibit cell cycle progression by binding to and inactivating cyclin/CDK complexes (Sherr and Roberts, 1995). Expression of $p27^{kip1}$ has been shown to be of prognostic significance in the patients with breast, colorectal and gastric carcinoma (Catzavelos *et al.*, 1997; Porter *et al.*, 1997; Loda *et al.*, 1997). The potential value of $p27^{kip1}$ expression in RCC has not been explored. The analysis of $p27^{kip1}$ expression along with Ki 67 may enhance our understanding of the biological behavior of RCC.

Chapter 2

Literature Review

1. Overview of Renal Cell Carcinoma

1.1 Epidemiology

Renal cell carcinoma (RCC) is the most common malignant tumor of the kidney in adult. It represents almost 1% of all malignant diseases and is the third most common urologic cancer. RCC is rare in children; its peak incidence is in the fifth and sixth decades of life. It occurs three times as frequently in males as in females (Nasser, 1984). The incidence of RCC in the United States and northern Europe is higher than in Africa, Asia, and South America (Brodsky and Garnick, 1994).

1.2 Etiology

Despite numerous investigations, there is little evidence linking a specific carcinogen to human RCC. Several environmental factors have been implicated. Smoking appears to be a major risk factor (La Vecchia *et al.*, 1990). Obesity, especially in women, also has been implicated as risk factor (Asal *et al.*, 1988). Chemical and physical agents can induce cancer in experimental animals. Other risk factors include exposure to industrial chemicals, for examples, aromatic hydrocarbons, aromatic amines and lead compounds (Brodsky and Garnick, 1994) and long term phenacetin and acetaminophen use (McLaughlin *et al.*, 1985).

Between one third and one half of patients with von Hippel-Lindau disease developed RCC. von Hippel-Lindau disease is transmitted in an autosomal dominant manner, which is associated with retinal angiomas and hemangioblastomas of the central nervous system and renal cell carcinoma (Horton, Wong and Eldridge, 1976). Tuberous sclerosis (an autosomal dominant syndrome, in which hamartomatous lesions occur in the brain, retina, skin, heart, bone, lung, and kidney) not only associated with renal cystic lesions, angiomyolipomas, but also has increased risk for RCC (Bernstein *et al.*, 1991).

Acquired renal cystic disease arising in the patients with chronic renal failure is also strongly associated with RCC (Fallon *et al.*, 1989). The association of RCC with autosomal dominant polycystic kidney disease remained uncertain (Gregoire *et al.*, 1987).

1.3 Clinical Features

1.3.1 Symptoms and Signs

The classic triad of pain, hematuria, and a flank mass is seen only in 10 percent of patients, and usually in those with advanced disease. Other common presenting symptoms include weight loss, abdominal pain and anorexia (deKernion and Belldegrun, 1992).

Some of the clinical features are attributed to para-neoplastic syndrome and occur in about 30 percent of patients with renal cell carcinoma. These include pyrexia, hypertension, hypercalcemia, erythrocytosis, gynecomastia and hepatic dysfunction (Sufrin *et al.*, 1989; Chisholm, 1974). Hypertension may be related to renin secretion, and gynecomastia related to gondotropin or prolactin production. Other laboratory findings may include anemia and elevation of the erythrocyte sedimentation rate.

About one third of patients with RCC have metastasis at the time of diagnosis (Ritchie and deKernion, 1987), although this number should fall with the increased incidental detection of small renal masses (Thompson and Peek, 1988). RCC is notorious for presenting as metastatic carcinoma of unknown primary.

1.3.2 Clinical Staging and Treatment

Imaging study include sonogram or CT scan was frequently used to investigate the primary tumor. Arteriogram may be performed in selected cases in some centers. Staging procedure may also include chest tomogram, CT scan of abdomen and bone

scan. Pre-operative trucut biopsy or aspiration may be required in selected patients (Nasser, 1984).

The extent of local and systematic spread of the neoplasm is of prime importance in the therapy and prognosis of RCC. There are several staging systems. The system proposed by Robson and coworkers (1968) serves as the most widely used scheme for staging RCC because of its relative simplicity and its prognostic validity (Table 2.2).

Table 2.2 The staging system described by Robson and coworkers (1968)

Stage I	Tumor confine to the kidney
Stage II	Perirenal involvement but confined within Gerota's fascia
Stage III	Regional invasion
III a	Renal vein or inferior vena cava involvement
III b	Lymphatic involvement
III c	Combination of a and b
Stage IV a	Involvement of adjacent organs other than the adrenals
IV b	Distant metastasis

Radical nephrectomy is the procedure of choice for the treatment of primary RCC. However, in the patients with metastatic disease, nephrectomy itself seldom has any influence on metastatic lesions and prognosis. Palliation of symptoms is, however, a reasonable rationale for nephrectomy provided that the primary tumor can be completely removed without undue morbidity (Sokoloff *et al.*, 1996).

Radiotherapy has been applied to RCC as both an adjuvant to surgical therapy and as a treatment for metastatic lesions. Palliative radiotherapy has been successful in treating painful metastasis and is a powerful tool for pain management. The potential role of preoperative radiotherapy in delaying tumor recurrence and shrinking tumor size has been suggested (Rabinovitch *et al.*, 1994; Van der Werf-Messing, 1973). However,

the role of radiotherapy as a primary treatment for locally extensive RCC has failed to show a beneficial effect (Montie, 1994).

The results of chemotherapy in treating RCC patients have been poor (Yagoda, 1989). In the past two decades, immunotherapy has also investigated in RCC patients. Various attempts including systemic interferon-α (IFN-α), combination of IFN-α/interleukin-2 (IL-2), administration of TILs (tumor-infiltrating lymphocytes) or CD8+/TILs have been tried (Sokoloff, 1996). Further studies are required to elucidate the potential value of immunotherapy.

1.4 Pathology

1.4.1 Classification of Renal Cell Carcinoma

The most common type of renal cell carcinoma was clear cell type, granular cell type or mixed clear cell and granular cell type, which comprised of more than 70 % of RCC. The next common type is papillary RCC and also named as chromophil RCC according to Mainz's classification. Other subtypes included chromphobe RCC, sarcomatoid RCC and collecting duct carcinoma (Eble, 1997).

I. Clear Cell and Granular Cell RCC

Clear cell and granular cell are the most common histological types of RCC.

Gross, microscopic and ultrastructural pathology:

Gross appearance of the tumor usually reveals multiple, fairly regular lobules, generally between 4 and 12 cm in diameter. The left and right kidneys are involved with approximately equal frequency. In 84% of cases the tumors are single; the remaining cases are multiple or extensive. Most tumors involve a single pole; the upper and lower poles are involved equally often, but the middle lobe is involved slightly less frequently.

The cut surface of the tumor usually reveals a variegated appearance. The color varies from yellow, reflecting lipid-containing clear cell carcinoma, to tan or grayish representing the granular cell type. Necrosis and hemorrhage are commonly seen (Javadpour, 1984).

In about 10% of cases the tumors are intrinsically cystic. In multilocular cystic RCC, the tumors are wholly cystic.

The clear cells are rich in lipid and/or glycogen, giving the typical clear cytoplasm microscopically. Granular cell tumors are characterized by cells which have eosinophilic homogeneous or granular cytoplasm. The mitotic rate is highly variable. Multinucleated giant cells are uncommon. The major architectural patterns are compact (alveolar), tubular and cystic with a prominent vascular stroma (Eble, 1997).

In multilocular cystic renal cell carcinoma, the septa are lined by and contain clear cells with small dark stained nuclei (Murad *et al.*, 1991)

Ultrastructurally, the clear cell type contain large amounts of glycogen, triglycerides, and phospholipids but little endoplasmic reticulum, a poorly developed Golgi apparatus, and few mitochondria and cytosomes. In contrast, granular cells contain more mitochondria, more highly developed Golgi apparatus, endoplasmic reticulum with less lipid and glycogen. Both cell types may have a brush border of tightly packed microvilli, membrane-associated vesicles involved in pinocytosis and membrane coatings of glycocalyx. Infolding of plasma membranes and abundance of tortuous and elongated mitochondria provide strong support that RCC originates from proximal convoluted tubular epithelium (Mostofi and Davis, 1984).

Cytogenetic findings:

Loss of genetic material in 3p is the most frequent and consistent abnormality (Kovacs G *et al*, 1988). The results suggest the presence of tumor suppressor gene in this region.

1.4.2 Chromophil RCC

This is the second most common type of RCC and comprised 10 to 15 % of RCC (Mancilla-Jimenez *et al.*, 1976; Bard, Lord and Fromowitz, 1982). This type of tumor is also referred as papillary or tubulopapillary carcinoma.

Gross, microscopic and ultrastructural pathology:

It is typically circumscribed, tan to brown in color. Cut surface frequently has a friable granular appearance, reflecting the papillary structures seen microscopically. A rim of fibrous tissue is not uncommon and giving an appearance of cystadenocarcinoma (Reznicek, Narayana and Culp, 1985).

The typical features are the papillary or tubulopapillary architecture. The carcinoma cells tend to have low cytoplasmic volume, high nuclear to cytoplasmic ratio with variable cytoplasmic staining (Thoenes *et al.*, 1990).

Ultrastructurally, some investigators suggested that the cells might resemble distal tubular cells rather than proximal tubular cells (Reznicek, Narayana and Culp, 1985).

Cytogenetic findings:

This type of tumor typically has gain of chromosomes, most often trisomy or tetrasomy 17 or 7. Loss of chromosome Y is often seen in male patient. Consistent loss of DNA in 3p as in clear cell type RCC is not found (Kovacs *et al.*, 1991).

III. Chromophobe RCC

This is a recently described subtype of RCC (Thoenes *et al.*, 1986). It affects men and women equally.

Gross, microscopic and ultrastructural pathology:

It is typically circumscribed, solid, beige or light brown. Histologically, it has two variants: typical and eosinophilic. The typical variant has compact architecture. The tumor cells tend to have large amount of cytoplasm, prominent cytoplasmic membranes and pale flocculent cytoplasm. Hale's colloidal iron stain positivity is diagnostically useful (Vieillefond *et al.*, 1992). Ultrastructurally, the cytoplasm is filled with microvesicles measured 150-300 nm (Thoenes *et al.*, 1988).

The eosinophilic variant is composed of cells with abundant brightly eosinophilic granular cytoplasm. The cytoplasm surround the nuclei may be pale and creating halo. Hale's colloidal iron stain is strongly positive. Ultrastructurally, numerous mitochondria mixed with cytoplasmic vesicles (Thoenes *et al.*, 1988).

IV. Sarcomatoid RCC

This type of tumor comprised about 2% of RCC (Farrow *et al.*, 1960). The tumor composed mainly of spindle cells, arranged in fascicles, whorls or sheets. Areas of more typical renal cell carcinoma usually present. The epithelial nature can be confirmed by immunohistochemical stain for epithelial markers or ultrastructural examination.

V. Collecting Duct Carcinoma

This tumor appears arising in the renal medulla. A subgroup of young adult patient with sickle cell anemia has been described (Davis *et al.*, 1995). Grossly, the tumor is centered in the renal medulla and extended to the cortex or hilar region. Histologically,

it consists of irregular tubular and glandular pattern with prominent desmoplastic stroma. The tumor cells tend to have high-grade nuclei with hobnail cells. Dysplastic changes in the collecting ducts may be seen.

1.4.2 Nuclear Grading

Riches, in 1963, made the first systematic attempt at tumor grading, finding that 45% were well differentiated (grade I), 36% moderately differentiated (grade II), and only 18% "pleomorphic" (grade III). Fuhrman and associates (1982) expanded on and proposed modifications to this scheme, with similar findings. The Fuhrman system, most widely used today, relies entirely on nuclear features. The details are listed below (Table 2.1).

Table 2.1 Criteria of Fuhrman and Colleagues for Nuclear Grade in RCC

Nuclear Grade	**Description of nuclear features**	**% of all RCCs**
1	Small(about 10 μm), round, uniform nuclei with inconspicuous or absent nucleoli	14
2	Larger(about 15 μm), nuclei with irregularities in outline and small nucleoli noted on high-power view	50
3	Larger(about 20 μm), nuclei with obviously irregular outline and prominent, large nucleoli appreciated even at low power view	26
4	Similar to grade 3 tumors, but with the addition of pleomorphic, bizarre, multilobed or giant nuclei and markedly clumped chromatin	10

1.4.3 Prognosis and Correlation with Conventional Clinical- pathological Factors

Overall 5-year survival rates after radical nephrectomy for stage I tumors range from 60% to 75%; for stage II, from 40% to 65%; for stage III, from 15% to 30%; and for stage IV, a dismal 10% to 20% (Brodsky and Garnick, 1994). Generally, nephrectomy does not prolong survival for patients with distant metastasis (Montie, 1977; Johnson, 1975).

The single most important determination of prognosis in the patients with RCC is the stage of the tumor at presentation (Hofmockel *et al.*, 1995; Inomiya, 1996). Grading appears less important than accurate staging in determining prognosis (Mostofi, 1967). Few studies have been large enough to allow for stage-independent evaluation of the effect of grading on prognosis. Inter-observer variation (Medeiros *et al.*, 1988), sampling variation and fixation artifacts further hamper the reliability of nuclear grading. Observers nonetheless agree on the validity of grading as a prognostic factor in RCC when applied rigidly and uniformly (Fujii *et al.*, 1996; Bretheau *et al.*, 1995).

Histologic features of the primary tumor have some bearing on prognosis. The sarcomatoid RCC is considered by virtually all investigators to have a poor prognosis. (Ro *et al.*, 1987; Tomera, 1983; Bertoni *et al.*, 1987; Uwatoko *et al.*, 1996) Sarcomatous components increase with tumor size and are independently associated with a poor prognosis. (Kanamaru *et al.*, 1996) The pathological stage and amount of necrosis also correlates with survival (Ro *et al.*, 1987). Collecting duct carcinomas appear to have a poor prognosis. The limited data suggest a rapid, aggressive course (Kennedy *et al.*, 1990).

Multilocular cystic RCCs are reported to have an excellent prognosis. Murad and colleagues (1991) observed six patients for a minimum of two years, with no recurrence or metastasis. Of note is that all of the cases in that series were Fuhrman grade I, thus the excellent prognosis may be due to low tumor grade.

Although the number of reported cases of chromophobe cell carcinoma is small, they appeared to have an overall good prognosis, with less than 10% developing metastasis (Thoenes *et al.*, 1988). Onishi *et al.* (1996) studied the clinicopathological characteristics of 34 cases of chromophobe cell carcinoma and showed the hypovascular/avascular pattern in angiography, low rate of laboratory abnormality, low stage/low grade and a favorable prognosis compared with the common types of RCC. Chromophil carcinoma was suggested to have a better prognosis, and this remained to be confirmed (Mancilla-Jiminez *et al.*, 1976).

Microscopic patterns may also suggested to have prognostic values. The papillary pattern, usually hypovascular on arteriography, is associated with a better prognosis, even stage for stage (Mancilla-Jimenzez *et al.*, 1976). Some studies (Kanamaru *et al.*, 1996; Uwatoko *et al.*, 1996) revealed that the solid architecture pattern was an independent variable which correlated with a poor prognosis.

Epidemiological factors are not prognostically important in RCC; reported survival differences based on age, sex, or race is small and inconsistent. Laterality, multiplicity of tumors, and location has no bearing on outcome, nor do other histological variables, such as calcification, lymphoid infiltration or fibrosis. There are no reliable serum markers that have a consistent bearing on prognosis (Brodsky and Garnick, 1994). However, hemoglobin, C-reactive protein, erythrocyte sedimentation rate, immunosuppressive acidic protein were suggested to have prognostic significance in a recent study (Inomiya, 1996).

2. The Biological Cell Cycle

2.1 Cell Cycle

In order to understand the nature of DNA ploidy status and the proliferative activity, a brief overview of the cell cycle is described (Figure 2.1). The observations of Howard and Pelc, who used ^{32}P incorporation and autoradiography during the early 1950s, led to

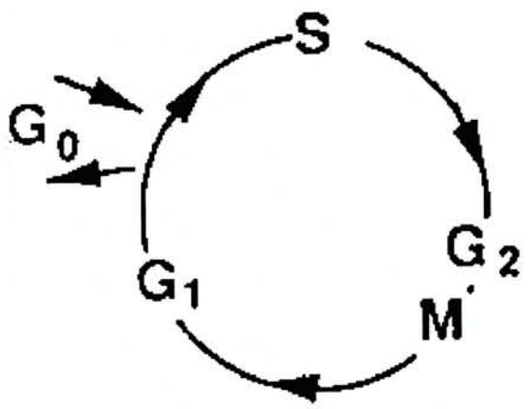

Figure 2.1 The cell cycle is divided into discrete phases. The gaps between mitosis (M) phase and DNA synthetic (S) phase, and between S phase and the next mitosis are called G_1 and G_2 phase, respectively. G_0 phase was introduced for cells not in cycle (Kvaloy et al., 1985).

the introduction of the concept of cell cycle and its subdivision into several phases (Kvaloy *et al.*, 1985).

Every dividing cell goes through the cell cycle with mitosis as the start and end points, giving rise to two cells after each cycle. During the first gap (G_1) phase which precedes the synthetic (S) phase, the cell synthesizes ribonucleic acid and proteins. This phase is highly variable in duration and is generally the longest in the proliferative cell cycle.

The G_1 phase is followed by the synthetic phase when the cell synthesizes DNA and doubles its DNA content in preparation for cell division. The S phase generally last for about ten to twenty hours. After that, the cell enters a period of apparent inactivity known as the second gap phase (G_2) which comes before the next mitosis. This premitotic phase lasts for two to ten hours during which the cellular components such as the spindle apparatus are synthesized and made ready for mitosis. During G_1 and G_2 phase of the cell cycle, most proteins, carbohydrates and lipids are synthesized.

Interphase comprises successive G_1, S, and G_2 phases and forms the largest part of the cell cycle. When not in the process of preparing for cell division, cells remain in the G_1 portion of the cell cycle. The cell cycle is completed in the mitotic (M) phase where the cell divides into two daughter cells. This is a very short phase which last 30 minutes to one hour. Within the mitotic phase, the cell proceeds through four steps of mitosis: prophase, metaphase, anaphase and telophase, before completing the cell division and generating two new daughter cells. These new cells may re-enter the next G_1 phase of the cycle or become non-proliferating cells in the G_0 phase. Cells in G_0 phase are quiescent regarding to the proliferative activity and not belong to the proliferative pools of the cells. However, under suitable stimulations, cells in G_0 phase can rejoin into the proliferative cycle.

2.2 Cell Cycle Control

Although many areas remain unclear, recent advances have been made and enhance our understanding of the regulation of the eukaryotic cell cycle. Some important cellular proteins involved directly or indirectly in the control of cell proliferation have been identified. For example, cyclins are a group of proteins, which accumulate progressively through interphase and disappear at the end of mitosis (Dunphy *et al.*, 1988). Several histone proteins vary in synchrony with the cell cycle and may be suitable markers for assessing changes associated with cellular proliferation (Schumperli, 1986). The regulation of genes related to the cell cycle by specific promoter sequences is also now becoming better understood (Breeden, 1988). Finally, there seem to be specific genes associated with growth arrest in cells, although these are as yet only poorly characterized. There seems to be numerous functionally interrelated substances that vary in level or activity during the cell cycle, whose functions (whether structural or regulatory) are to permit the initiation and completion of normal cell division.

3. Overview of DNA Ploidy and the Relationship with the Biological Behavior of Renal Cell Carcinoma

3.1 Overview of DNA Ploidy

The DNA ploidy is the amount of DNA in cells that are in the G_1/G_0 phase of the cell cycle. All cells in G_1/G_0 phase in an organism, with few exceptions, have the same DNA content and the same chromosomal complement. In mammals, this is referred to "diploid DNA content" by cytogeneticists (who actually look at chromosomes), and the designation "2N" is used to describe this value (where N refers to a single complement of chromosomes, the haploid DNA content).

Cells in G_2 phase and mitotic cells have twice the normal G_1 DNA content, gametes have haploid DNA contents and a few cells in the body have tetraploid (4N) DNA contents (as in adult liver), other exceptions include several types of multinucleated

cells. All of these DNA contents are together referred to as "euploid values", and all share the distinction that the chromosomes are in intact sets and each chromosome is itself an unaltered subunit.

Cells containing abnormal amounts of DNA are said to be aneuploid. They have either an abnormal set of chromosomes or abnormally constructed chromosome. Aneuploid cell populations are almost always, but not exclusively, associated with malignancy. Cells with less than the DNA diploid content are termed hypodiploid, which is generally a relatively infrequent finding in tumors. Conversely, hyperdiploid cells contain more than the diploid DNA content and the degree of abnormality can be expressed as DNA index (DI) relative to the normal DI of 1.0 in diploid cells. For examples, triploid cells have a DI of 1.5, tetraploid cells have a DI of 2.0 (Macartney and Complejohn, 1995).

Aneuploidy implies the presence of an abnormal quantity of genomic material. These assayable aberrations of cellular DNA content presumably reflect the more extreme alterations at the molecular level (Evans and Podratz, 1996). Thus, gross DNA abnormality can be detected by ploidy analysis. Sub-microscopic abnormality or genetic alterations at molecular levels may not be reflected by abnormality in ploidy status.

In vitro studies (Burholt *et al.*, 1989; Kubbies *et al.*, 1986; Laffin *et al.*, 1989) suggest that diploid tumor cells can become aneuploid by first doubling their chromosome sets leading to an unstable tetraploid genotype, followed by subsequent chromosome loss. This phenomenon can contribute to tumor progression by generating cells with a new genotype. Those with a selective advantage will give rise to a more aggressive tumor subpopulation. Flow cytometric data from many laboratory supported this hypothesis, as most of the aneuploid tumor cell populations have DNA indices between 1.5 and 2, with a gap in the DNA distribution below and above these two values (Devonec *et al.*, 1987; 1989; Ljundberg *et al.*, 1985; 1986; Norming *et al.*, 1989).

Another hypothesis involves a loss or gain of some chromosomes after unequal mitosis, leading to hypodiploid or hyperdiploid cells. The acquisition of genetic instability seems to be a critical event in tumor progression (Shackney *et al.*, 1989), particularly for the attainment of the metastatic phenotype (Fidler and Hart, 1982; Ichikawa *et al.*, 1990). Duplication of the genome may be associated with a markedly increased growth rate and dedifferentiation (Wake, Isaacs and Sandberg, 1982). Chromosome loss will result in a modification of the equilibrium between genes which positively and negatively regulate cell proliferation and invasiveness (Weinberg *et al.*, 1989). Thus, the likelihood that aggressive clones emerge in these tumors is higher, and this may explain the poor prognosis associated with aneuploidy in certain types of tumors.

Genomic instability as reflected by gross DNA content potentially contributes to both diagnosis and prognosis of the disease. Aneuploidy has been shown to occur in some tumor types, such as malignancies originating in the oral cavity, esophagus, bronchi, stomach, colon-rectum, uterine cervix, urinary bladder and skin. The in-situ lesions may also exhibit aneuploid (Bauer *et al.*, 1993; Shankey *et al.*, 1993; Seckinger *et al.*, 1989; Shapiro *et al.*, 1989). Abnormality in ploidy status can be of value in distinguishing between non-specific cellular alterations and true pre-malignant or malignant tumors.

In general, aneuploid tumors appear to behave in a more aggressive manner. DNA ploidy analysis has been demonstrated to be of prognostic value in some, but not all, of the tumor types. This included carcinoma of the breast, prostate, thyroid gland, ovary and endometrium (Auer, Steinbeck and Zetterberg, 1995).

3.2 Intratumoral Heterogeneity

Nowell has provided a model for tumor progression in 1986. He suggested that tumor cells tend to be genetically unstable, and therefore subject to a high rate of random mutation during clonal expansion from a single cell of origin. These mutations

or genetic alterations may be of growth advantages or disadvantages. The genetic alterations may be lethal or place the tumor cells at a growth disadvantage; these subclones may eventually disappear from the tumor populations. Some of the genetic alterations may convey greater autonomy and a selective growth advantage; these subclones will tend to become dominant in the populations, leading to tumor progression.

As predicted by Nowell model, cells within human and animal tumors demonstrated considerable heterogeneity in their properties (Heppner, 1984). This heterogeneity extends to almost any property that can be assessed and includes morphology, cell proliferation, karyotype, surface markers, biochemical products, metastatic behavior, and sensitivity to therapeutic agents.

Stemline heterogeneity can be assessed in several levels. In DNA ploidy analysis, heterogeneity designates the presence of at least one aneuploid stemline. Co-existing tumor stemlines often display a DI ratio of 2, reflecting their close genetic relationship (Mellin, 1990).

Evaluation of tumor cell heterogeneity by DNA ploidy assessment, as argued by Ljundberg *et al.* (1985; 1996), has gained increasing interest because of the potential implications in the biological and possible clinical behavior. Numerous studies have confirmed that the rate of aneuploidies and the stemline heterogeneity of a tumor are directly correlated with its growing size and local spread (Vindelov *et al.*, 1982; Tytor *et al.*, 1987; Ewers *et al.*, 1984; Frankfurt *et al.*, 1984; BÜchner *et al.*, 1975). Different tumor entities will show different degrees of stemline heterogeneity. In general, heterogeneity may increase with the grade or stage of malignancy (Mellin, 1990).

3.3 Controversial Prognostic Value of DNA Ploidy Analysis in RCC

During the last decade, DNA cytometry-both FCM and ICM have become established techniques to obtain information about the nuclear DNA content in different

cellular populations. Various investigators have demonstrated that DNA ploidy as a predictor of the clinical behavior for a variety of neoplasm (Bauer *et al.*, 1993; Shankey *et al.*, 1993; Seckinger *et al.*, 1989; Shapiro *et al.*, 1989). But the prognostic value in RCC is, however, uncertain.

Some authors reported a better prognosis in the patients with diploid or near-diploid tumor in comparison with patients with an aneuploid pattern (Otto *et al.*, 1984; Ljungberg *et al.*, 1985; Ekfors *et al.*, 1987; Raviv *et al.*, 1993). As described by Baisch *et al.* (1982) and Ljundberg *et al.* (1985), DNA aneuploid populations have higher S-phase fraction than DNA diploid ones, indicating a higher proliferative activity.

Studies which have used multivariate analysis, comparing ploidy with grade and/or tumor category, have disagreements on the significance of its influence on prognosis (deKernion *et al.*, 1989; Grignon *et al.*, 1989 Currin *et al.*, 1990). There is disagreement also on whether a correlation exists between these factors and tumor ploidy. As argued by Ljundberg *et al.* (1985), the histopathological grade is considered to be an important prognostic factor (Ljundberg *et al.*, 1985; Skinner *et al.*, 1972; Amtrup *et al.*, 1974). The most widely used and reliable histological grading systems in RCC are based on nuclear morphology. It's reasonable to expect that a relationship exist between this parameter and ploidy, as has been found, for example, in breast tumors. In literature, most authors (Baisch *et al.*, 1982; Grignon *et al.*, 1989; Rainwater *et al.*, 1987; Kiesewetter *et al.*, 1987; Kleinhans *et al.*, 1987; Ljundberg *et al.*, 1985; Oosterwijk *et al.*, 1988; Otto *et al.*, 1984) , but not all (Currin *et al.*, 1990; Ekfors *et al.*, 1987), found an association between nuclear grading and the DNA ploidy status by flow cytometry studies.

Published data on the frequency of DNA aneuploidy in RCC also showed great variations, ranging widely from 29% to 77% (Baisch *et al.*, 1982; 1984; Ekfors *et al.*, 1987; Grignon *et al.*, 1989; Kleinhans *et al.*, 1987; Ljundberg *et al.*, 1986; 1991; Rainwater *et al.*, 1987; Schwabe *et al.*, 1983; Silverio et at., 1992; Nakano *et al.*, 1993). This variation may probably contribute to the contradictory prognostic value of DNA

ploidy on RCC. No study has focused on the point that whether this variation is due to methodological discrepancies or to intratumoral heterogeneity, or both.

3.4 Assessment of DNA Ploidy

Flow cytometry and static image cytometry are the most commonly used methods in quantitative DNA analysis. The DNA content is determined by measuring the fluorescent intensity in flow cytometry or integrated optical density of the DNA specific dyes that are bound stoichiometrically to DNA in static image cytometry.

The measurement of DNA content by either flow or image cytometry is based on the assumptions that the amount of stain represents the amount of DNA and this amount of stain is correctly measured by the instrument. These assumptions imply that: 1. the DNA labeling procedure (fluorescent dye, chromogenic reaction or staining) is specific (all DNA is labeled and only DNA), stoichiometric (staining intensity proportional to DNA content) and stable (staining intensity does not change with time or repeated measurements); 2. the instrument used to measure either the light emitted by the fluorescent dye or absorbed by the stain is accurate (giving a result close to the true amount of stain) and reproducible (giving very similar measurements when repeated on the same nucleus), and linear (giving a result that is perfectly proportional to the amount of stain) (Schulte *et al.*, 1995).

3.4.1 DNA content analysis by flow cytometry

Flow cytometry (FCM) is the most commonly employed method in DNA ploidy analysis. Flow cytometry is a unique combination of electric, optical and biochemical technique. This is a complex measurement device that can detect small intensities of light either scattered or emitted from a cell. If the intensities are proportional to the cellular components causing them, light measurement (photometry) will allow these features to be quantified.

A variety of dyes are available to serve this function, all of which have high binding affinities for DNA. The location to which these dyes bind on the DNA molecule varies with the type of dye used. The two most common categories of DNA binding dyes are the blue-excited dye Propidium Iodide (PI) and the UV-excited dyes Diamidino-phenylindole (DAPI) and Hoechst dyes 33342 and 33258. PI is an intercalating dye which bind to DNA and double stranded RNA (and is thus almost always used in conjunction with RNase to remove RNA), while DAPI and Hoechst dyes bind to the minor groove of the DNA helix and have essentially no binding to RNA. Darzynkiewicz *et al.* (1984) and Evenson *et al.* (1986) have noted that the accessibility of DNA to dyes in nuclei decreases with increasing degrees of chromatin condensation, resulting in lower staining intensity. Accessibility of DNA to dye and staining intensity can be increased by acid extraction of nuclear histones (Rabinovitch, 1993).

The particles (cells, nuclei, chromosomes and bacteria etc.) for analysis are dispersed in suspension. This sample suspension is fed into a central stream as a single file. A very-high-intensity light source (laser or arc lamp) is focused on this stream and as each particle physically passes through the laser beam, light is scattered in all directions. Optical channels collect forward-angle light scatter (FALS) and light scattered at an angle of 90° (90 ° LS) to the direction of the laser. If the cells have been specifically stained with a fluorochrome, excitation by the light source will cause the fluorochrome molecules to fluoresce. Fluorescence is also collected in the 90° light channel and a pinhole aperture excludes extraneous light. Specific wavebands of light can be selected for measurement using dichroic mirrors and absorptive filters. Photodetectors measure the intensity of scattered and fluorescent light, the electrical output signal of that is directly proportional to the quantity of incident light. Analogue-to-digital conversion of this signal allows the quantitative data to be stored in the computer memory and retrieved for analysis.

Most flow cytometers have an on-board computer that can store and display the data for interpretation and statistical analysis. The data may be stored in the form of a histogram, which allows analysis of histogram characteristics only. Alternatively, it can

be collected in list mode that stores each data point to memory. It allows manipulation and reanalyzes of the original flow cytometric measurements (Hamilton and Crockard, 1995).

During the last 10 years there has been an explosive increase in the number of ploidy studies of human cancer using the technique of DNA flow cytometry. This has been related to Hedley's discovery (1983) that pathological material processed for histological examination can also be used for FCM analysis. It greatly facilitated the application of DNA analysis in routinely processed material, making it possible to correlate DNA ploidy status with the biological behavior of tumors both in retrospective and prospective studies.

Since single parameter measurements of DNA content are commonly done in isolated nuclei (Vindelov *et al.*, 1982), Hedley *et al.* developed a technique for DNA analysis of nuclei from paraffin-embedded materials. After sections are deparaffinized in xylene and rehydrated in alcohol solutions, acid pepsin treatment is used for nuclear isolation. Results have been good using material originally fixed in formaldehyde solution or formaldehyde/acetone/acetic acid. Although the resolution of DNA histograms is somewhat reduced when compared to that in fresh or ethanol-fixed tissue, but DNA ploidy can be reliable evaluated (Coon *et al.*, 1986; Franzen *et al.*, 1986; Johnson *et al.*, 1985; Ljundberg *et al.*, 1987).

The principles of flow cytometry, in brief, involve the examination of a single cell suspension passing a given point, by a suitably tuned laser beam, with reflected and/or transmitted light, being detected by suitably placed detectors and converted into electronic signals. Information about the number of cells and their DNA content can be obtained from these data, providing kinetic information if suitably analyzed. In the absence of aneuploidy, cells in G_0/G_1 will be diploid, cells in G_2 will be tetraploid, and cells in S phase will have intermediate amounts of DNA (Figure 2.2).

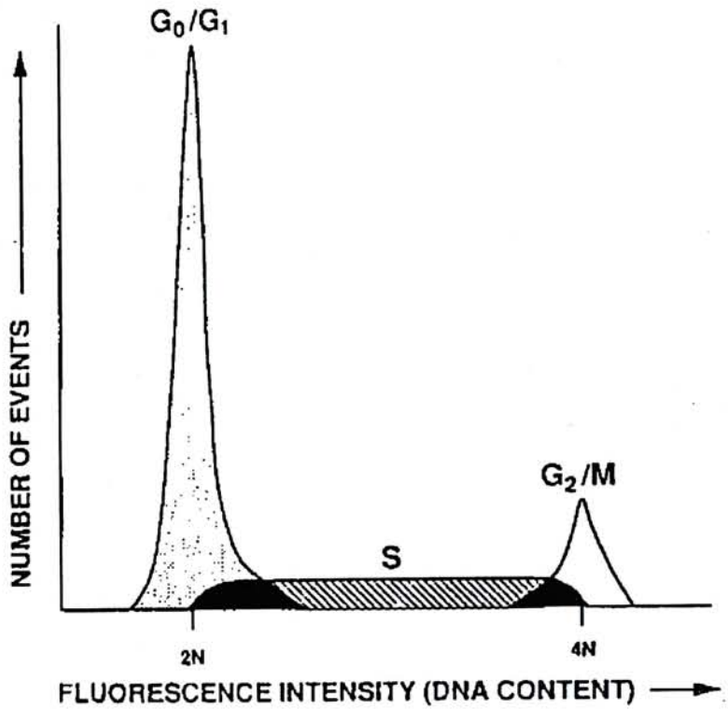

Figure 2.2 A normal diploid population
Flow cytometric histogram display of different fluorescent intensity areas which are separable into corresponding phases of the cell cycle (Zarbo, 1993).

As shown in Figure 2.2, the measured fluorescence from G_1 cells is a normally distributed Gaussian peak. This bell-shaped distribution is characteristic of the variation in measurement such as instrumentation errors and variability in DNA dye binding. The greater the observational variation, the broader the Gaussian peak will be.

The measurement of precision is the coefficient of variation (CV) of the G_0/G_1 peak. The CV, expressed as a percentage, is defined as 100 times the SD divided by the mean. Lower the CVs imply higher precision.

Similarly, G_2 and mitotic cells, described as having twice the normal G_1 DNA content, produce a Gaussian peak in the DNA content histogram with a mean position approximately twice that of the G_1 peak - i.e. 4N.

Assessment of kinetic variables is considerably complicated by the presence of aneuploidy, but with suitable mathematical analysis, the S phase fraction can be determined in most cases (Figure 2.3).

The DNA histogram of an aneuploid tumor usually has two overlapping cell cycles, as aneuploid and a diploid. The latter consists of normal cells, for examples, lymphocytes, endothelial cells, fibroblasts and other stromal elements that are always present in tissue in a greater or lesser extent. In case of intratumoral heterogeneity, the diploid population may also consist of diploid tumor cells. More sophisticated model for cell cycle analysis is required (Rabinovitch, 1992). The important limitation of flow cytometry is the lack of morphological correlation. Visual selection of target cells for analysis is not feasible.

In general, the normal and abnormal DNA peaks must differ by 5% to 20% in DNA content in order to be distinguishable as separate populations. The distinction of near-tetraploid DNA aneuploidy from DNA tetraploidy is even more challenging than the detection of near-diploid aneuploid.

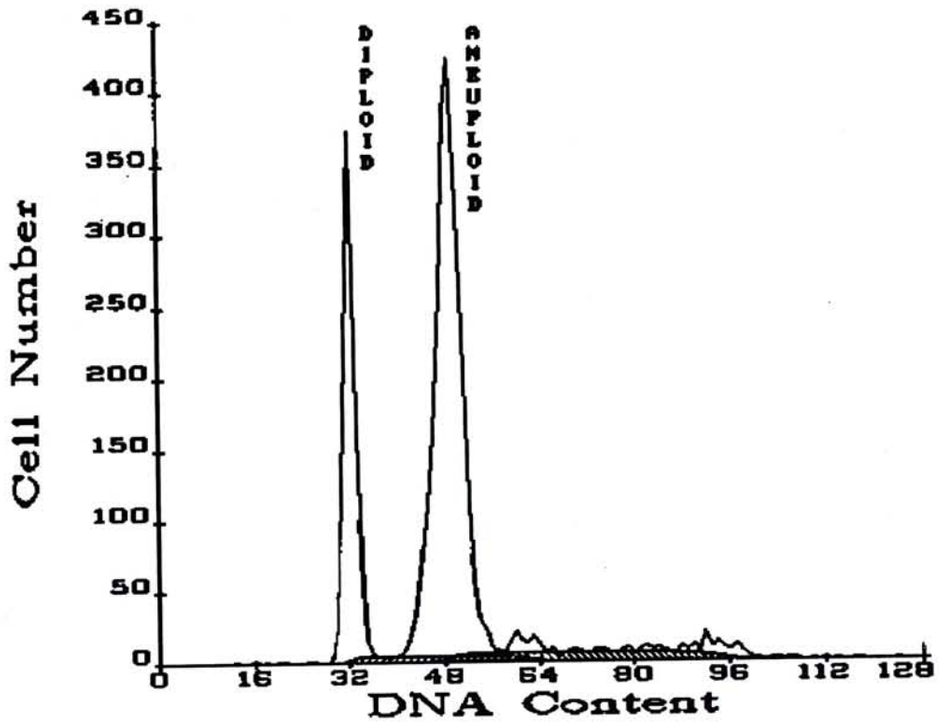

Figure 2.3 A typical flow cytometric aneuploid histogram
By definition, the left most (first) peak is composed of diploid population (Zarbo,1993) and the DNA contents of aneuploid cells are higher than diploid cells.

3.4.2 DNA content analysis by static image cytometry (ICM)

Static image analysis (ICM) has become an important tool in the pathology laboratory for DNA ploidy evaluation. Application of this method in cytological specimens is wildly used (Russack, 1994; Lanigian *et al.*, 1992; Papadopoulos *et al.*, 1995). However, recently, application in tissue sections has also been advocated (Mellin, 1990; Askensten *et al.*, 1990; Veloso *et al.*, 1992).

The ICM DNA assessments are nowadays performed by means of microscope-based and charge coupled-devices (CCD) camera-equipped systems. A typical image analysis system consists of a microscope, a high-quality video camera and color monitor, and a computer (Russack *et al.*, 1994).

The technology uses computer to acquire image, measure, interpret and store extracted data for subsequent retrieval and analysis (Simonson, 1985). The main steps of image analysis are image capturing, image storage (compression), correcting image defects (e.g. non-uniform illumination, electronic-noise, glare effect), image enhancement, segmentation of objects in the image and image measurement (Oberholzer *et al.*, 1996).

The real-life light microscopic image is converted to an analog electronic signal by the video camera. This signal is then digitized by an imaging board or frame-grabber installed in the computer with an analog-to-digital converter (ADC). This results in a matrix of picture elements called pixels. The digital image is composed of pixels arranged in rows and columns like individual tiles of a mosaic. The larger the number of pixels in the image, the better the detail (resolution). The digital signal may also be converted back to an analog signal by a digital-to-analog converter (DAC) for display on a color monitor. They offer high resolution and allow visual inspection and cytodiagnostic identification of the cells during the measurement (Cohen *et al.*, 1996).

By image segmentation, the digitized object of interest is distinguished from the background by human discretion with semiautomatic image cytometers, or by use of gray levels assigned to each pixel by fully automatic instruments. A pixel with a gray level greater than the threshold for background is considered significant. Each pixel gray value may be manipulated by an intensity transformation function before being converted back to a pulse of voltage to be displayed on the computer monitor. Position and optical information of each pixel in the image are stored in the computer's memory as bits that can be integrated for each nucleus or for all nuclei in the image. Eight bits are summarized in one byte. Therefore, gray values can have a value between 0 and 256 (2^8). The human eye seems to be quite content with a display of 5-bit images (corresponding to 64 different gray values) (Oberholzer *et al.*, 1996).

After having been stained by DNA specific dye, the microscopic preparation is scanned by the image cytometry system that measures the optical density (OD) at each point of the image. The digital values belonging to the nucleus are selected through a segmentation procedure. The summed measurement called the integrated optical density which is closely correlated to the quantity of DNA-specific stain in the nucleus.

The microscope is the cornerstone of the system. It is not necessary to be exceedingly complex, but should have a bright, stable and uniform illumination source, quality optics, and be mechanically stable. Maximum contrast is achieved interposing a narrow bandpass filter corresponding to the maximum absorption of a particular histochemical dye. For example, a 588-nm filter is often used to enhance the contrast of Feulgen stained specimens. A solid-state CCD camera is ideal for image analysis since it produces a very stable video signal. For accurate densitometric measurements, the video signal voltage must be directly proportional to the light intensity over a wide range of brightness. The computer must have an imaging board or image processor, which permits the isolation and selection of individual objects (pixels) in the image. Storage of images may require additional peripheral devices such as optical disks, because of the large amount of data obtained in any given image. The output monitor should have sufficiently high resolution for the operator of the instrument to be able to

identify features of interest. Output devices such as printers are necessary for preparing reports and hard copies of data. Commercial systems such as the CAS 200 (Cell Analysis systems, Inc., Lombard, IL) or SAMBA (Dynatech Laboratories, Chantilly, VA) are user-friendly but are expensive.

CAS 200 Image Analyzer

The CAS 200 Image Analyzer is a recently introduced microscope-based, computerized image analysis system designed for analysis of cellular and histological samples.

In brief, the system consists of a Nikon LabPhot 2 trinocular microscope, an IBM PC compatible 486/33-MHz microcomputer equipped with 4 MB RAM, a 120 MB hard disk and two floppy disk drives, a PC Vision Plus video frame grabber (Image Technology, Woburn, MA), two high-resolution VGA monitors, a dot matrix printer, and a Microsoft mouse interactive peripheral device. The image sensor is a solid-state CCD monochrome video camera (Cohu, San Diego, CA).

The system provides a set of calibration slides for system calibration. The standard staining kits are also available. The Quantitative DNA Analysis (QDA) software is an interactive program designed for DNA content analysis. Using the 40 x objective, the pixel size is 0.1935 μm^2. Optical density values for each pixel are mapped by look-up tables. Gray levels from 0 to 130 are mapped from 1.50 to 0.00 optical density levels, respectively, with 2 decimal places retained for internal computation. Images were taken at 620 nm with 10-nm half-width, narrow-band spectral filtering. Subtractive shading correction with image averaging is used in the QDA software module.

A variety of types of specimens are suitable for image analysis. Surgical pathology material from biopsies or excisions, cytological material of all types (effusions, brushes, smears, and fine needle aspirates), and cells grown in culture are all suitable specimens. Fresh or frozen tissue is ideal, but paraffin-embedded materials can also be used. Fresh

tissue can be used to make imprints or disaggregated to make whole cell suspensions from which smears or cytospins are prepared.

Various stains and chromogenic reagents for quantitative staining of DNA have been recommended in the literature, but only one of them has gathered worldwide acceptance for DNA cytophotometry. This is the reaction named after Feulgen and Rossenbeck, often simply named Feulgen reaction. Strictly speaking, the Feulgen reaction is not a stain but a chromogenic reaction. The reaction starts with acid hydrolysis. The previously fixed specimens are immersed in hydrochloric acid (HCl) which splits off the purine bases adenine and guanine from the DNA molecule. Thereby, it generates aldehyde groups in the purine-free DNA molecule, which is then called apurinic acid (APA). In the second step, the specimens are immersed in Schiff's reagent containing a dye that binds covalently to the aldehyde groups. After removal of surplus dye, the slides are dehydrated and mounted as usual. In correctly stained material, cell nuclei are stained red-violet, the cytoplasm and background are unstained.

The most common graphic representation of DNA image analysis data is a linear scale for DNA content, with even intervals between 2c (diploid), 3c, 4c, etc. This assumes that the total OD increases linearly with the absolute amount of DNA (Wied *et al.*, 1989).

Typical DNA distribution patterns measured by ICM are showed in Figure 2.4. Non-proliferating (G_0) or proliferating (G_1, S, G_2/M) normal diploid human cell populations result in regular DNA histograms, characterized by a narrow peak in the diploid (2C) region, with or without varying fractions of cells in the S-phase and G_2/M phase (4C) region (Fig. 2.4a, b). Benign non-neoplastic tissue can sometimes show DNA values distinctly located within the 4C or 8C region. This polyploidization is a phenomenon that can occur, for example, in endocrine tissues and in the liver (Fig. 2.4c). Aneuploid histograms characterized by a prominent peak (or peaks) in the region between 2C-4C (Fig. 2.4d), 4C-8C or 8C-16C.

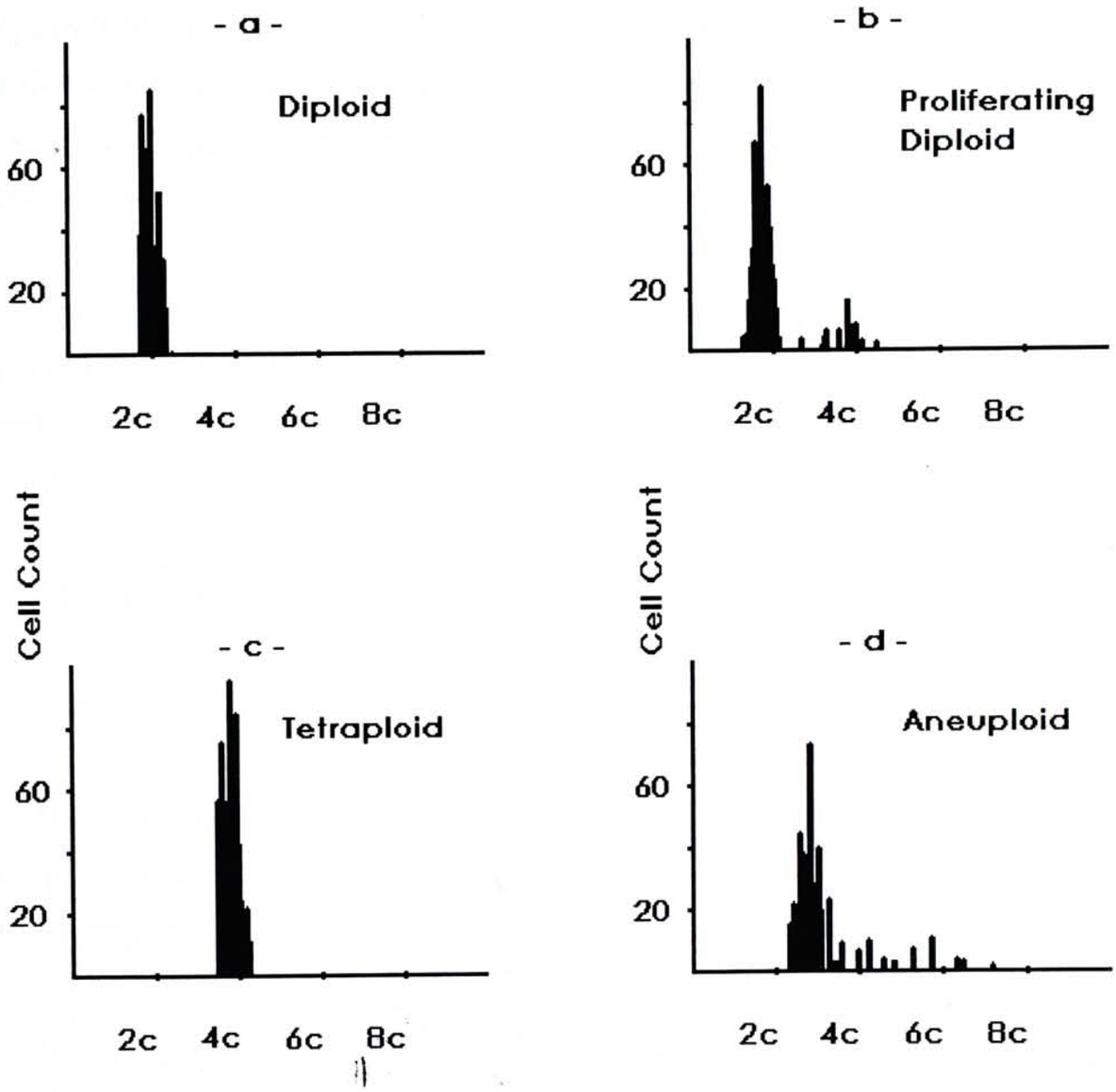

Figure 2.4 Typical image cytometric histograms.
a: Diploid; b: Proliferating diploid; c: Tetraploid; d: Aneuploid.

4. Cell Proliferation and its Assessment by Immunohistochemical Methods

4.1 Proliferation Activity and Tumor Growth

The cellular proliferation is one of the fundamental biological processes (Alberts *et al.*, 1989). The proliferative or growth fraction of any cellular population can be defined as the ratio of cycling to cycling plus non-cycling cells. Proliferation activity results from cell cycling and contributes to tumor growth. The mechanism relating proliferation activity is the speed of the cycle that is inversely proportional to the generation time.

Tumor growth is the overall increase in the cell number and thus the tissue mass. It is the net result of the balance between the cell gain, which directly results from proliferation activity, and the cell loss either related to necrosis or apotosis (Tannock, 1992).

4.2 Basic Principles of Immunohistochemistry (IHC)

Introduction

Immunohistochemistry is a method for specific identification of cellular components according to their antigenic constituents. It can be considered as the demonstration of antigens in cells by the specific antigen-antibody reactions.

Biological macromolecules such as proteins, carbohydrates, lipids and nucleic acids, which are capable of evoking antibody production (Rosen, Steiner and Unanue, 1989) can be theoretically detected by IHC. Many types of antibodies are commercially available and the technique is employed in routine diagnostic serves.

The antibody

The antibody is central to the success of IHC labeling. A good antibody is highly specific, possesses a high titre (amount of antibody activity) (Rosen, Steiner and Unanue, 1989), high affinity (the exactitude of stereochemical fit of an antibody-combining site to its complementary antigenic determinant) (Catty, 1988), and high avidity (the total binding strength of a multivalent antigen with the antibody) (Beltz and Burd, 1989). Both polyclonal and monoclonal antibodies can be used for IHC.

A polyclonal antisera is a mixture of high affinity antibodies against different epitopes on the antigen. Epitopes refer to sites on the complex antigenic molecule that are recognized by antibody (Beltz and Burd, 1989). They are produced by injecting an antigen into a host animal, usually either rabbit, sheep, or goat. After booster injections, the serum is periodically collected and tested for antibody. Antibodies are produced in the spleen of the host animal by B-lymphocytes and plasma cells.

A monoclonal antibody is a pure preparation of one of the constituents of polyclonal antiserum. Monoclonal antibodies are useful as diagnostic and research tool since large amounts of antibody with high specificity, titre, and homogeneity in all batches can be produced (Beesley, 1993).

The initial phase of preparation is to induce synthesis of a polyclonal antiserum in the host animal as described above. The plasma cells are removed from the host animal and each fused with a malignant myeloma cell to form hybridoma cells (Kohler and Milstein, 1975). Hybridoma cells are isolated and cultured and theoretically each will produce unlimited monoclonal antibodies raised against a specific epitope. Each antibody is identical in reactivity and titre. These hybridoma cells are either cultured *in vitro,* in which the tissue culture supernatant fluid contains antibodies, or *in vivo* in the peritoneal cavity of a suitable host and the ascites fluid contains antibodies.

The microscopically dense marker

The microscopically dense marker enables the site of the antigen-antibody reaction to be correlated with the morphology of the specimen. The marker contains two components, a microscopically dense reagent and a reagent that binds to the primary antibody. For light microscopy, the microscopically dense reagent could be an enzyme, such as peroxidase or alkaline phosphatase, which is developed to a colored reaction product (Beesley, 1993).

Conjugation of a binding protein to the dense reagent ensures linkage of the dense marker to the primary antibody. If the primary antibody has been biotinylated the marker will contain streptavidin (Beesley, 1993).

Immunolabeling techniques

The antigen, the antibody, and the microscopically dense probe must be linked together by successive incubations. There are numerous IHC techniques that may be used to localize antigens. The selection of a suitable technique should be based on parameters such as the type of specimen under investigation and the degree of sensitivity required (Jackson and Blythe, 1993).

ABC (Avidin-Biotin-peroxidase Complex) method (Hsu, Raine and Fanger, 1981) is a three-step immunoperoxidase method that utilizes the high affinity of avidin for biotin, with a dissociation constant of 10^{-19} M. The staining procedures include adding of normal serum to the tissue prior to unlabeled primary antibody and followed by a layer of biotinylated secondary antibody. The third layer is a complex of avidin and biotinylated horseradish peroxidase which forms a tertiary structure possessing four biotin binding sites that enable binding of biotin which is conjugated to the secondary antibody (Figure 2.5).

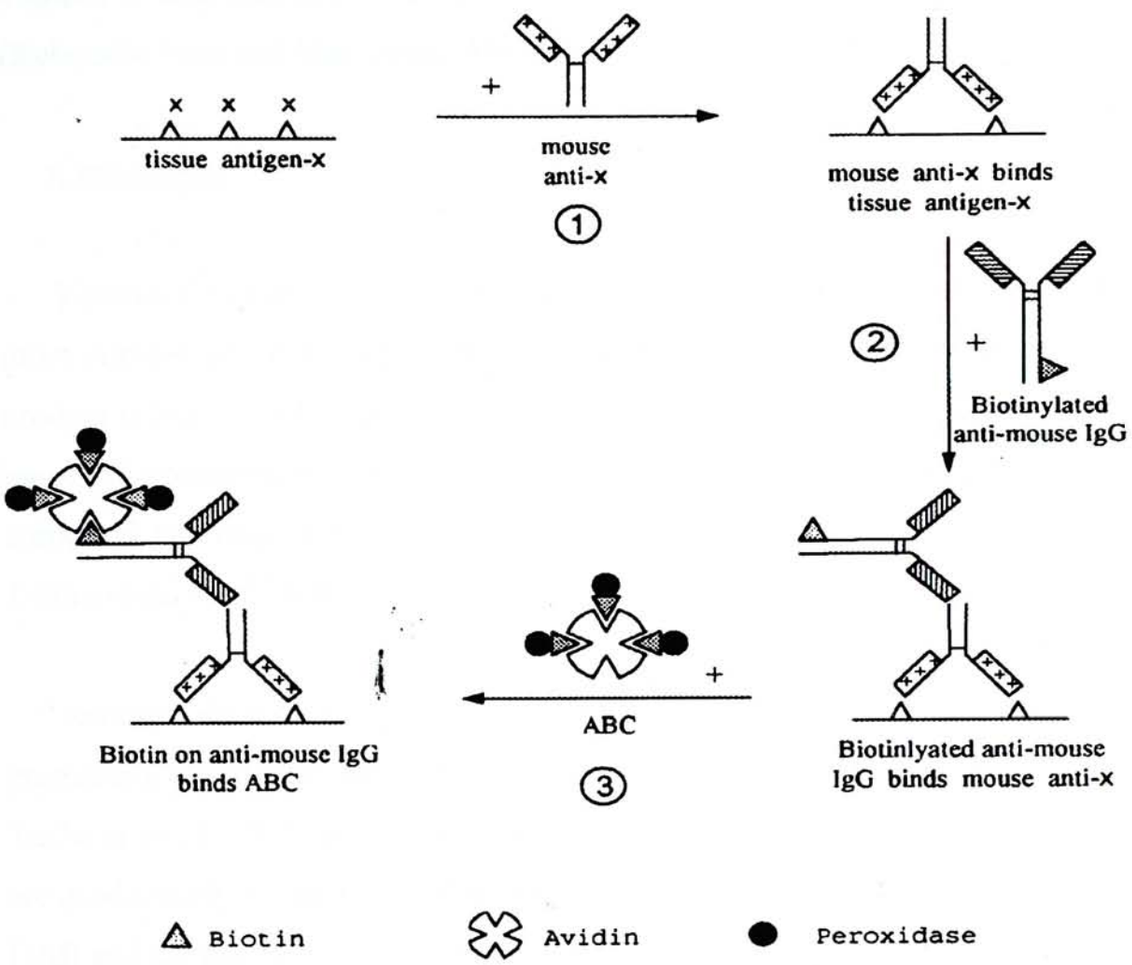

Figure 2.5 Staining sequence in the Avidin-Biotin-peroxidase Complex (ABC) method (Hsu, Raine & Fanger, 1981).

One of the disadvantages of this technique is that avidin is a glycoprotein and thus it can bind to lectins in the tissue via its carbohydrate groups to produce non-specific or false positive staining (Bussolati and Gugliotta, 1983). This problem can be overcome by changing the buffer pH from 7.4 to 9.0 or replace avidin with streptavidin (a bacterial protein which does not contain sugars). Streptavidin has an isoelectric point at 7 and it is near that of the tissue and it is less prone to attach to charged binding sites (Robinson, Euis and Maclennan, 1986).

Chromogens

Various Chromogens are available for the different immunoenzyme systems. The most popular one currently used is 3,3'-diaminobenzidine (DAB). Its brown reaction product is clearly visible and insoluble in alcohol, making it suitable for use with a wide range of counterstains and mounting media. One of the drawback of DAB is its suspected carcinogenecity (Marcollet *et al.*, 1980; Tubbs and Sheibani, 1981; 1984; Trojanowski *et al.*, 1983; DeJong *et al.*, 1985; Scopsi and Larsson, 1986).

Another chromogen commonly used is 3-amino-9-ethylcarbazole (AEC). It produces a cherry-red color which is soluble in organic solvents (Graham *et al.*, 1965; Tubbs *et al.*, 1979; Trojanowski *et al.*, 1983). Other chromogens are available and they are used mainly because they offer an alternative to the brown color reaction product of DAB and the cherry-red color of AEC. These chromogens include tetramethylbenzidine (Sheibani *et al.*, 1981; Tubbs *et al.*, 1981), *p*-phenylenediamine-pyrocaterchol or the Hanke-Yates reagents (Hanker *et al.*, 1977; Tubbs *et al.*, 1979; Sheibani *et al.*, 1981) and *etc*. Their action is dependent on the ability of peroxidase to mediate an oxidation-reduction reaction in the presence of hydrogen peroxide to produce a visible, oxidized product that precipitates at the site of tissue-bound antibody-enzyme complexes.

Unmasking of antigens

Although formalin is the most common fixative used in pathologic laboratory for preserving tissue morphology, it is not an ideal fixative for preserving antigenicity of tissue to be used in IHC study. Prolong fixation reduces the immunoreactivity of many antigens and fixations in old buffered formaldehyde which becomes acidic is damaging to some antigenic determinants (Taylor, 1978).

There are several methods to restore immunoreactivity, the most common used are enzyme digestion and microwave. The proteolytic digestion of the enzyme cleaves the cross-link introduced by formalin and re-exposed the hidden antigenic sites. But it is not always successful. False negative staining, morphologic degradation or no enhancement of staining had been reported.

Microwave (MW) treatment was initially described by Shi *et al.* (1991). But the lead-containing solution is hazardous for routine laboratory used. Alternative medium solutions were reported including inorganic, organic and metal salts solution, denaturant agents such as urea (Cattoretti *et al.,* 1993), and antigen retrieval solution (Biogenex) (Van den Berg *et al.,* 1993). MW irradiation gives dramatic enhancing effect on the recovery of many antigens when compare with enzyme digestion. Enhancement of immunoreactivity can also be achieved through autoclave or pressure cooker with preheating of sections immersed in an aqueous salt solution (Bunkfalvi *et al.,* 1994; Miller *et al.*, 1995).

4.3 Ki 67, A Cell Proliferation Marker

Antibodies have become an important means of assessing cell proliferation in modern pathology. Recent interest has focused on the immunohistochemical determination of cell cycle-associated antigens.

One of the most widely used reagents in this field is the antibody Ki 67 (Gerdes *et al.*, 1983), which reacts with a nuclear non-histone protein of 395 and 345 kD (Gerdes *et al.*, 1991) present in all active parts of cell cycle, i.e., G_1, S, G_2, and mitosis, but is absent in G_0 phase (Gerdes *et al.*, 1984). The corresponding protein which is coded by a gene on chromosome 10 in human has been highly conservative during evolution. It accumulates in the nucleoli during the cell cycle and releases at the onset of mitosis. It appears to play a key role in chromosome packaging. Recent studies using a variety of techniques, including confocal microscopy, suggest that the antigen is a component of the nuclear matrix (Verhuijen *et al.*, 1989).

Although the original Ki 67 labeling is sensitive to fixation procedures and is thus usable on fresh and frozen materials only. A new family of antibodies such as MIB-1 (Key *et al.*, 1993) directly against the same protein is becoming available and can be used in routinely formalin fixed paraffin embedded materials.

Cattoretti *et al.* (1992) demonstrated that antibodies MIB-1 can be regarded as true Ki 67 equivalents. The initial applications of MIB-1 on routinely fixed and processed materials were disappointing. MIB-1 staining was limited to mitotic figures. However, following microwave antigen retrieval, the nuclear staining pattern seen in paraffin sections with MIB-1 coincides well with that of Ki 67 in frozen sections and with data on normal cell proliferation obtained by incorporation of radiolabeled DNA precursors. Thus, their data showed that it is now possible to identify the Ki 67 antigen by MIB-1 antibody in formalin-fixed paraffin-embedded tissue.

In nutritionally deprived cells, which are not uncommon in tumors, there can be a discrepancy between Ki 67 immunoreactivity and other variables of cellular proliferation (Verhuijen *et al.*, 1989; Dierendonck *et al.*, 1989). In practice, some underestimation of the growth fraction may occur due to the rapid disappearance of the antigen in postmitotic cells. Nevertheless, Ki 67 immunostaining has been extensively used as an marker of cellular proliferation and, although certain caveats have been raised, it will probably remain a popular method.

Studies have shown that there is a close correlation between Ki 67 immunoreactivity and other variables of cellular proliferation such as thymidine labeling, bromodeoxyuridine incorporation and flow cytometry (Schwarting *et al.*, 1986; Silvestrini *et al.*, 1988; Veroni *et al.*, 1988; Kamel *et al.*, 1989; Sasaki *et al.*, 1988).

Ki 67 immunostaining has been used in numerous disease states including tumor such as non-Hodgkin's lymphomas (Shrape *et al.*, 1987; Hall *et al.*, 1988), breast tumors (Querzoli *et al.*, 1996), brain tumors (Striepecke *et al.*, 1996), cervical tumor (Brown *et al.*, 1988) and etc. Ki 67 expression seems to provide prognostically useful information in these tumors. In RCC, Jochum *et al.* (1996) found that Ki 67 immunoreactivity was significantly related to nuclear grade, pT stage, Robson's stage, DNA ploidy, mitotic count and lymph node involvement. They also demonstrated that Ki 67 was significantly correlated with recurrent rate as well as survival of RCC patients. Tannapfel *et al.* (1996) also described Ki 67 as being valuable in the prognostic assessment of RCC.

4.4 $p27^{kip1}$, A Cell Cycle Arrest Protein

Cell proliferation is regulated by many factors. Progression through the cell cycle is governed by cyclins and their partners the cyclin-dependent kinases (CDKs) (Morgan, 1995). Recently, two families of cyclin-dependent kinase inhibitors (CKIs) have been identified that inhibiting cell cycle progression by binding to and inactivating cyclin/CDK complexes (Sherr and Roberts, 1995). The INK family, Including $p15^{INK4b}$, $p16^{INK4a}$, $p18^{INK4c}$ and $p19^{INK4d}$ bring about G_1 arrest by specific inhibition of D-cyclins complexed with cdk4 or cdk6. The other group of CKIs, the p21 family, includes $p21^{waf1.cip1.sdi1}$, $p27^{kip1}$ and $p57^{kip2}$, which are proteins that inhibiting kinase activities of preactivated G_1 cyclin E-CDK2, cyclin D-CDK4/6, and other cyclins (Xiong *et al.*, 1993; Ei-Deiry *et al.*, 1993; Polyak *et al.*, 1994; Toyoshima and Hunter, 1994; Matsuoka *et al.*, 1995; Lee, Reynisdottir and Massague, 1995).

Over expression of kip proteins causes cell cycle arrest. However, the role of kip proteins in regulating cell cycle progression in normal and neoplastic cells has not been elucidated. Recent studies with $p27^{kip1}$-deficient mice that developed multiple organ hyperplasia indicate that this CDK inhibitor has anti-proliferative activity *in vivo* (Nakayama *et al.*, 1996; Kiyokawa *et al.*, 1996; Fero *et al.*, 1996). Although p21 and $p27^{kip1}$ can inhibit many cyclin/CDK complexes in vitro, their in vivo activity appears to be restricted to the G_1 cyclin/CDK complexes (Sherr and Roberts, 1995). Although genetic alterations are common in INK family members, mutations in p21 and $p27^{kip1}$ appear to be surprisingly rare in tumors, suggesting that tumor cells retaining such inhibitors may have a survival advantage (Ferrando *et al.*, 1996; Spirin *et al.*,1996).

A recent study of the expression of $p27^{kip1}$ protein by immunohistochemistry in normal and abnormal tissues (Ricardo *et al.*, 1997) has shown that there is widespread aberrant $p27^{kip1}$ expression in hyperplastic tissues, in benign and malignant neoplasms compared with normal tissues. $p27^{kip1}$ expression was appeared to be inversely related to the proliferation marker Ki 67 (MIB-1). Other authors reported that reduced expression of $p27^{kip1}$ correlated with poor survival in cohorts of breast and colorectal carcinoma patients (Catzavelos *et al.*, 1997; Loda *et al.*, 1997; Porter *et al.*, 1997).

Immunohistochemical analysis of $p27^{kip1}$ along with Ki 67 may be useful in the assessment of the biological behavior of neoplasms, to classify hyperplastic or neoplastic tissues, and to study cell cycle regulation during tumor progression.

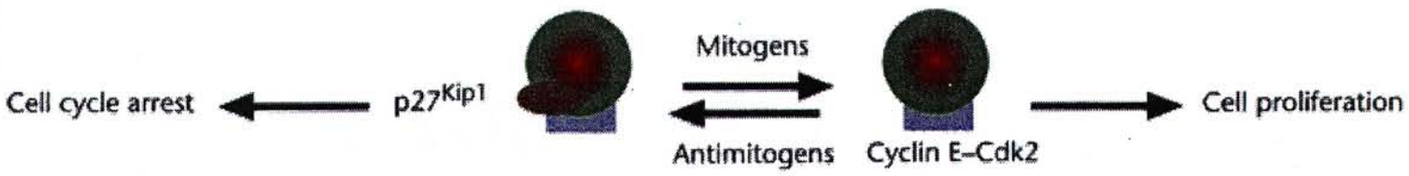

Figure 2.6 Regulation of the G_1 to S-phase transition point by the cyclin E-cdk2 complex and its inhibitor, $p27^{kip1}$ (Catzavelos *et al.*, 1997).

Chapter 3

Aims of the study

The principal purpose of this study is to assess the DNA ploidy status of renal cell carcinoma (RCC) using three different methods: 1. flow cytometry; 2. static image cytometry using cytospin preparation; 3. static image cytometry using tissue sections. By comparing three different methods, DNA ploidy status of RCC may be more accurately assessed and factors which might lead to any discrepancies could be established.

Assessment of proliferative activity also appears to be of prognostic significance. The proliferation activity of renal cell carcinoma was assessed by immunohistochemical method using two cell cycle-related monoclonal antibodies: Ki 67 (MIB1) and $p27^{kip1}$. The potential relationship among ploidy status, expression of the proliferative markers and other clinical-pathological factors would be explored.

Chapter 4

Materials and Methods

1. Tissue Samples

1.1 Sample Retrieval

Formalin-fixed paraffin-embedded surgical specimens of renal cell carcinoma were used for our study. The surgical specimens were collected during 1985 to 1995 and they were retrieved from the files of the department of Anatomical and Cellular Pathology, Prince of Wales Hospital, the Chinese University of Hong Kong.

Slides stained with haematoxylin and eosin were retrieved and examined by a pathologist to confirm the diagnosis. For each case, the section contained the most high-grade tumor area was selected. One additional tumor section was randomly selected. Thus for each case, two representative tumor blocks and a normal renal tissue block were selected and subjected to DNA content analysis by three methods. Paraffin blocks from 46 patients were available, including 43 cases of renal cell carcinoma (RCC) and 3 cases of oncocytoma.

1.2 Tissue Processing

Surgical specimens were fixed in 10% neutral buffered formalin for at least 4 hours. Then they were processed according to the procedures as shown in Table 4.1.

1.3 Preparation of Tissue Sections

Tissue sections with three different thickness for different purposes were cut by Reichert Jung 2030 rotary microtome.

- 4 μm sections mounted on APES coated glass slides* : for immunohistochemical staining
- 6 μm sections mounted on APES coated glass slides* : for Feulgen staining

- 50 μm sections placed in 15ml centrifuge tubes : for preparation of nuclear suspension

Table 4.1 Procedure of rotary tissue processor

Model : Citadel 2000 (Shandon)

Step No.	Reagent	Time (hour)
1	10% neutral buffered formalin	3
2	70% ethanol	1
3	95% ethanol	1
4	absolute ethanol I	1
5	absolute ethanol II	1
6	absolute ethanol III	1
7	absolute ethanol IV	2
8	Xylene I	0.5
9	Xylene II	0.5
10	Xylene III	1
11	Paraffin I	1
12	Paraffin II (vacuum)	2
	Total:	15

*Pretreatment of glass slides:

The microscopic glass slides were soaked in 5% chromium tritroxide in 10% sulphuric acid overnight, washed thoroughly with running water then coated with 2% 3-aminopropyl triethoxysilane(APES, Sigma)-Acetone solution. The slides were then rinsed in acetone, followed by distilled water and dried at 37°C in the oven. Using APES coated slides can prevent detachment of sections during staining.

2. Methods for Quantitative DNA Analysis

2.1 Instrumentation

Both Flow Cytometry (FCM) and Static Image Cytometry (ICM) were used in our study to perform the quantitative DNA analysis.

2.1.1 Flow Cytometry

The FCM used in our study was COULTER® EPICS XL Flow Cytometer from Hematological laboratory, Prince of Wales Hospital, Hong Kong.

The following reagents were used for quality control of FCM analysis:

- COULTER Standard-Brite: to standardize fluorescence intensity.
- DNA-CHECK EPICS Alignment Fluorospheres: for optical alignment.
- CEN (Chick Erythrocyte Nuclei) DNA Calibrators: to calibrate FL3 high voltage.
- COULTER INDEX DNA Controls: for verification of the staining procedure, instrument performance, and software analysis.

The instrument and all of the reagents are products of COULTER Corporation, Miami, Florida, USA.

2.1.2 Static Image Cytometry

The CAS (Cell Analysis System) 200 Image Analyzer were used for ICM DNA quantitation.

The following materials were provided by the manufacturer to integrate staining and quantitative analysis.

- CAS™ Quantitative DNA Staining Kit (BDCIS Cat. No. 54100140), which uses the Feulgen staining reaction to stain DNA specifically and quantitatively.

- DNA Calibration Slides (BDCIS Cat. No. 54100120), which containing cells with a standard DNA content, produce a biological reference for assessment of DNA content and calibration of instrument and staining procedures.

The instrument and materials are products of Becton Dickinson and company, San Jose, California, USA.

2.2 Procedures for Quantitative DNA Analysis

The DNA ploidy profiles of RCC were investigated by two different approaches: flow cytometry and static image cytometry. FCM DNA analysis was performed using disaggregated nuclei from archival paraffin-embedded materials. Propidium iodide was used as a stain. While in image cytometric analysis, two specimen types were used: paraffin-embedded sections and cytospin preparations of disaggregated nuclei. Both types of specimens were stained quantitatively with Feulgen reaction.

2.2.1 Flow Cytometry

2.2.1.1 Preparation of nuclear suspension *The protocol was kindly provided by Dr. WC Tsoi, Hematology, Department of Anatomical and Cellular Pathology, Prince of Wales Hospital.

Tissue preparation:

- Histological review to define representative tumor area free of necrosis and inflammation.
- Prepare 3-5 50-μm sections as mentioned above.
- Place the cut sections in appropriately labeled 15-ml polypropylene centrifuge tubes

Dewax and rehydration:

- Dewaxed using two changes of xylene and rehydrated through a series of graded alcohol.
- Add 10 ml of distilled water, cap tubes and leave at room temperature for a minimum of overnight.

Tissue disaggregation:

- Make fresh 0.5% pepsin solution with 0.9% saline solution (pH = 1.5).
- Wash the tissues twice with distilled water and decant. Transfer the tissue to a petri dish with applicator stick.
- Mince tissue into small pieces using scissors, rinse tissue into centrifuge tubes with 1-2 ml 0.5% pepsin solution.
- Place in 37°C waterbath for 30 minutes.
- Filter the cells through a 41-μm nylon mesh (Spectral/Mesh, SPECTRUM medical industries, Inc.) into another 15-ml centrifuge tube.
- Fill the new tubes with 15-ml HEPES-Hanks solution to neutralize the pH.
- Centrifuge at 1000 rpm for 10 minutes. Pour off and resuspend in 4 ml of HEPES-Hanks solution.

Adjust nuclear concentration:

- Measure the nuclear concentration using a hematocytometer.
- Make sure that recovery > 100,000 nuclei, nuclei count in the range of 3-10 x 10^6 nuclei/ml.
- If count < 3 x 10^6 nuclei/ml, centrifugation and resuspension required.
- If count > 10 x 10^6 nuclei/ml, dilution required.

At this point the specimens were split into two parts. One would be cytocentrifuged for ICM analysis. And the other part would proceed to Propidium Iodide-based (PI) DNA staining for FCM analysis.

2.2.1.2 Rapid PI-based DNA Staining for FCM Analysis

Preparation of staining solution and salt solution:

Staining Solution (10 ml)

0.3 g PEG 6000 (Sigma # P-2139)

0.5 ml PI (Sigma # P-4170) stock (1 mg/ml)

0.5 ml RNase (Pharmacia # 27-0323-01) stock (4 mg/ml)

0.1 ml 10% Triton X stock (Dilute 5 ml to 50 ml PBA)

8.9 ml 4 mM citrate buffer pH 7.8

(Adjust final pH to 7.2)

Salt Solution (10 ml)

0.3 g PEG 6000

0.5 ml PI stock

0.1 ml 10% Triton X stock

9.4 ml 0.4 M NaCl

(Adjust final pH to 7.2)

Staining procedure:

1. Spin the nuclear suspension at 1000 rpm for 10 minutes, discard the supernatant.
2. Add Stain Solution at a volume that yields 2-4 x 10^6 nuclei/ml final concentration.
3. Incubate in the dark for 30 minutes at 37°C.
4. Double the volume with Salt Solution.
5. Store in the dark at 4°C for at least one hour.
6. Proceed to Flow Cytometry Analysis.

2.2.1.3 FCM DNA Analysis

Quality assurance:

Precision is critical in DNA cytometry that is monitored by following procedures.

System warm up A warm up period of 30 minutes to 1 hour is advisable for the system.

Running Standard Brite The uniform microspheres contains a fluorescent dye. The fluorescent dye emits from 525 nm to 700 nm when excited at 488 nm. The peak emission in the spectrum is located at about 560 nm. (COULTER) Using Stand-Brite is to ensure that the instrument provides the same intensity value on a day-to-day basis for a standard fluorescent particle.

Running DNA-Check The DNA-Check fluorospheres are uniform polystyrene particles containing a fluorescent dye. The dye's fluorescence emission spectrum is located at about 560 nm. (COULTER) The running if the DNA-Check fluorospheres is to optimize the FCM optical alignment.

Running Chicken Erythrocyte Nuclei (CEN) CEN have a DNA content of 35% of the human diploid value. (Howard, 1989) Prepare the CEN DNA calibrators along with each batch of specimens. Run CEN to adjust the DNA High Voltage to place the major singlet peak at a standardized channel, for example, 100 of 1024 channel histogram. At this setting normal human cell DNA intensity will be at about channel 200. This is optimal for visualization of most types of samples.

Running DNA Controls COULTER Index DNA Controls are fixed preparation of a Normal Control, containing normal human peripheral blood lymphocytes (PBL), and an Abnormal Control, containing a mixture of normal human PBL and a tumor cell line.

Each control contains different levels of DNA content, detectable by DNA staining and flow cytometry. The mean assay values should be within the expected ranges given in the Assay Table below (Table 4.2). The purpose of using these materials is to provide quality control for verification of the staining procedure, instrument performance, and software analysis used in making DNA measurements.

Table 4.2 Expected assay mean values and ranges

Parameter	Normal		Abnormal			
	Diploid Cycle		Diploid Cycle		Aneuploid Cycle	
	Mean	Range	Mean	Range	Mean	Range
CV G1	2.6%	1.7-4.4%	2.8%	1.9-4.6%	5.3%	3.8-8.3%
% Total			33%	13-53%	67%	47-87%
DNA Index					1.5	1.3-1.7

Data acquisition and processing:

- Flush each specimen through a 25-gauge needle several times to reduce clumping.
- Transfer the samples to test tubes. For each patient, totally 5 samples were measured by FCM. A sample from normal renal tissue, 2 samples from different tumor blocks, and 2 mixtures of tumor and normal samples.
- Put the sample onto the sample stage of FCM.
- Start data acquisition. The intensity of fluorescence emitted by each of the 10,000 nuclei per sample was measured on a linear scale of 1024 channels.
- The data were display and stored in the form of single parameter histograms. The raw data were analyzed employing Multicycle DNA cell cycle analysis program (Phoenix, San Diego, CA, USA)

2.2.1.4 Interpretation of FCM Histograms

The FCM histograms were considered as acceptable for analysis when the CVs of G_0/G_1 peak was less than 10%. Histograms with CVs greater than 10% were rejected and required repeat of the measurement.

According to DNA cytometry consensus conference (1992), the tumor samples were denominated diploid (DNA index = 1.0) when only one peak was detected. Aneuploidy was assigned when identification of two separate discernible G_0/G_1 peaks containing ascending and descending components. The aneuploid peak should have no less than 5 - 10% of total cells. Peaks composed of fewer cells, with shoulders or wide CVs were suspicious for two or more incompletely discriminated stemline cell population that may warrant reanalysis. A tumor sample was regarded as tetraploid when more than 15% of the cells had a tetraploid DNA index (1.8 - 2.2).

2.2.2 Static Image Analysis on Cytospin Preparations

The cytospin is a special purpose instrument designed to deposit cells onto glass slides. The instrument produces monolayer cell deposition in a defined area of the slide, using centrifugal force. The cell preparation system we used is the Shandon Cytospin® 3 (Shandon Scientific Limited, Pittsburgh, Pennsylvania, USA)

2.2.2.1 Procedures for Preparing Cytospin Specimens

The preparation of nuclear suspension was described in the previous section.

1. Load 100µl nuclear suspension (previous prepared) into cytospin sample chamber.
2. Cytocentrifuged at 800 rpm for 5 minutes.
3. Remove the slides and air-dried for 30 minutes to 2 hours.
4. Fixed in 10% neutral buffered formalin for 30 minutes.
5. Rinse the slides for 5 minutes in running deionized water.

6. Air-dried the slides completely.
7. Stored at room temperature (dust free) until staining.

2.2.2.2 Feulgen Staining for Static Image Analysis

Two commercially available DNA Calibration Slides (CAS) were stained along with each batch of specimen slides.

Preparation of reagents:

1. Stain Solution (100 ml) for a Single Coplin Jar
   Place 100 ml 0.1N HCl and the entire content of one Stain Reagent vial into a 125-ml conical flask. Cover the flask tightly with parafilm to prevent SO_2 loss. Stir on a magnetic stirrer for 1 hour. At the end of 1 hour, filter the stain solution through #1 grade filter paper.

2. Rinse Solution (300 ml)
   Place 300 ml of 0.05N HCl into a 500-ml conical flask and add the entire content of one Rinse Reagent vial. Parafilm the flask tightly and mix until completely dissolved.

Staining procedure:

1. Start the preparation of the Quantitative DNA Stain Reagent no more than 15 minutes before the initiation of hydrolysis.
2. Place the slides into 5N HCl and hydrolyzed for 60 minutes. Filter the DNA Stain solution no mare than 10 minutes before the end of hydrolysis.
3. Fill the Coplin jar with freshly prepared stain. Transfer the slides directly from the 5N HCl to the stain. Parafilm and cap the Coplin jar to prevent the excess SO_2 loss. Stain for 60 minutes.
4. Rinse the slides with three changes of Rinse Solution for 30 seconds, 5 minutes and 10 minutes respectively. Keep the Coplin jar parafilmed to prevent SO_2 loss.

5. Wash the slides in several changes of deionized water for 5 minutes.
6. Put slides into 1% acid alcohol for 5 minutes.
7. Directly from acid alcohol, dehydrate slides in absolute ethanol and clear slides in xylene.
8. Coverslip slides with a synthetic mounting medium and ready for ICM analysis.

2.2.2.3 Performing ICM Analysis

ICM DNA analysis was performed on CAS 200 Image Analyzer using version 3.0 of Quantitative DNA Analysis program (QDA). Each QDA analysis consists of two steps: calibration and analysis.

System standardization and calibration:

System Warm up The microscope lamp and camera should have sufficient time to warm up (10-15 minutes). Otherwise the light settings will probably drift, and could possibly cause an incorrect calibration of the system.

Set light Set light is necessary to set the proper reference light level so that the camera can acquire images with a constant background light level. Set light also corrects for irregularities in the field of view.

Measurement of calibration slides Two calibration slides were stained along with each batch of specimens. The calibration slides contain rat hepatocytes of a known DNA content. It is necessary to calibrate the system for every staining batch, and for best results, should be done for every specimen. It controls for variations in staining intensity, differences in daily microscope setup, light quality, and instrument tolerances (CAS QDA user guide).

Analysis specimen slides:

Check light to set the microscope lamp intensity to a standard, optimum level.

To check the Boundary or Threshold. Setting the Boundary is to set a threshold that defines the level of optical density has to be achieved before the system recognize it as an object and attempt to measure it. Nuclear objects below the threshold won't be selected as objects for measurement. At least 100 representative nuclei were measured per histogram..

2.2.2.4 Interpretation of ICM Histograms

For each case, normal renal tubular epithelial cells from the same patient, preferably from the same block were measured. The DNA index of the tumor sample was determined by comparison of the DNA content with normal control cells. A DNA index range of 0.85 to 1.15 was considered to be diploid. DNA indexes ranging from 1.85 to 2.15 were considered to be tetraploid. Other DNA indexes were considered aneuploid.

2.2.3 Static Image Analysis on Tissue Sections

Formalin-fixed paraffin-embedded 6 μm-sections were stained following deparaffinization, hydration and rinse in several changes of distilled water to remove excess alcohol. Slides then were placed directly in 5N HCl for hydrolysis followed DNA staining procedure.

When using tissue sections, most often partially cut nuclei rather than whole intact nuclei were measured. A proper filter in the QDA software program was used to filter out the unwanted debris and nuclear fragments. A thickness correction based on the measured DNA mass of normal diploid nuclei has to be performed when tissue sections were measured. As we know that DNA mass of normal human diploid cells are 7.18 picogram (pg). For each sample, we measured at least 100 normal tubular epithelial cells of the same patient, preferably on the same section, and corrected the DNA mass of each

nucleus to 7.18 pg. The corresponding tissue thickness for this particular section was automatically computed by the software program. This tissue thickness was applied to the tumor sample to calculate the actual DNA mass of each nuclear fragment under this particular thickness.

Detail of ICM performances and measurements were described in the previous section.

2.2.4 Assessment of Nuclear Area

Nuclear area was measured simultaneously during ICM analysis of the DNA content on tissue sections. The mean nuclear areas of the cellular populations at the peaks in the histogram of each sample were recorded.

3. Immunohistochemical (IHC) Studies of Proliferative Activity of RCC

3.1 Antibodies Used

Ki 67

Monoclonal mouse anti-human Ki-67 antigen, Clone: MIB 1 (08-0156 ZYMED LABORATORIES, INC.)

This antibody reacts with a nuclear antigen expressed on all human proliferating cells. It recognizes all stages of the cell cycle, including late G_1, S, M, and G_2 phases, but not in G_0 phase.

$p27^{kip1}$

Monoclonal mouse anti-human Kip 1, Clone 57 (K25020 Transduction Laboratories)

3.2 Other Reagents

3.2.1 Normal Rabbit Serum (X902)

(DAKO Corporation, Carpinteria, California, USA)

Working solution: 5% normal rabbit serum in 0.05 M TBS pH 7.6

3.2.2 Secondary Antibody:

Biotinylated Rabbit Anti-mouse Immunoglobulins (E354)

(DAKO Corporation, Carpinteria, California, USA)

Working solution: 0.5% biotinylated rabbit anti-mouse immunoglobulins in 0.05 M TBS pH 7.6

3.2.3 Avidin/Biotin Complex/HRP (K355)

(DAKO Corporation, Carpinteria, California, USA)

Working solution:

A: Avidin solution

B: Biotinylated horseradish peroxidase solution

Reagent A and B were mixed in 0.05 M TBS to a final concentration of 1%. The mixture should be prepared 30 minutes before use.

3.2.4 DAB Solution

3,3'-Diaminobenzidine tetrahydrochloride (DAB)

(Sigma Chemical Company, St. Louis, M. O., USA)

Stock solution: DAB 1.25 g was dissolved in 0.05 M TBS pH 7.6.

The stock solution was aliquoted into one milliliter per tube, store at -20^{0}C.

Working solution:	0.05 M TBS pH 7.6	49 ml
	30% H_2O_2	50 µl
	DAB stock	1 ml

The working solution should be prepared just before use.

3.2.5 Buffers

3.2.5.1· Tris Buffer Saline (TBS)

Trizma base Tris [Hydroxymethyl] aminomethane

(Sigma Chemical Company, St. Louis, M. O., USA)

Stock solution:	Tris	242 g
	NaCl	360 g
	Conc. HCl	130 ml
	Add distilled water to	4 L

Adjust the pH of the solution to 7.6 using NaOH or HCl.

Working solution: (0.05 M Tris/HCl, 0.1 M NaCl, pH 7.6)

Stock solution	200 ml
Distilled water	1800 ml

Mixed and filtered before use.

3.2.5.2 Citrate Buffer (0.1 M, pH 6.0)

Stock solution:	Citric acid monohydrate	2.1 g
	2 M NaOH	13 ml
	Add distilled water to	1 L

Adjust pH to 6.0.

Working solution:

Stock solution	30 ml
Distilled water	270 ml

Mixed thoroughly.

3.3 Unmasking of Antigens

For the best results, we used combination of enzyme digestion and Microwave retrieval.

Antigen Retrieval Procedure

1. All 4-μm sections were dewaxed in three changes of xylene and followed two changes of absolute ethanol, and further rehydrated in a series of graded alcohols and rinsed well with distilled water.
2. Digest with 0.01% Trypsin solution for 20 minutes at room temperature.
3. Wash in tap water and rinse well with distilled water.
4. Immerse to a plastic slide box containing 10 mM citrate buffer (pH 6.0) and heated in a MW oven with high power until boiling. Change to median-low power, keep boiling for 6 minutes.
5. Leave the sections at room temperature in the buffer for 20-30 minutes to cool down.
6. Wash with distilled water.
7. Proceed to immunostaining.

3.4 ABC Method for Monoclonal Antibodies with Avidin/Biotin Blocking

ABC (Avidin-Biotin-peroxidase Complex) method (Hsu, Raine and Fanger, 1981) is a three-step immunoperoxidase method that utilizes the high affinity of avidin for biotin. Certain tissues, especially liver, kidney and spleen, are rich in biotin. This may result in non-specific binding of streptavidin to endogenous biotin or to biotin-binding proteins

when using the streptavidin immunoenzyme method (Bussolati and Gugliotta, 1983). Endogenous biotin can be blocked by incubation with avidin followed by biotin. Pretreatment of tissue with the Avidin/Biotin Kit (BioGenex) will help eliminate the problem that can block the endogenous biotin, biotin receptors, or avidin binding sites present in the section.

Endogenous peroxidase which produces non-specific or false positive staining, for example, presented in erythrocytes, can be inactivated by hydrogen peroxide prior to immunostaining.

Protocol of ABC Method with avidin/biotin blocking

1. Quench endogenous peroxidase by incubation of sections in 0.03% hydrogen peroxide in distilled water for 20 minutes at room temperature.
2. Wash the sections with three changes of 0.05M Tris buffer saline (TBS) pH 7.6.
3. Incubate in 5 % normal rabbit serum (DAKO) in TBS for 10 minutes at room temperature.
4. Rinse briefly with TBS.
5. Complete Avidin-Biotin blocking with Avidin/biotin Blocking Kit (BioGenex) (step 6-8).
6. Apply Avidin Blocking Reagent for 20 minutes at room temperature.
7. Rinse with TBS.
8. Apply Biotin Blocking Reagent for 20 minutes at room temperature.
9. Rinse with three changes of TBS for 10 minutes.
10. Incubate in primary antibodies at room temperature overnight.
11. Rinse with three changes of TBS for 10 minutes.
12. Incubate in secondary antibody, biotinylated rabbit anti-mouse (dilution 1:200, Dako) for 45 minutes at room temperature.
13. Rinse with three changes of TBS for 10 minutes.
14. Incubate in avidin-biotinylated peroxidase complex (dilution 1:100, Dako) for 45 minutes at room temperature.

15. Rinse with three changes of TBS for 10 minutes.
16. Develop using 3,3-diaminobenzidine tetrahydrochloride and counterstain with methyl green.

Table 4.3 Summary of the Antibodies Used in the Study

Antibodies	Antigen retrieval		Dilution	Incubation time	Method
	MW	*Trypsin*			
MIB-1	4+6*	0.01%, 20 min	Prediluted, ready to use	overnight, room temperature	ABC
$p27^{kip1}$	4+6*	0.01%, 20 min	1:1000	overnight, room temperature	ABC

* Four minutes' high power followed by six minutes' median-low power.

3.5 Interpretation and Scoring of Immunostaining

Visual evaluation of immunostaining was performed under light microscope. Both MIB-1 and $p27^{kip1}$ staining showed nuclear localization. Nuclei were considered positive if any nuclear staining was present, regardless of staining intensity. In each case, the highest expression areas were selected for assessment (deRiese *et al.*, 1991; 1993). The percentage of positive cells was then assessed by scoring ten high power fields (× 400) in selected areas. The scores were determined according to the average of these ten high power fields. It was scored between 1 to 10 according to the criteria listed in Table 4.4. The assessments were done by two investigators without prior knowledge of the other clinical-pathological data. Discordant cases required re-examination under microscope.

4. Clinical Data Retrieval

Clinical data were retrieved from the patient's medical record. The parameters include age, sex, clinical stage, date of surgery, date of recurrence, distant metastasis, death and last follow up.

Table 4.4 Interpretation of Ki 67 and $p27^{kip1}$ immunostaining

Score	Percentage of positive cells
1+	0 to ≤ 10%
2+	>10% to ≤ 20%
3+	>20% to ≤ 30%
4+	>30% to ≤ 40%
5+	>40% to ≤ 50%
6+	>50% to ≤ 60%
7+	>60% to ≤ 70%
8+	>70% to ≤ 80%
9+	>80% to ≤ 90%
10+	>90% to ≤ 100%

5. Statistical Analysis

Clinical and pathological findings were subjected to statistical analysis. Comparisons of the data were performed by chi-square test and Spearman's correlation was calculated. Survival functions were estimated for each of the variables by the Kaplan-Meier method using log rank test. Multivariate analysis was performed using Cox regression.

All calculations were performed using a commercial available statistical software package (SPSS, version 7.5). A critical significance level of 0.05 was chosen.

Chapter 5

Results

In this chapter, the results of our studies are reported in detail. Clinicopathological data will be present first, followed by the results of DNA ploidy analysis under three different methods and immunohistochemical evaluation of proliferation activity using two cell cycle-related antibodies, and finally, the statistical analysis.

1. Clinical Information

The clinical data of the selected patients are summarized in Table 5.1. The average age of the patients at the time of diagnosis was 59.1 years (25-83 years). Male to female ratio was 1.5 to 1 (28:18). The follow-up data were drawn from hospital charts, which were available in 32 patients. The median follow up period was 53 months (3-123 months). Nine patients developed distant metastasis. Two patients died with tumor or tumor-related diseases and two died with other causes.

2. Pathological Features

2.1 Histological Subtypes

H&E stained sections were reviewed by pathologist to verify the diagnosis and selected appropriate areas for analysis. The most common histological subtypes of RCC are clear cell type and granular cell type, or mix of these two types. Other cell types include chromophil, sarcomatoid, chromophobe, and collecting (Bellini) duct carcinoma.

The histological classification of our tumor samples was as follows: 23 clear cell type, 7 granular type, 4 mixed clear and granular, 3 chromophil, 2 sarcomatoid, 1 chromophobe, 1 collecting duct carcinoma and 2 multilocular cystic renal cell carcinoma. 3 oncocytomas were also included in our study.

2.2 Nuclear Grading

The nuclear grading were assigned according to Fuhrman's nuclear grading system which has been reviewed in chapter 2. In our series, thirteen cases were nuclear grade I, fourteen were grade II, eleven cases were grade III, and eight cases were grade IV. For details, please refer to Table 5.2.

2.3 Clinical Stage

The classification of clinical stage was based on Robson's staging system. Twenty-eight patients were classified stage I, six were stage II, eight were stage III, and four patients were stage IV. Detailed information was listed in Table 5.2.

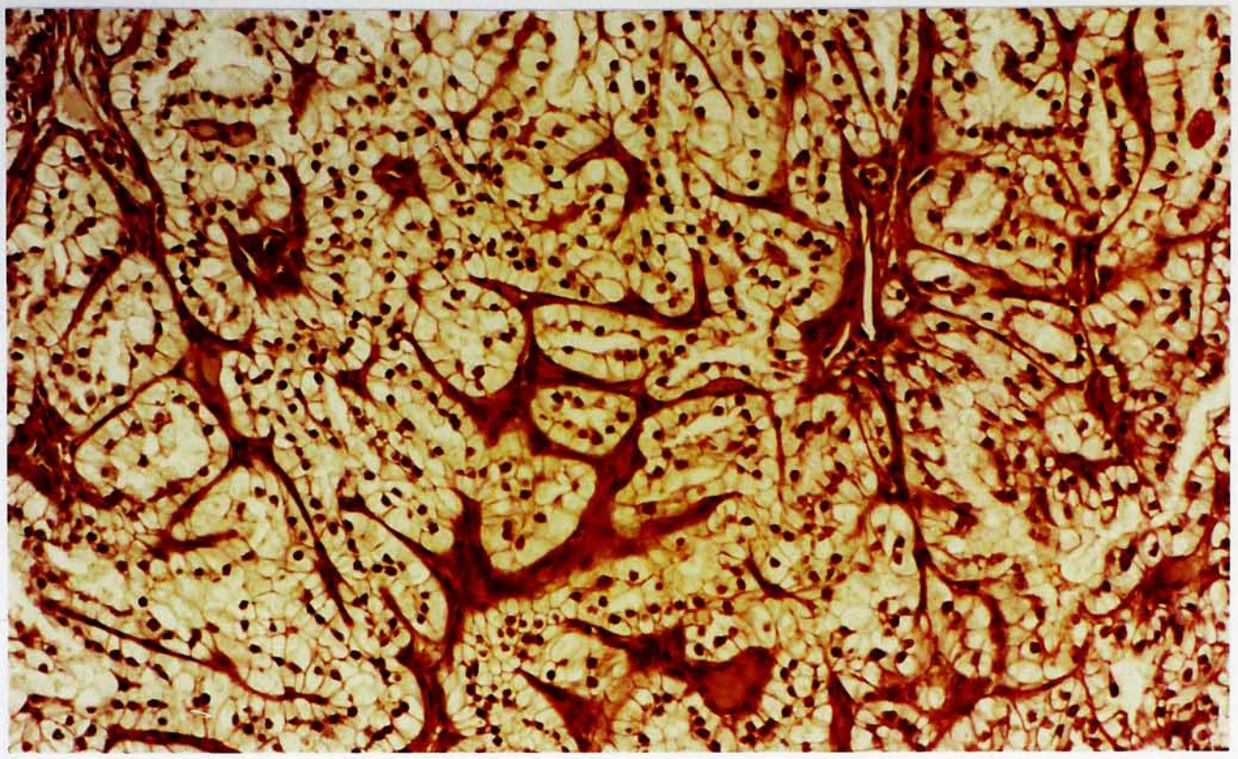

A

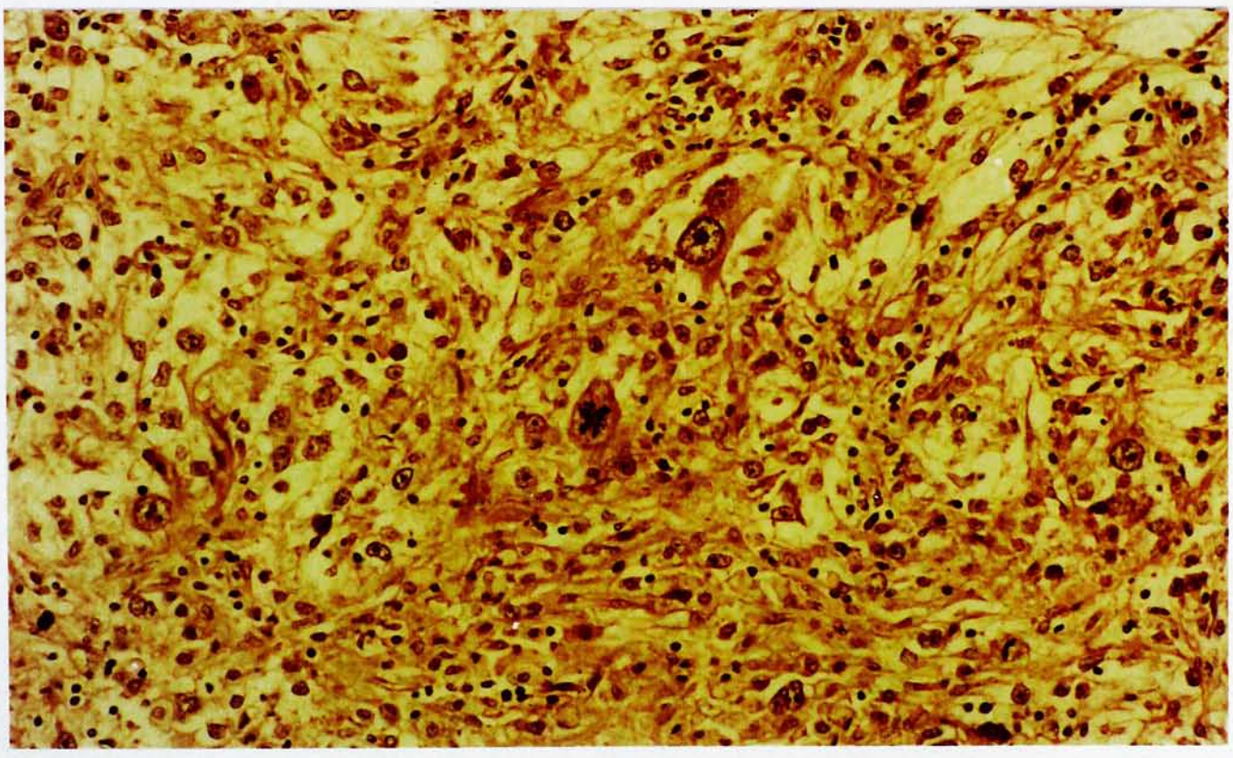

B

Figure 5.1

Panel A. Clear cell type renal cell carcinoma (Fuhrman's grade I). The tumor consists of clusters of clear cells separated by fine vascular septa. The cells have large amount of clear cytoplasm. The nuclei are small, round, uniform and absence of nucleoli (Case 12, HE ×100).

Panel B. Clear cell type renal cell carcinoma (Fuhrman's grade IV). The nuclei are much larger, vesicular and pleomorphic with prominent nucleoli. Mitoses is frequently seen (Case 10, HE ×200).

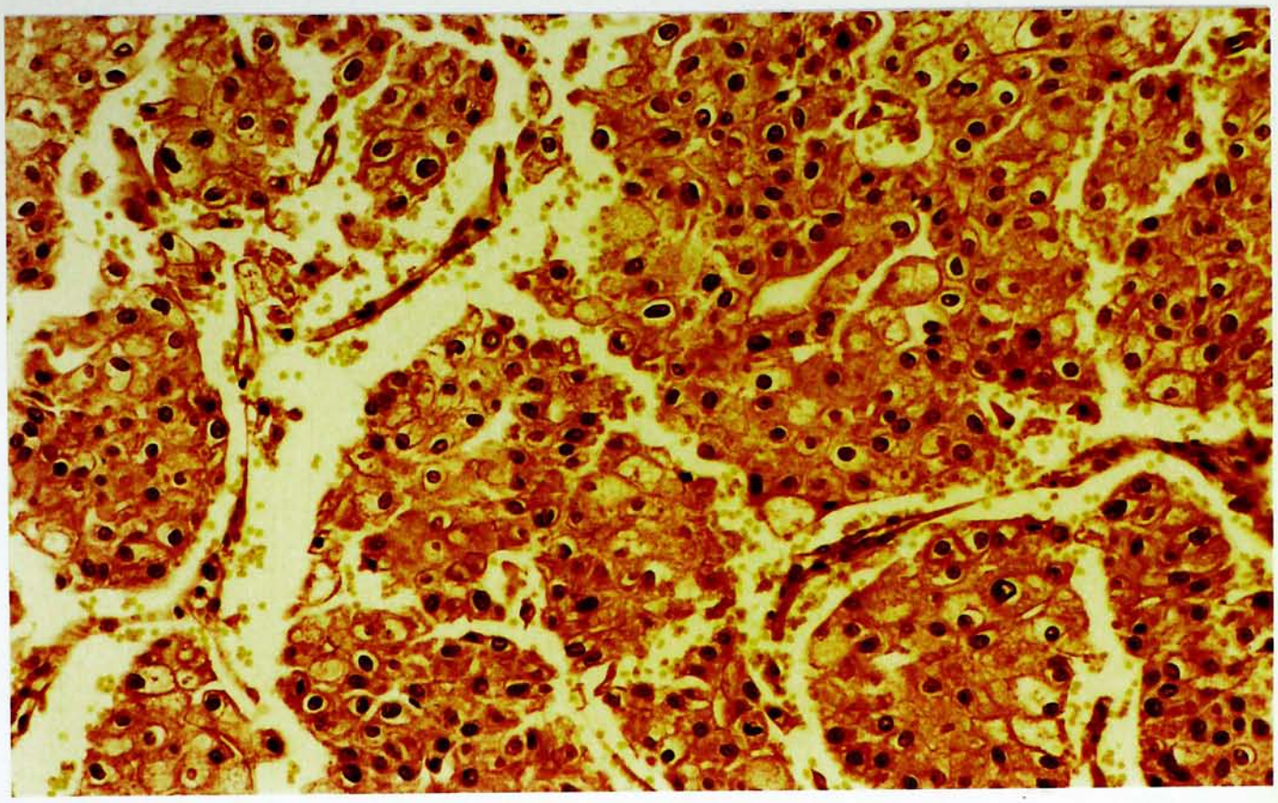

Figure 5.2 Granular cell type renal cell carcinoma (Fuhrman's grade II). Granular cell RCCs are characterized by their eosinophilic granular cytoplasm. The nuclei are larger than grade I nuclei with occasionally tiny nucleoli (Case 18, HE ×200).

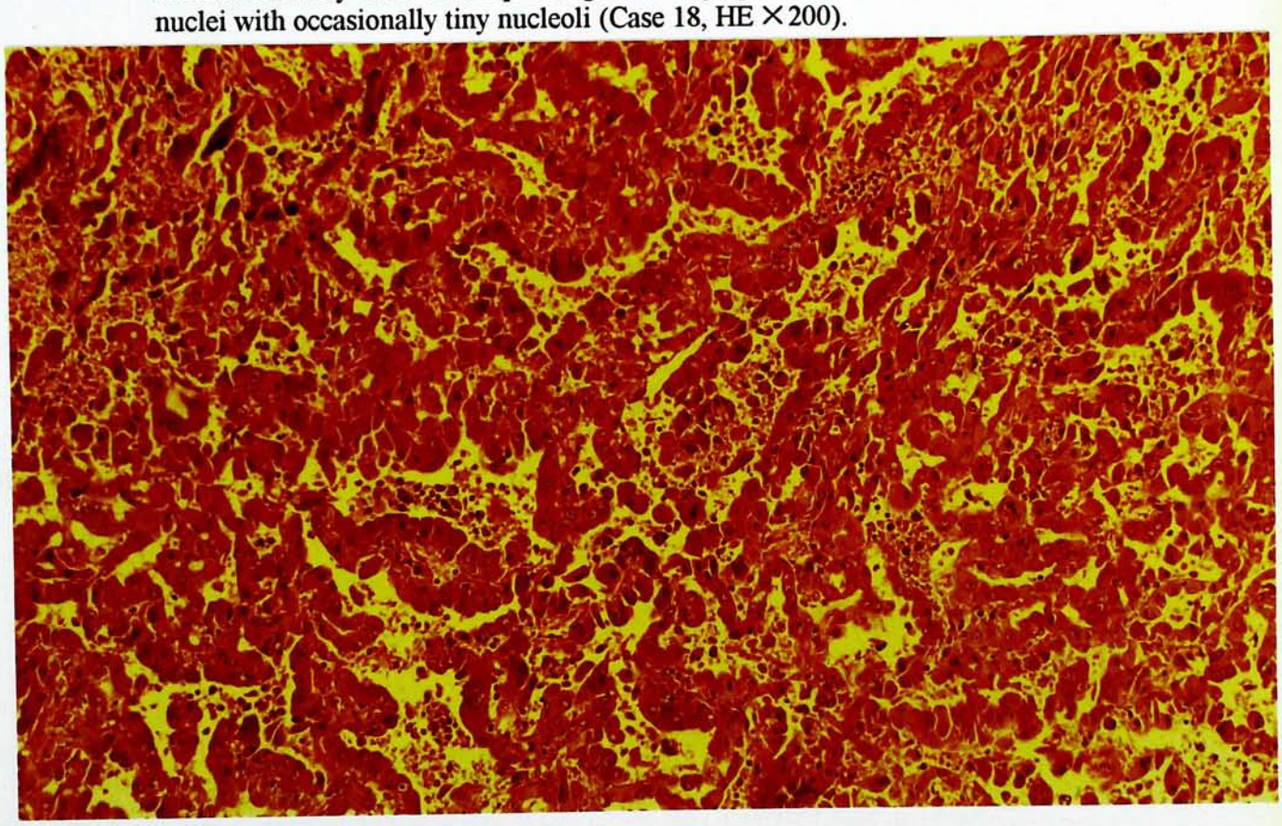

Figure 5.3 Chromophil cell carcinoma (Fuhrman's grade III). The tumor is composed of cells arranged mainly in thin papillae. The tumor cells exhibit moderate amount of eosinophilic cytoplasm. They were classified as tubular-papillary type previously (Case 37, HE ×200).

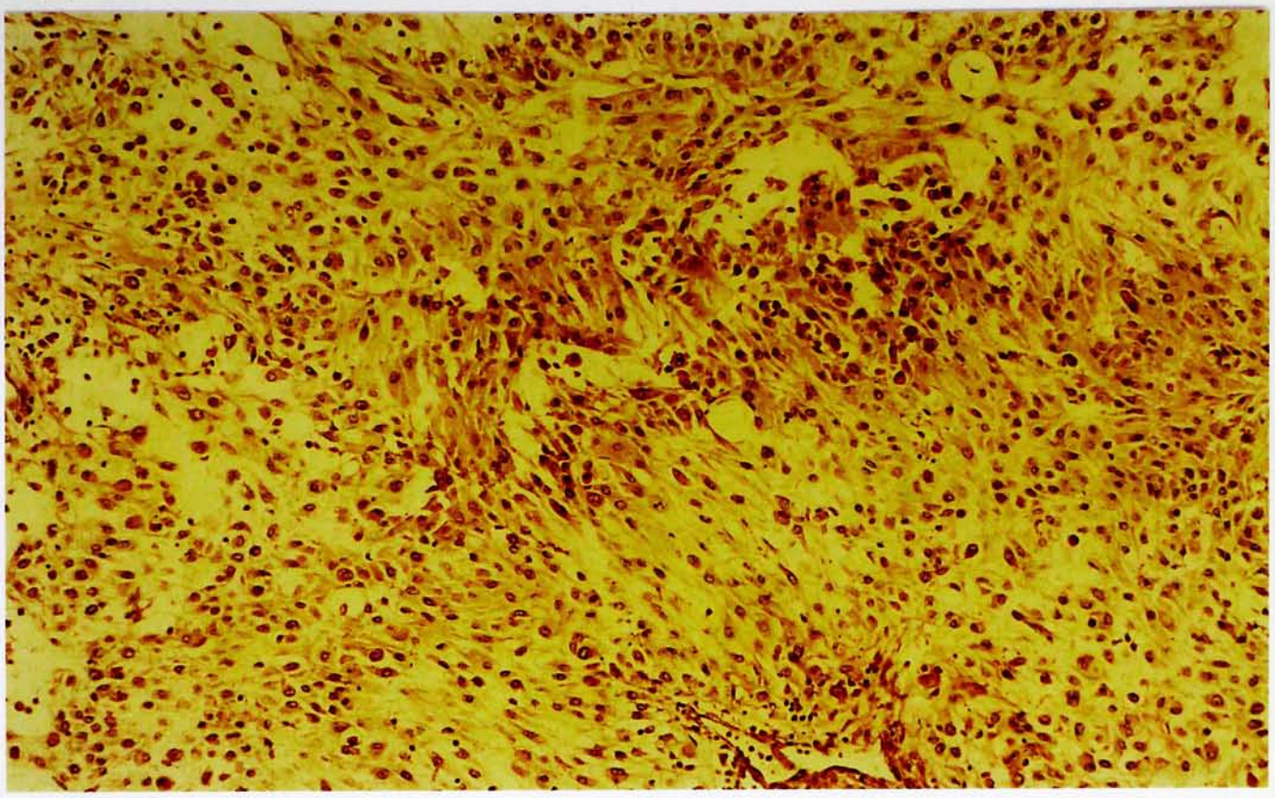

Figure 5.4 Sarcomatoid renal cell carcinoma (Fuhrman's grade IV). The tumor is composed of spindle-shaped cells arranged in fascicles, sheets, and whorls in the fibromyxoid stroma (Case 28, HE ×100).

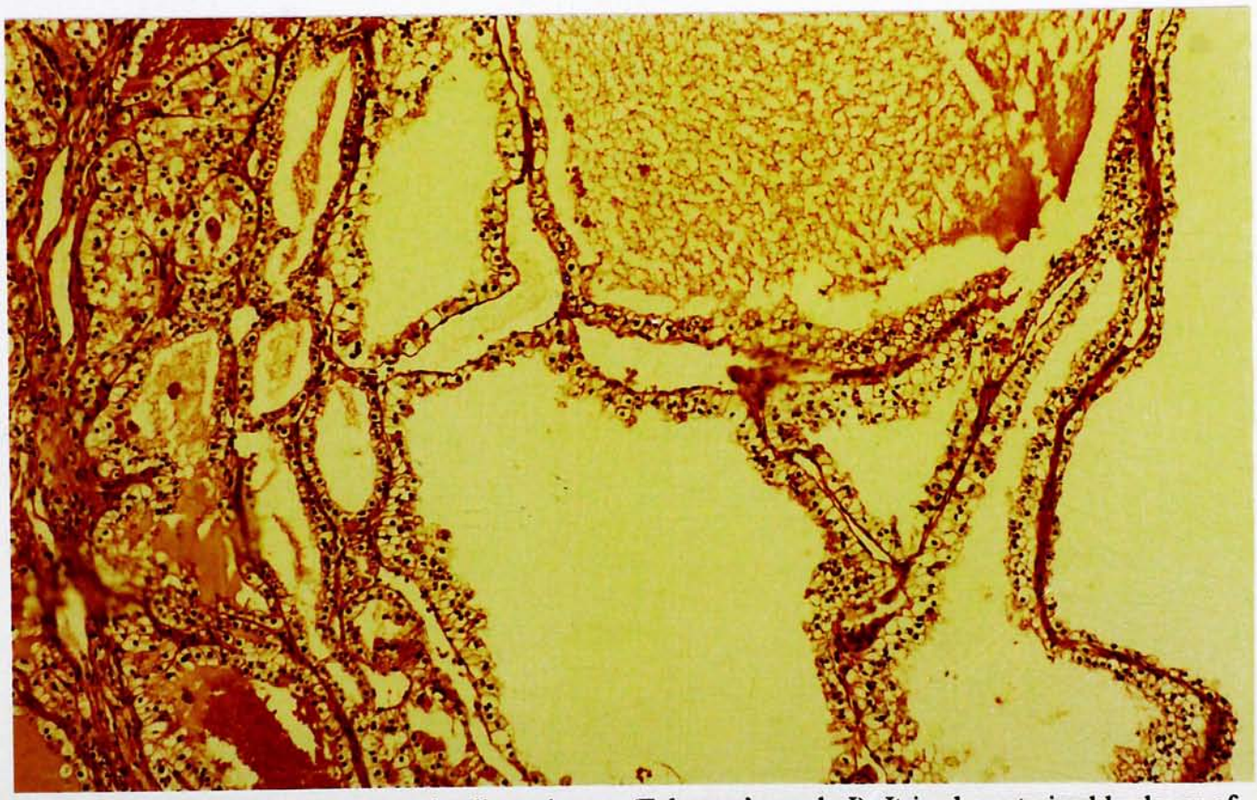

Figure 5.5 Multilocular cystic renal cell carcinoma (Fuhrman's grade I). It is characterized by layer of clear cell carcinoma cells lining the fibrous septa. The nuclei of carcinoma cells are small, dark stained and lack of nucleoli (Case 4, HE×40).

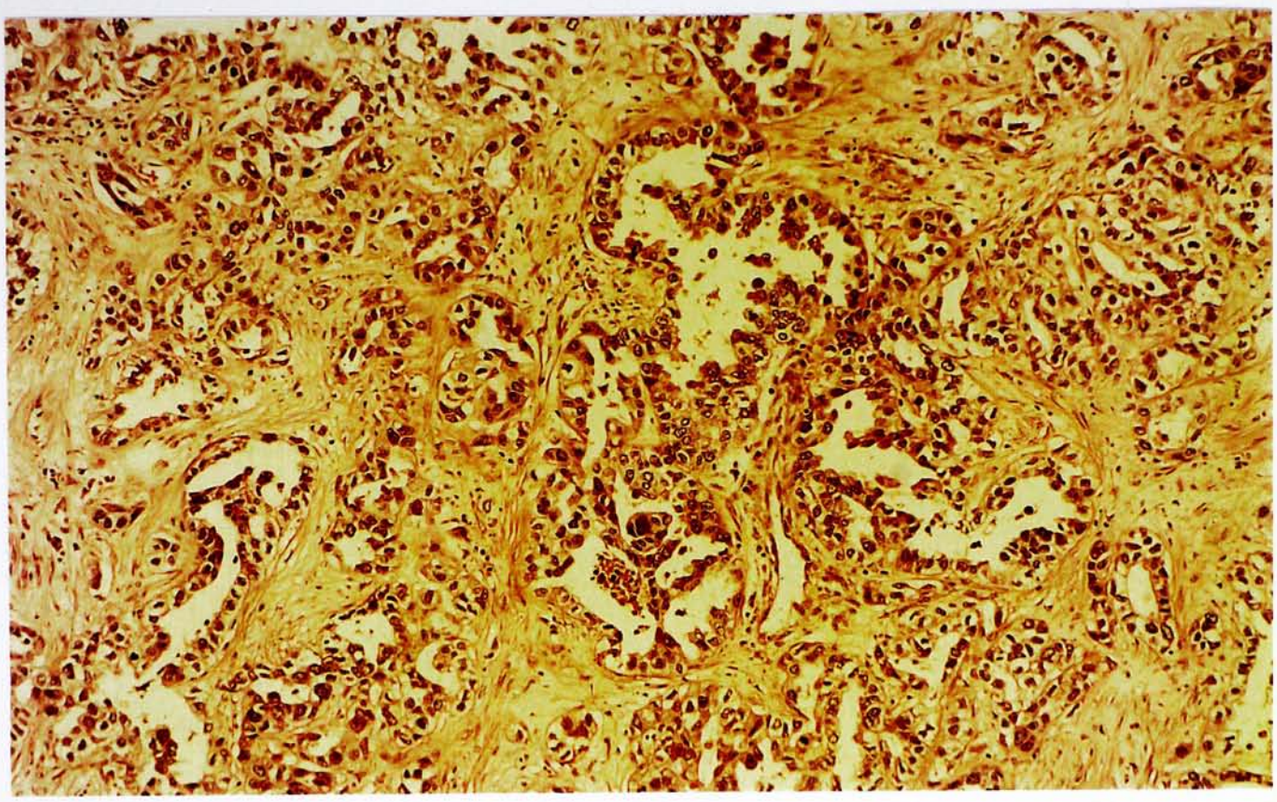

Figure 5.6 Collecting (Bellini) duct carcinoma (Fuhrman's grade IV). It is arranged in irregular tubulo-granular pattern and invade the desmoplastic stroma (Case 21, HE ×200).

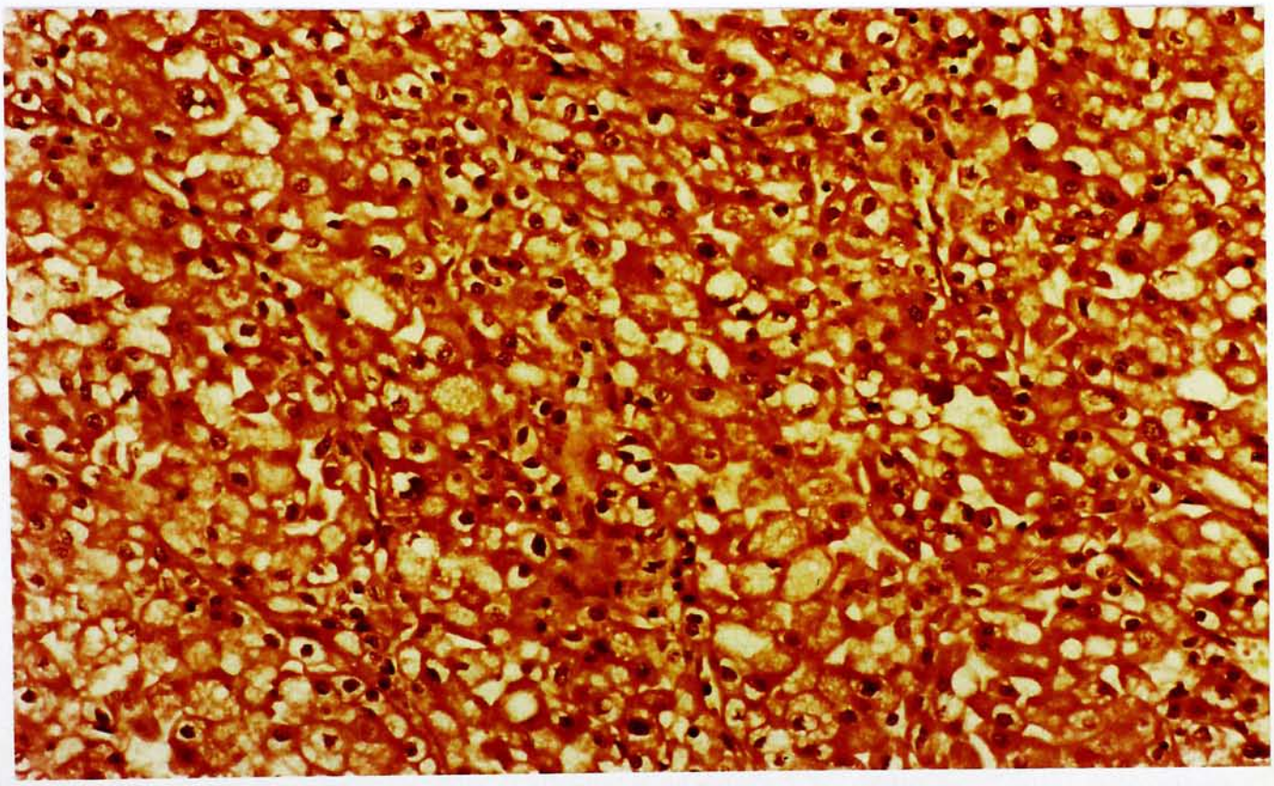

Figure 5.7 Chromophobe cell carcinoma (Fuhrman's grade II). It composes of sheets of tumor cells with fine granular and flocculent cytoplasm (Case 31, HE ×200).

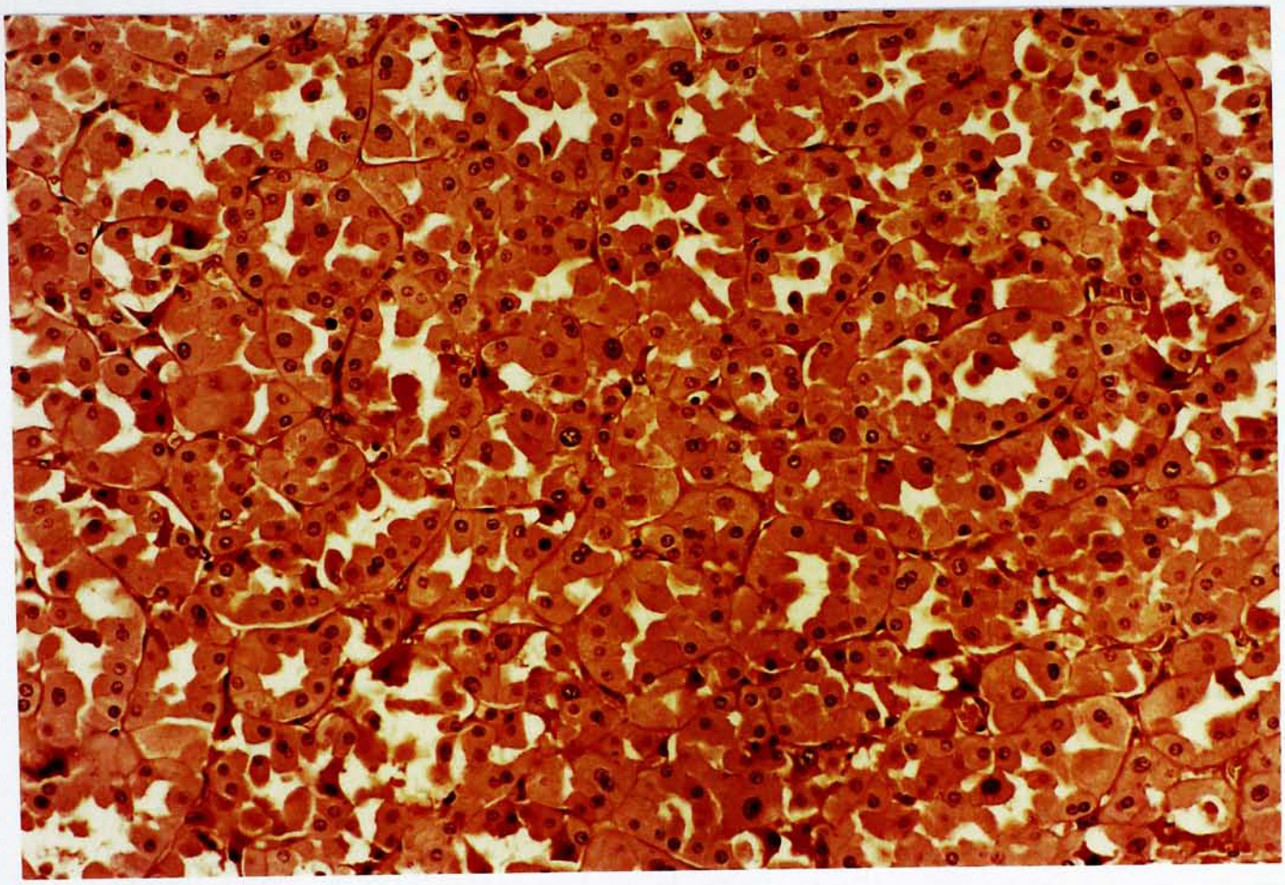

Figure 5.8 Oncocytoma. Oncocytes are typified by a large amount of dense eosinophilic cytoplasm. The tumor cells are arranged in closely packed clusters (Case 19, HE ×200).

Table 5.1 Clinical information of 46 patients

Case No.	Age	Sex	Event 1	Event 2	Event-free period (months)	Follow-up period (months)	Die
1	43	F					
2	46	M			29.4	29.4	
3	67	F			10.9	10.9	
4	54	M			27.6	27.6	
5	61	F			43.9	43.9	
6	78	M			46.2	46.2	
7	62	M					
8	62	M			30.6	50.9	
9	53	F			72.6	72.6	
10	70	M	M-GIB	M-Spinal	1.0	13.9	DWD
11	67	M	M-Colon	M-Liver	24.1	61.5	DWD
12	44	F			53.8	53.8	
13	71	M	M-Lung	M-Skin	0.97	22.3	
14	69	F			29.7	29.7	
15	76	M	M-Lung		57.1	66.2	
16	46	M			89.7	89.7	
17	40	M			78.1	78.1	
18	40	M	M-Lung		26.1	40.3	
19	59	M			95.7	95.7	
20	66	M			101.4	101.4	
21	67	F					
22	67	M					
23	61	M					
24	68	F					
25	65	F					
26	69	F			123.9	123.9	
27	61	M			106.5	106.5	
28	77	F					
29		M					
30	57	M					
31	33	F			20.1	20.1	
32	59	M	M-Liver	M-Colon	0	5.2	
33	69	M					
34	46	M			34.8	34.8	
35	63	M					DOD
36	34	F			41.8	41.8	
37	25	M			54.1	54.1	
38	59	M					
39	52	F			32.1	32.1	
40	53	M	M-Lung		0	4	
41	64	F	M-Lung		3.6	3.6	
42	58	M					
43	59	M			103.1	103.1	
44	56	F					
45	81	F			115.7	115.7	
46	83	F	M-Bone		49.1	77.6	DWD

M- : Metastasize to
DWD : Die With Disease
DOD : Die of Other Disease

Table 5.2 Pathological features of 46 cases

Case No.	Stage	Grade (Fuhrman)	Histologic type
1	I	I	multilocular cystic RCC
2	I	II	Clear cell
3	II	II	Clear cell
4	I	I	Multilocular cystic RCC
5	I	III	Clear cell and granular cell
6	IV	II	Clear cell
7	II	IV	Granular cell
8	II	II	Clear cell
9	II	III	Clear cell
10	IV	IV	Clear cell
11	III	IV	Granular cell
12	I	I	Clear cell
13	III	II	Clear cell
14	I	I	Clear cell
15	II	II	Clear cell
16	I	III	Granular cell
17	I	III	Clear cell
18	I	II	Granular cell
19	I	II	Oncocytoma
20	I	III	Chromophil
21	III	IV	Collecting duct carcinoma
22	I	III	Granular cell
23	I	II	Clear cell
24	I	II	Granular cell
25	III	IV	Clear cell and granular cell
26	I	II	Clear cell
27	I	I	Clear cell
28	III	IV	Sarcomatoid
29	I	IV	Sarcomatoid
30	I	I	Chromophil
31	I	II	Chromophobe
32	IV	III	Clear cell
33	I	I	Clear cell
34	I	I	Oncocytoma
35	I	III	Clear cell
36	III	I	Clear cell
37	I	III	Chromophil
38	I	I	Oncocytoma
39	I	I	Clear cell
40	IV	III	Granular cell
41	III	II	Clear and granular cell
42	II	IV	Clear and granular cell
43	I	II	Clear cell
44	I	I	Clear cell
45	I	I	Clear cell
46	III	III	Clear cell

3. DNA Ploidy Analysis

DNA ploidy analysis was performed using three different methods. In all cases where the initial CV was high or the results among methods were discordant, the whole process was repeated. The results will be shown separately in three sections.

3.1 By Flow Cytometry

Mean Coefficient of variation (CV) of the G_0G_1 peaks in our samples was 5.1±1.7% (range 1 - 9.1%). CVs above 10% were regarded as unacceptable.

COULTER INDEX DNA Controls were run along with each batch of samples. The mean values and ranges of both normal and abnormal control (Table 5.3) were within the expected ranges provided by the manufacturer, which has been described in chapter 4 (Table 4.2).

Table 5.3 Assay mean values and ranges of INDEX DNA controls

Parameter	Normal		Abnormal			
	Diploid Cycle		Diploid Cycle		Aneuploid Cycle	
	Mean	Range	Mean	Range	Mean	Range
CV G1	3.8%	3.3-4.2%	3.5%	2.9-4.6%	4.9%	4.5-5.7%
% Total			38.8%	28.6-48.2%	61.2%	51.8-71.4%
DNA Index					1.51	1.487-1.519

Figure 5.9 shows FCM histograms of normal control and abnormal control.

Tumor tissue for FCM analysis was derived from paraffin blocks in 46 cases and totally 92 samples were analyzed (2 samples per case). Evaluable histograms were obtained in 45 cases (90 samples). One case (case 36) was considered uninterpretable by FCM because of high CVs (despite repeats).

DNA content was homogeneously diploid in 30 tumors (67%, 30/45). Another 15 (33%,15/45) tumors had nondiploid DNA content, of which 13 (29%, 13/45) were homogeneously aneuploid, the other two contained heterogeneous DNA content. One case (2%, 1/45) was composed of both diploid and aneuploid, the other (2%, 1/45) was composed of diploid and tetraploid populations.

The DNA ploidy profiles of 46 cases measured by flow cytometry are shown in Table 5.4. Typical FCM histograms were shown in Figures 5.10 - 5.11.

A

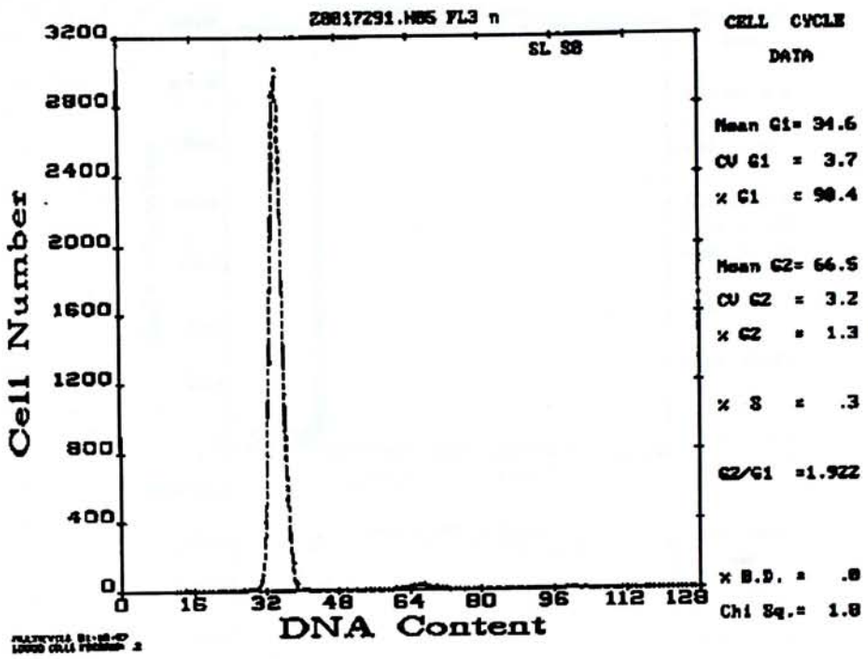

B

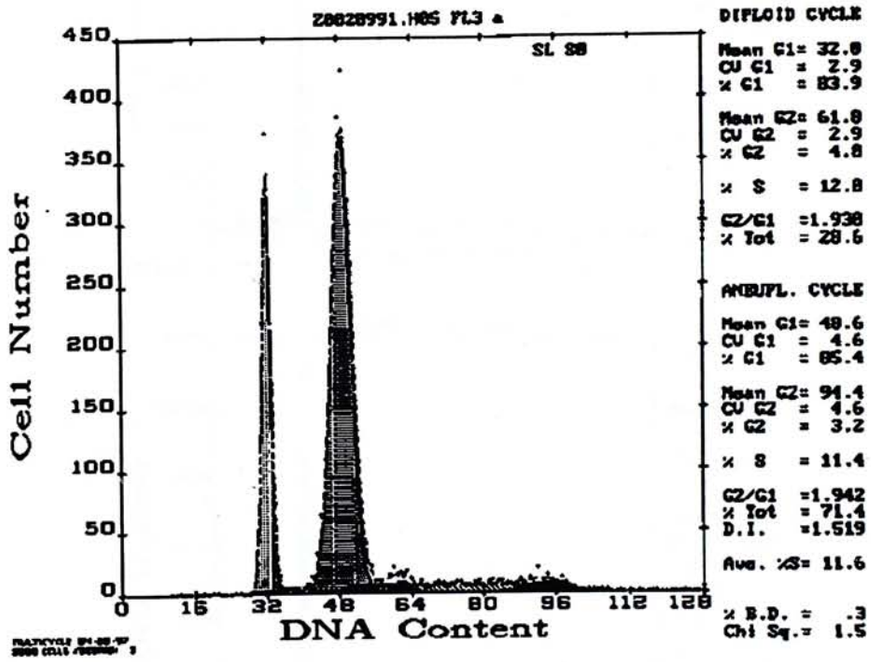

Figure 5.9 Flow cytometric histograms of DNA controls.
A: Normal control; B: Abnormal control.

A

B

C

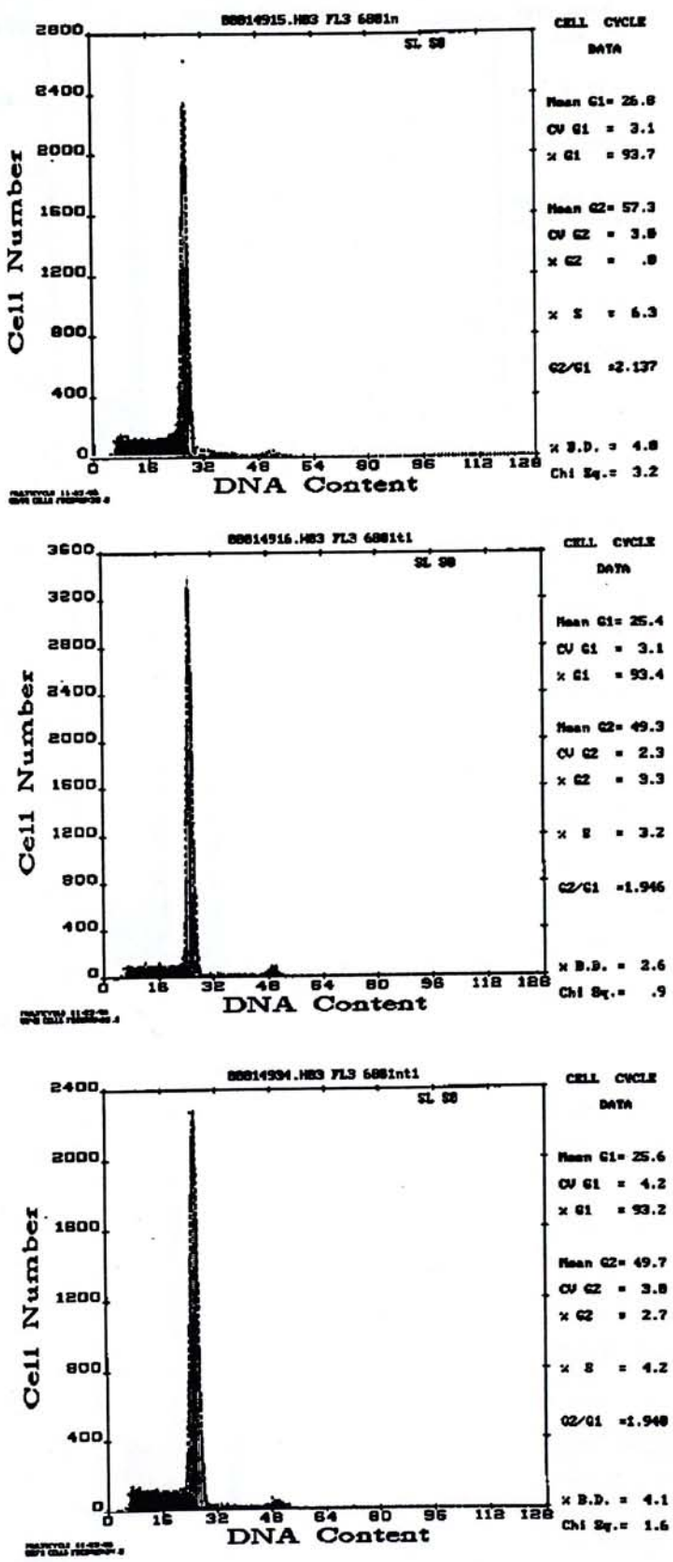

Figure 5.10 Flow cytometric histograms (case 6).
A: Normal kidney tissue; B: Tumor sample;
C: Mixure of normal control and tumor sample;
All three specimens showed diploid histograms.

A

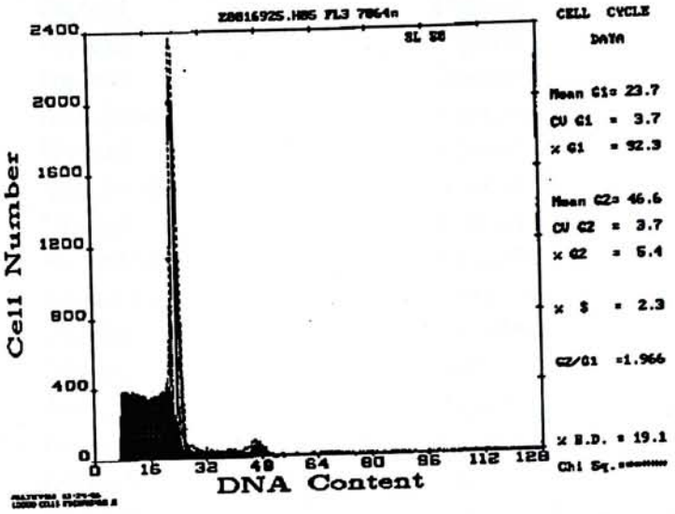

B

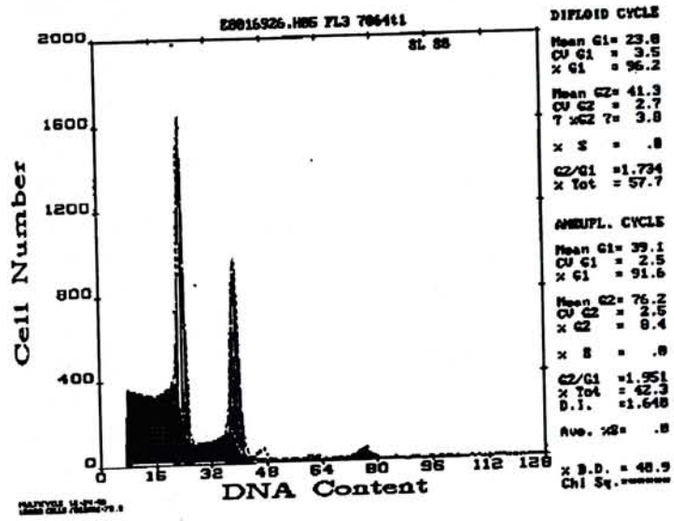

C

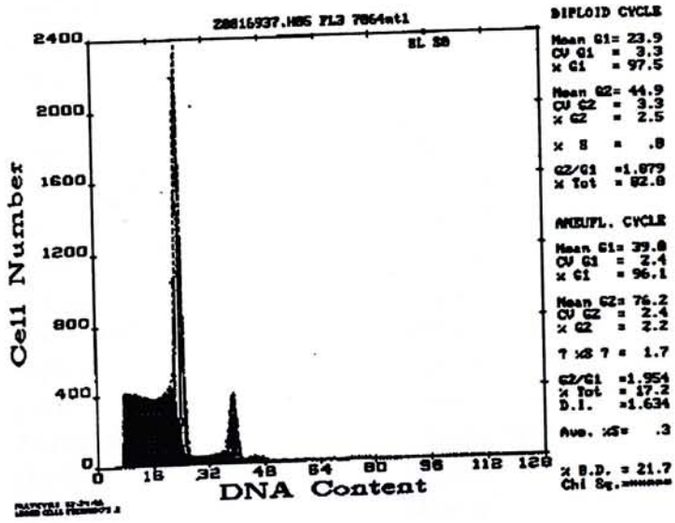

Figure 5.11 Flow cytometric histograms (case 22).
A: Normal kidney tissue showed a diploid histogram;
B: Tumor sample showed an aneuploid histogram;
C: When mixing tumor sample with normal control cells, the aneuploid peak decreased.

Table 5.4 DNA ploidy profiles measured by FCM

Case No.	*Tumor sample I*	*Tumor sample II*
1	Diploid	Diploid
2	Diploid	Diploid
3	Diploid	Diploid
4	Diploid	Diploid
5	Aneuploid	Aneuploid
6	Diploid	Diploid
7	Aneuploid	Aneuploid
8	Diploid	Diploid
9	Aneuploid	Aneuploid
10	Aneuploid	Aneuploid
11	Diploid	Diploid
12	Diploid	Diploid
13	Aneuploid	Aneuploid
14	Diploid	Diploid
15	Diploid	Diploid
16	Aneuploid	Aneuploid
17	Aneuploid	Diploid
18	Diploid	Diploid
19	Diploid	Diploid
20	Diploid	Diploid
21	Aneuploid	Aneuploid
22	Aneuploid	Aneuploid
23	Diploid	Diploid
24	Aneuploid	Aneuploid
25	Diploid	Diploid
26	Diploid	Diploid
27	Diploid	Diploid
28	Aneuploid	Aneuploid
29	Diploid	Diploid
30	Diploid	Diploid
31	Diploid	Diploid
32	Aneuploid	Aneuploid
33	Diploid	Diploid
34	Diploid	Diploid
35	Diploid	Diploid
36	Uninterpretable	Uninterpretable
37	Diploid	Diploid
38	Diploid	Diploid
39	Diploid	Diploid
40	Aneuploid	Aneuploid
41	Diploid	Diploid
42	Diploid	Diploid
43	Aneuploid	Aneuploid
44	Diploid	Diploid
45	Diploid	Diploid
46	Diploid	Tetraploid

3.2 By Static Image Cytometry Using Cytospin Preparations

All 46 cases were available for analysis. 37 out of 46 (80.4%) cases showed homogeneous DNA content. 21 (45.7%, 21/46) were homogeneous diploid and 15 (32.6%, 15/46) were aneuploid, and 1 (2.1%, 1/46) was tetraploid.

5 (10.9%, 5/46) cases contained both diploid and aneuploid populations. And 4 (8.7%) cases had both diploid and tetraploid stemlines.

The DNA ploidy profiles measured by ICM using cytospin preparations are shown in Table 5.5. Typical image cytometric histograms of DNA content analysis on cytospin preparations are shown in Figure 5.12 -5.14.

A

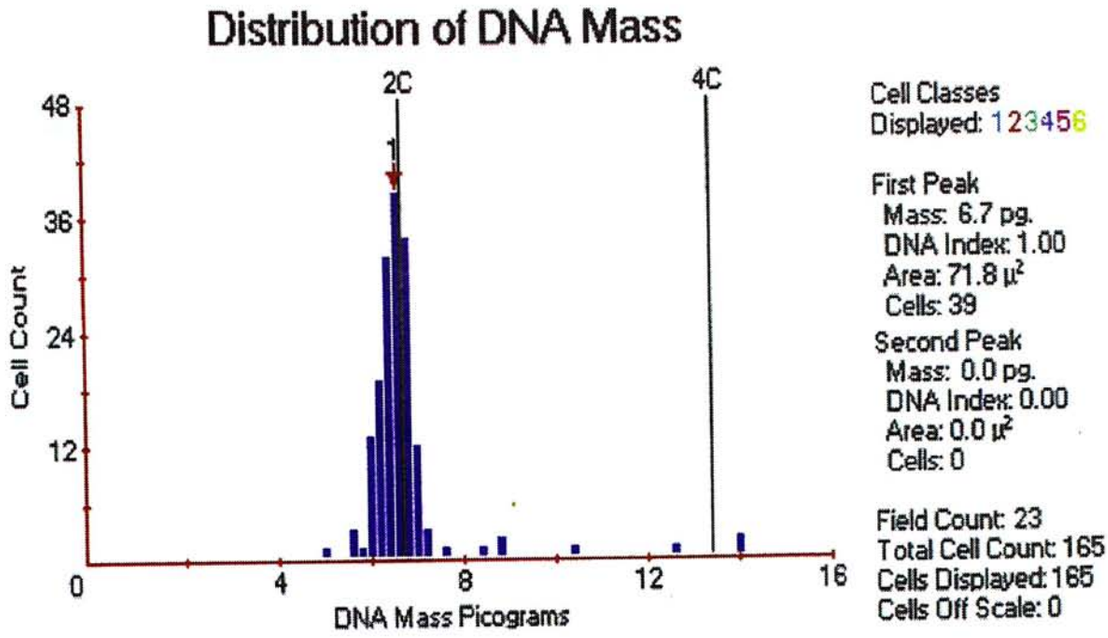

B

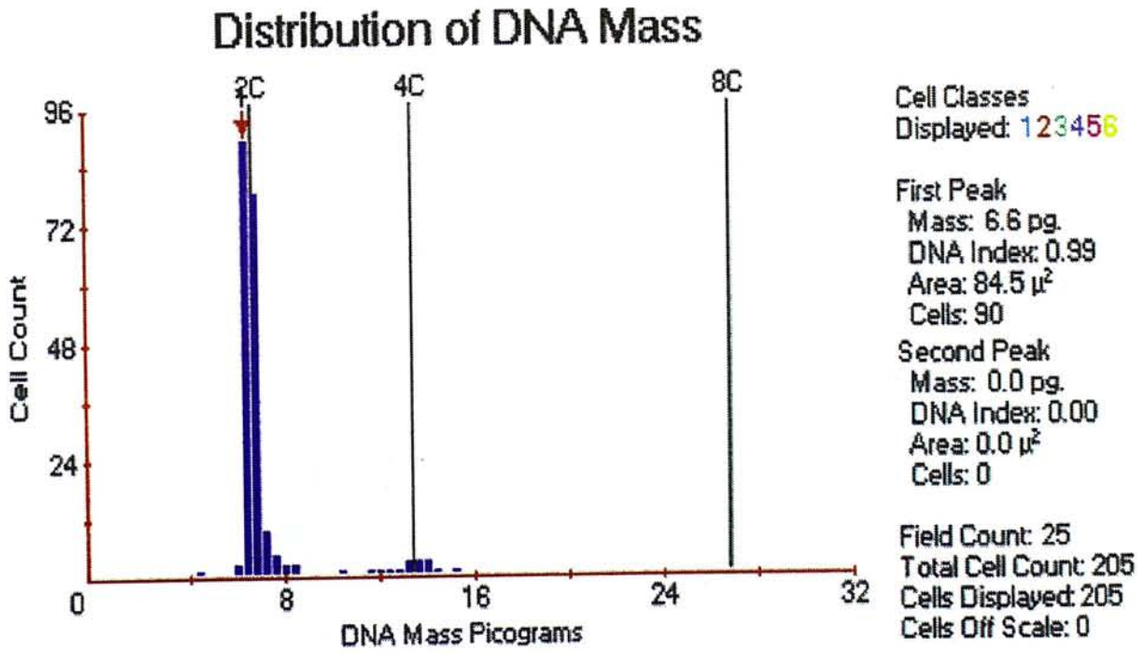

Figure 5.12 Case 1-I Image cytometric histograms (cytospin)
A: Normal control
B: Diploid RCC
(DNA index corrected according to the normal control)

A

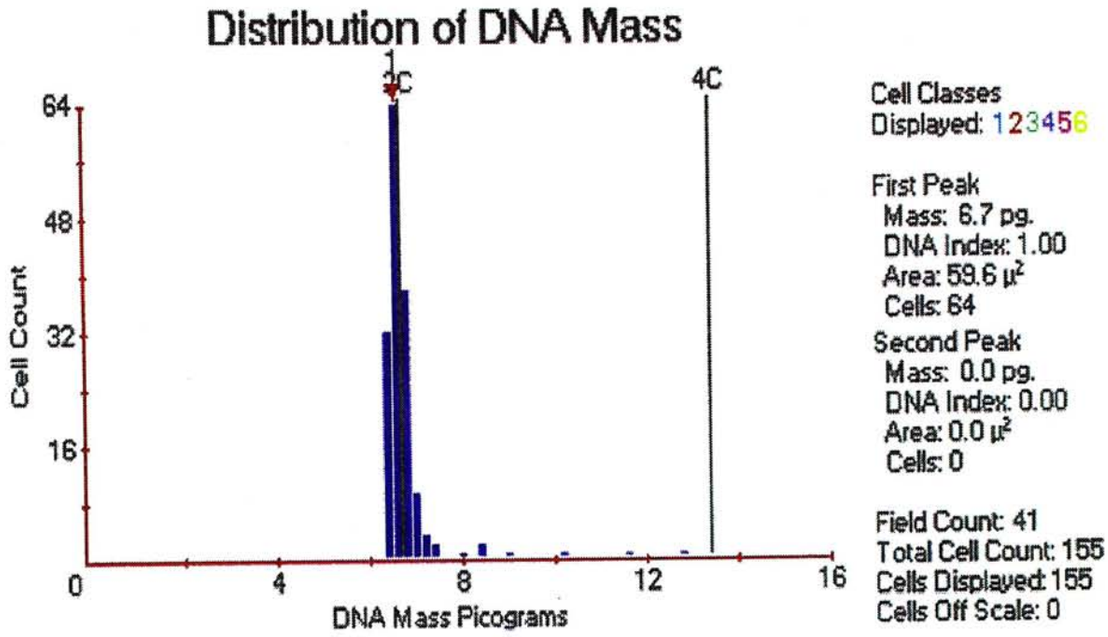

B

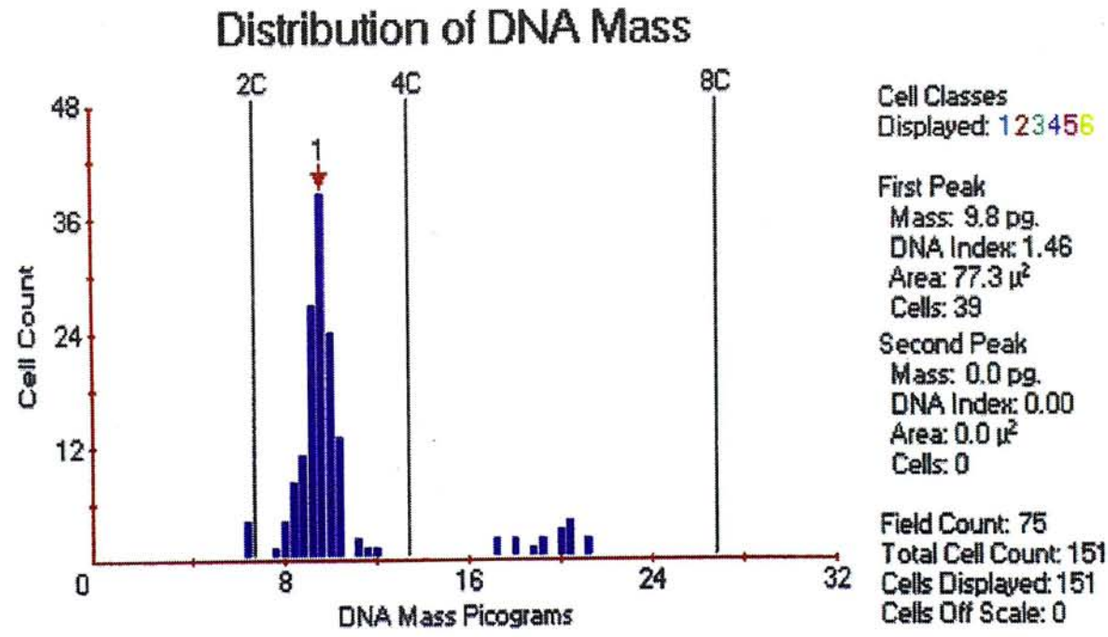

Figure 5.13 Case 5-I Image cytometric histograms (cytospin)
A: Normal kidney
B: Aneuploid RCC
(DNA index corrected according to the normal control)

A

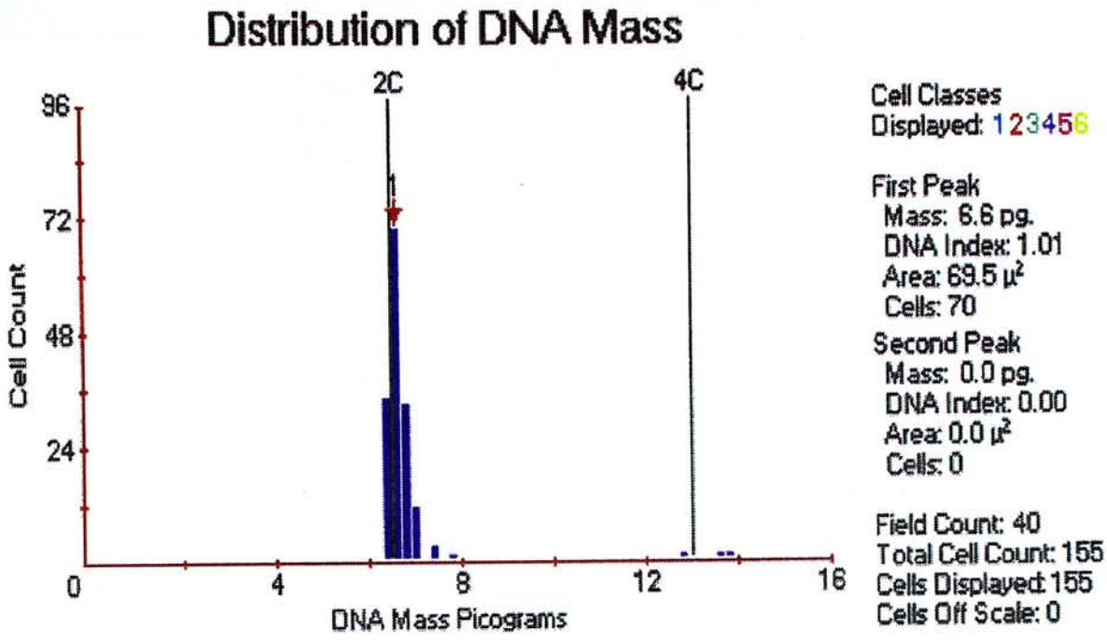

B

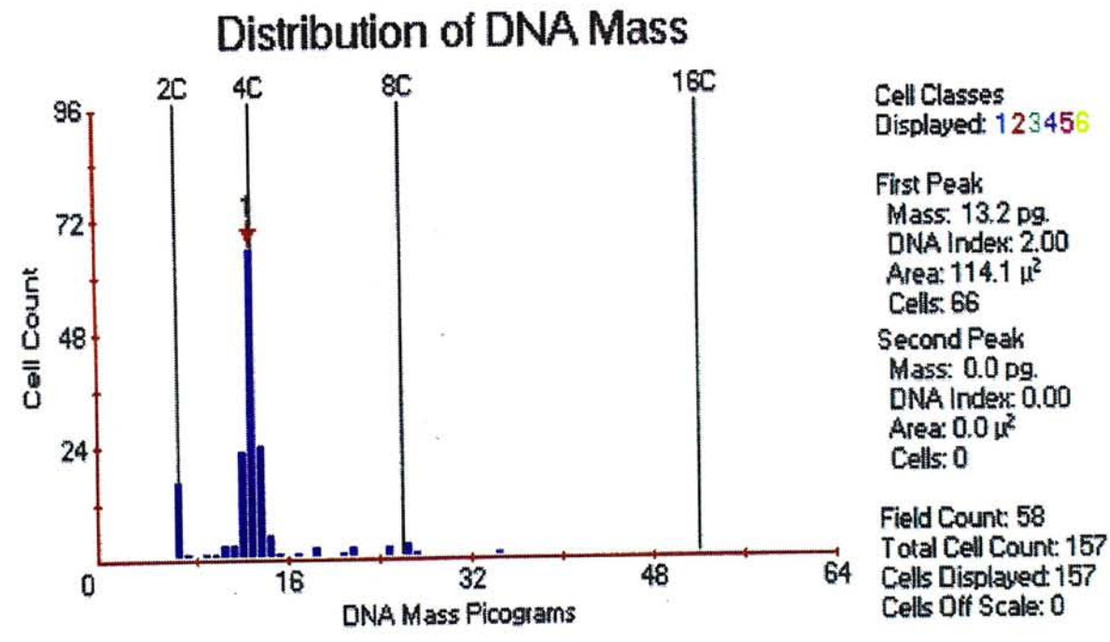

Figure 5.14 Case 20-I Image cytometric histograms (cytospin)
A: Normal kidney
B: Tetraploid RCC
(DNA index corrected according to the normal control)

Table 5.5 DNA ploidy profiles measured by ICM using cytospin preparations

Case No.	*Tumor sample I*	*Tumor sample II*
1	Diploid	Diploid
2	Diploid	Diploid
3	Diploid	Diploid
4	Diploid	Diploid
5	Aneuploid	Aneuploid
6	Diploid	Diploid
7	Aneuploid	Aneuploid
8	Diploid	Diploid
9	Diploid and Aneuploid	Aneuploid
10	Aneuploid	Aneuploid
11	Tetraploid	Tetraploid
12	Diploid	Diploid
13	Aneuploid	Aneuploid
14	Diploid	Diploid
15	Diploid	Diploid
16	Aneuploid	Aneuploid
17	Aneuploid	Diploid and Aneuploid
18	Diploid	Diploid
19	Diploid and Tetraploid	Diploid and Aneuploid
20	Diploid and Tetraploid	Diploid and Tetraploid
21	Aneuploid	Aneuploid
22	Aneuploid	Aneuploid
23	Aneuploid	Aneuploid
24	Aneuploid	Aneuploid
25	Aneuploid	Aneuploid
26	Diploid and Aneuploid	Aneuploid
27	Diploid	Diploid
28	Aneuploid	Aneuploid
29	Tetraploid	Diploid and Tetraploid
30	Diploid	Diploid
31	Diploid	Diploid
32	Aneuploid	Aneuploid
33	Diploid	Diploid
34	Diploid	Diploid
35	Diploid	Diploid and Aneuploid
36	Diploid	Diploid
37	Diploid	Diploid
38	Diploid	Diploid
39	Diploid	Diploid
40	Aneuploid	Aneuploid
41	Diploid	Diploid
42	Diploid	Diploid and Aneuploid
43	Aneuploid	Aneuploid
44	Aneuploid	Aneuploid
45	Diploid	Diploid
46	Diploid	Tetraploid

3.3 By Static Image Cytometry Using Tissue Sections

All 46 cases were available for analysis. 20 out of 46 (43.5%) cases had homogeneous diploid DNA content. 11 out of 46 (23.9%) cases had homogeneous aneuploid DNA content. Intratumoral heterogeneity was demonstrated in 15 (32.6%) cases.

The DNA ploidy profiles measured by ICM using tissue sections are shown in Table 5.6. Histograms are shown in Figure 5.15 - 5.17.

A

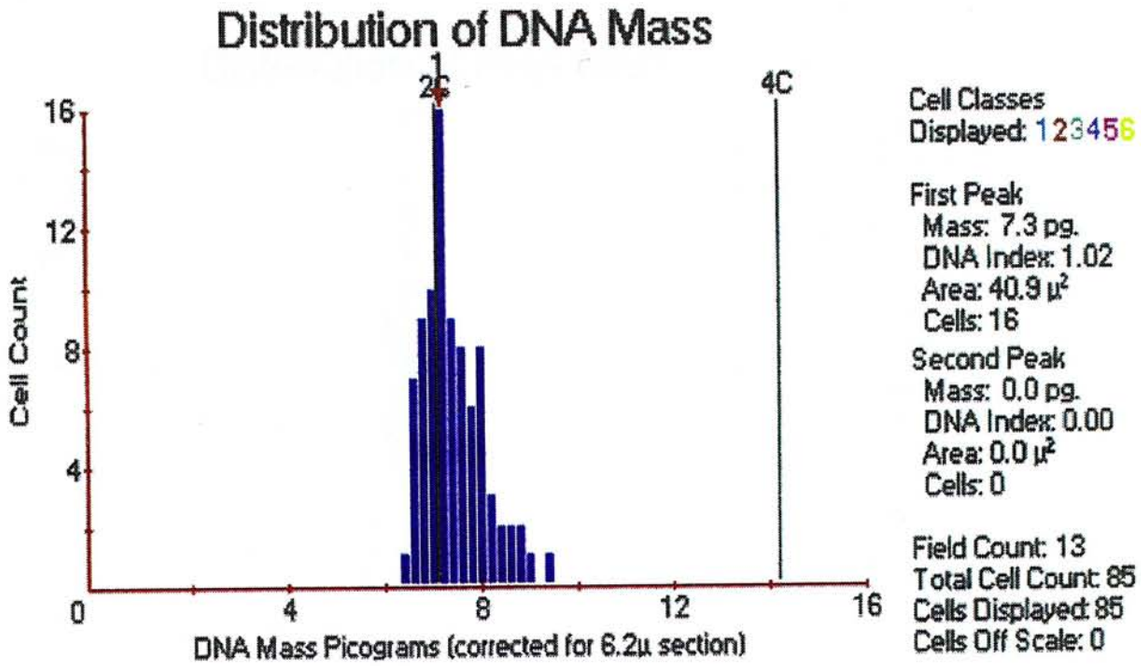

B

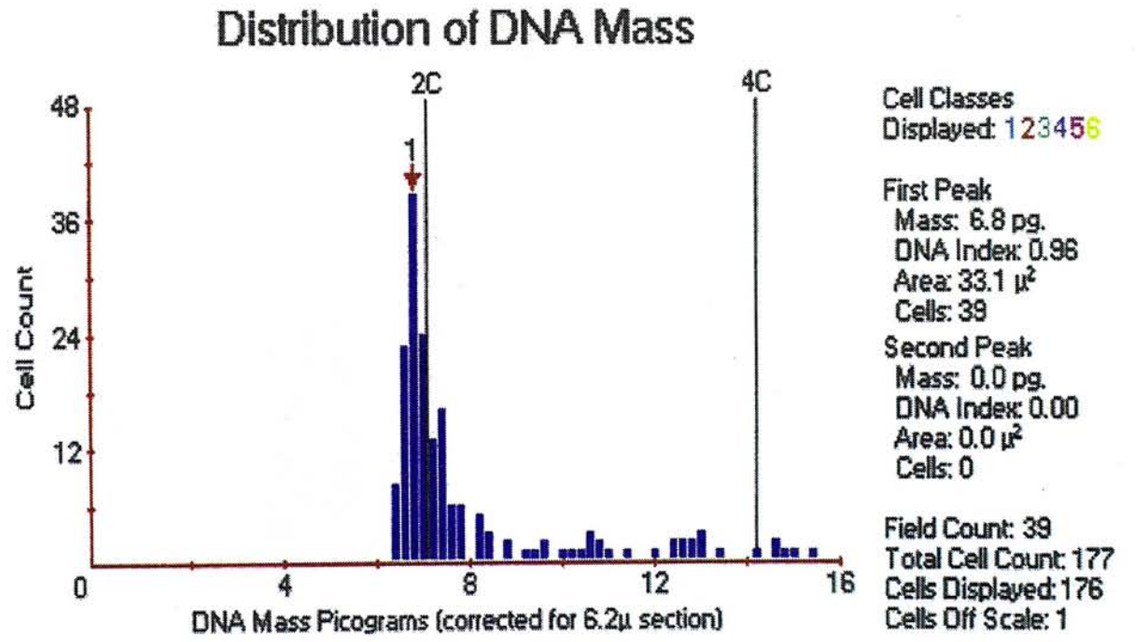

Figure 5.15 Case 2-I Image cytometric histograms (section)
A: Normal control
B: Diploid RCC
(Thickness corrected according to the normal control)

A

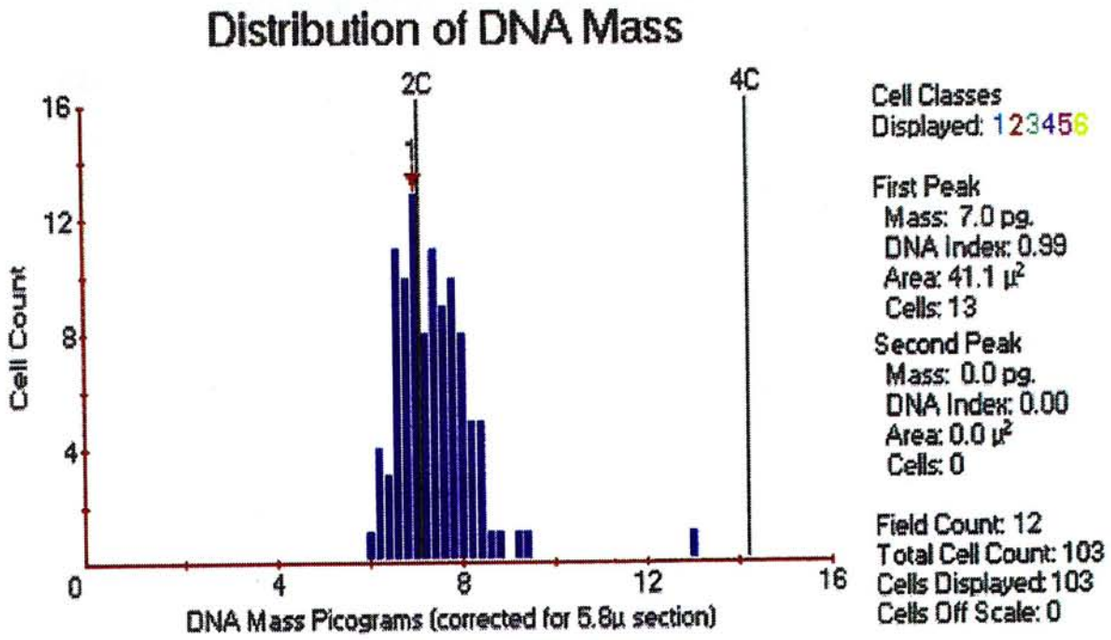

B

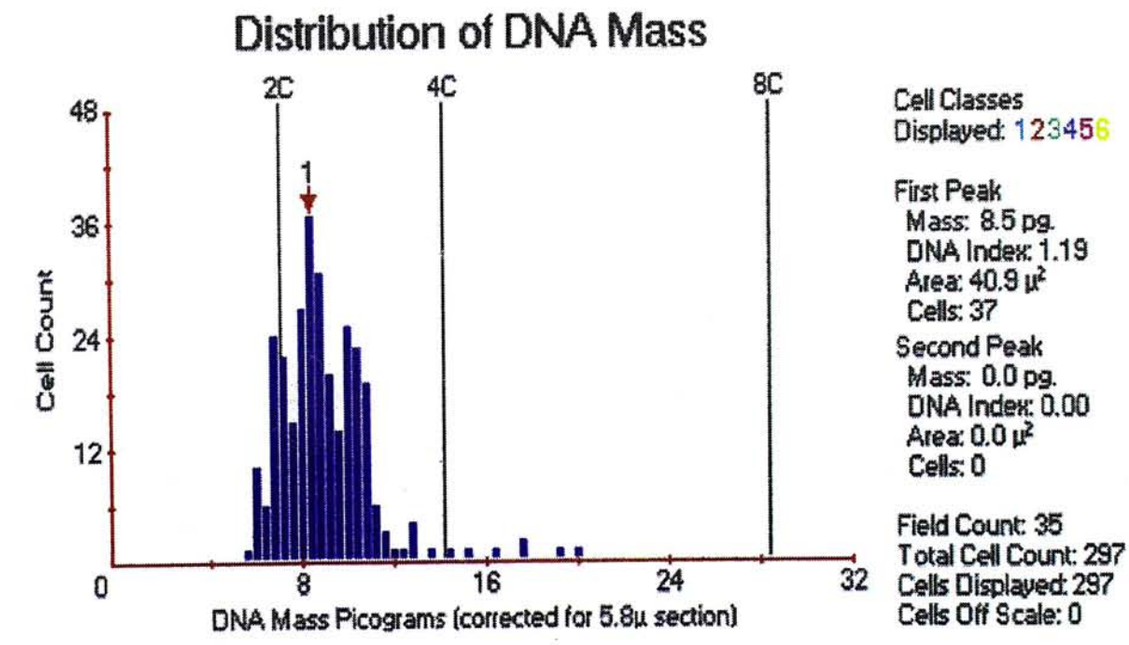

Figure 5.16 Case 10-I Image cytometric histograms (section)
A: Normal control
B: Aneuploid RCC
(Thickness corrected according to the normal control)

A

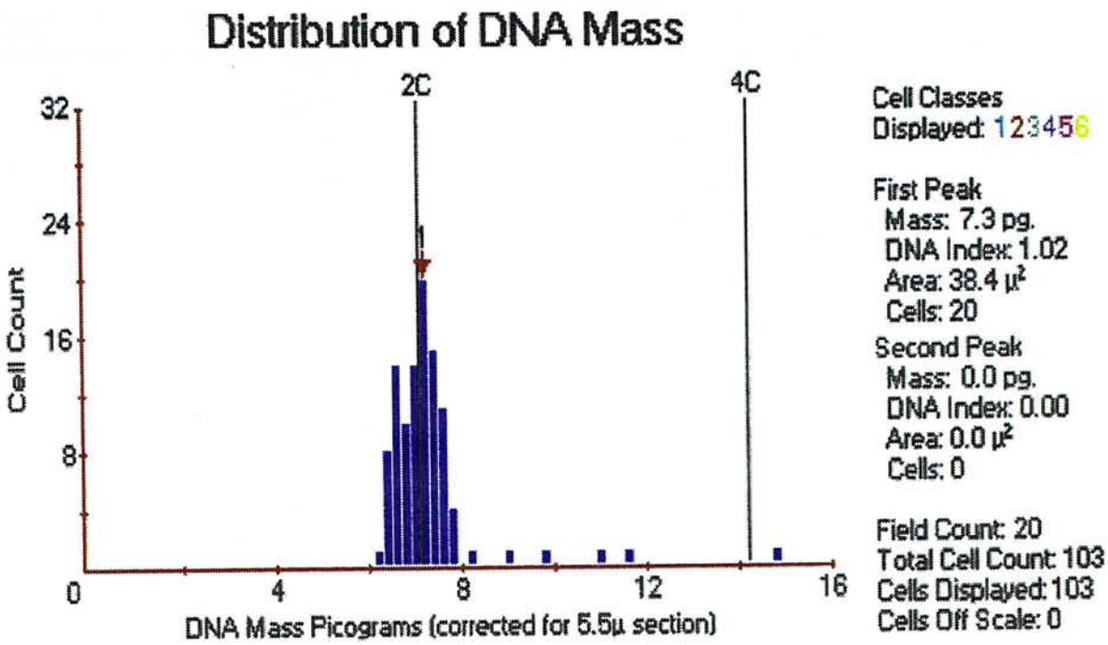

B

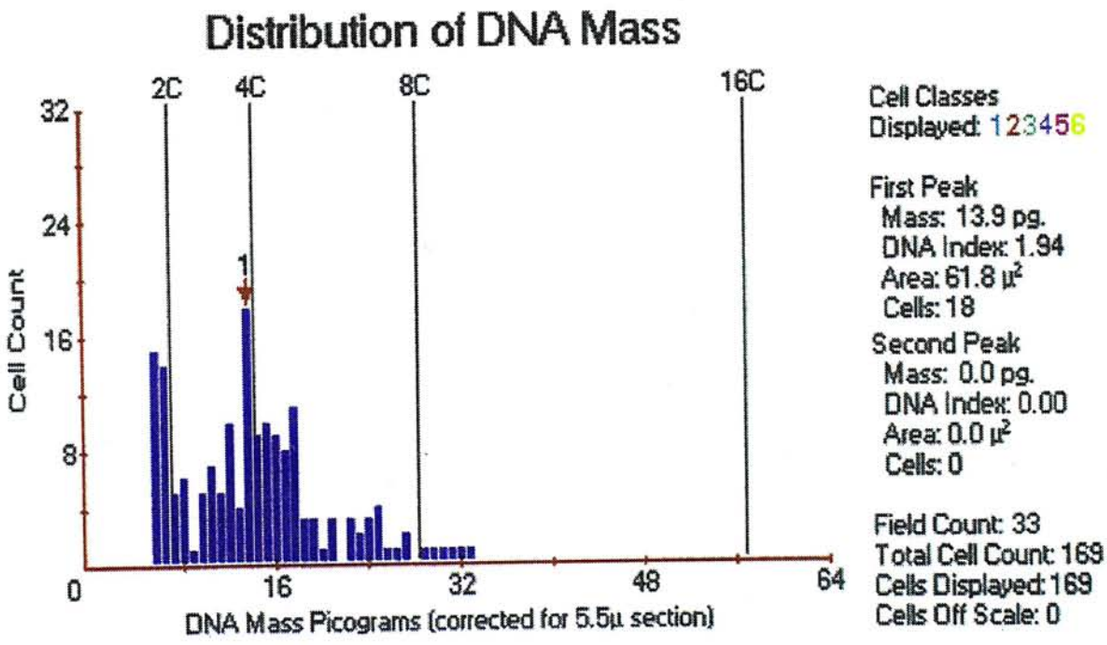

Figure 5.17 Case 35-II Image cytometric histograms (section)
A: Normal control
B: Tetraploid RCC
(Thickness corrected according to the normal control)

Table 5.6 The DNA ploidy profiles measured by ICM using tissue sections

Case No.	*Tumor sample I*	*Tumor sample II*
1	Diploid	Diploid
2	Diploid	Diploid
3	Diploid	Diploid
4	Diploid	Diploid
5	Aneuploid	Aneuploid
6	Diploid	Diploid
7	Aneuploid	Aneuploid
8	Diploid	Diploid
9	Diploid and Aneuploid	Aneuploid
10	Aneuploid	Aneuploid
11	Tetraploid	Aneuploid
12	Diploid	Diploid
13	Aneuploid	Aneuploid
14	Diploid	Diploid
15	Diploid	Diploid
16	Aneuploid	Aneuploid
17	Aneuploid	Diploid
18	Diploid	Diploid
19	Diploid and Aneuploid	Diploid and Aneuploid
20	Diploid and Tetraploid	Aneuploid
21	Aneuploid	Aneuploid
22	Aneuploid	Aneuploid
23	Diploid and Aneuploid	Aneuploid
24	Aneuploid	Aneuploid
25	Aneuploid	Tetraploid
26	Diploid and Aneuploid	Aneuploid
27	Diploid	Diploid
28	Aneuploid	Aneuploid
29	Diploid and Tetraploid	Diploid and Aneuploid
30	Diploid	Diploid
31	Diploid	Diploid
32	Diploid and Aneuploid	Aneuploid
33	Diploid	Diploid
34	Diploid	Diploid
35	Diploid	Diploid and Tetraploid
36	Diploid	Diploid
37	Diploid	Diploid
38	Diploid	Diploid
39	Diploid	Diploid
40	Aneuploid	Aneuploid
41	Diploid	Diploid
42	Diploid	Aneuploid
43	Aneuploid	Aneuploid
44	Diploid	Diploid and Aneuploid
45	Diploid and Aneuploid	Aneuploid
46	Diploid	Tetraploid

4. Immunohistochemistry

Evaluation of immunostaining was performed under microscope. Nuclei were considered positive if any brown nuclear staining was present, regardless of staining intensity. The staining was scored from 1+ to 10+ according to the scoring criteria described in chapter 4 (Table 4.4).

4.1 Ki 67 (MIB-1)

The Ki 67 (MIB-1) staining was heterogeneous in most cases. Areas with the highest expression of Ki 67 (MIB-1) positive cells were selected for assessment.

Expression of Ki 67 (MIB-1) in normal renal tubular epithelial cells was less than 1% (Figure 5.18). Ki 67 (MIB-1) immunostaining of representative cases were shown in Figure 5.19 and Figure 5.20.

The score of Ki 67 (MIB-1) immunostaining were listed in Table 5.7 in detail.

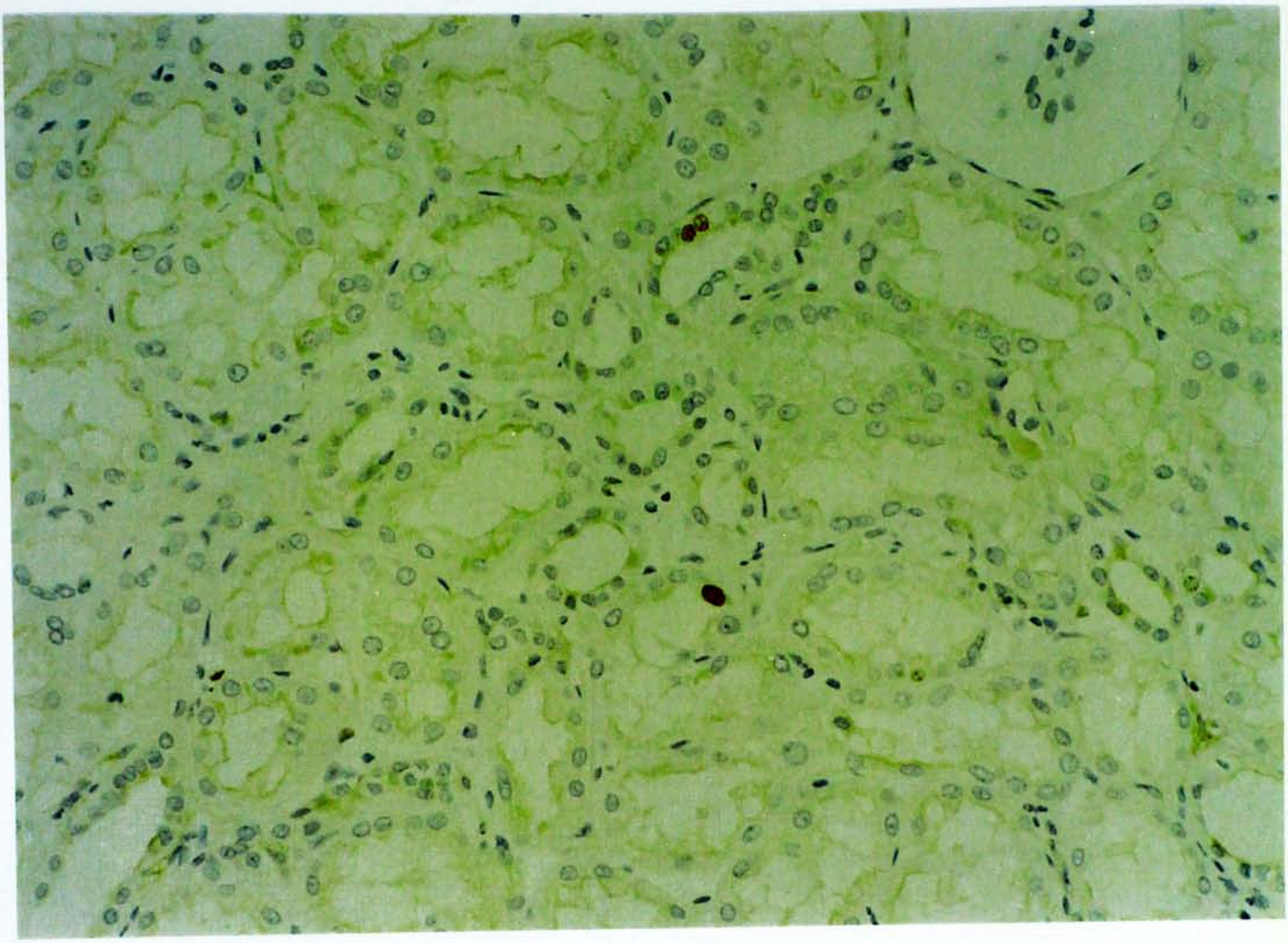

Figure 5.18 Normal renal tubular epithelial cells. Immunostaining for Ki 67 antigen (MIB-1). Counterstained with Mayer's haematoxylin. Only a small number of the tubular epithelial cells are positive (×200).

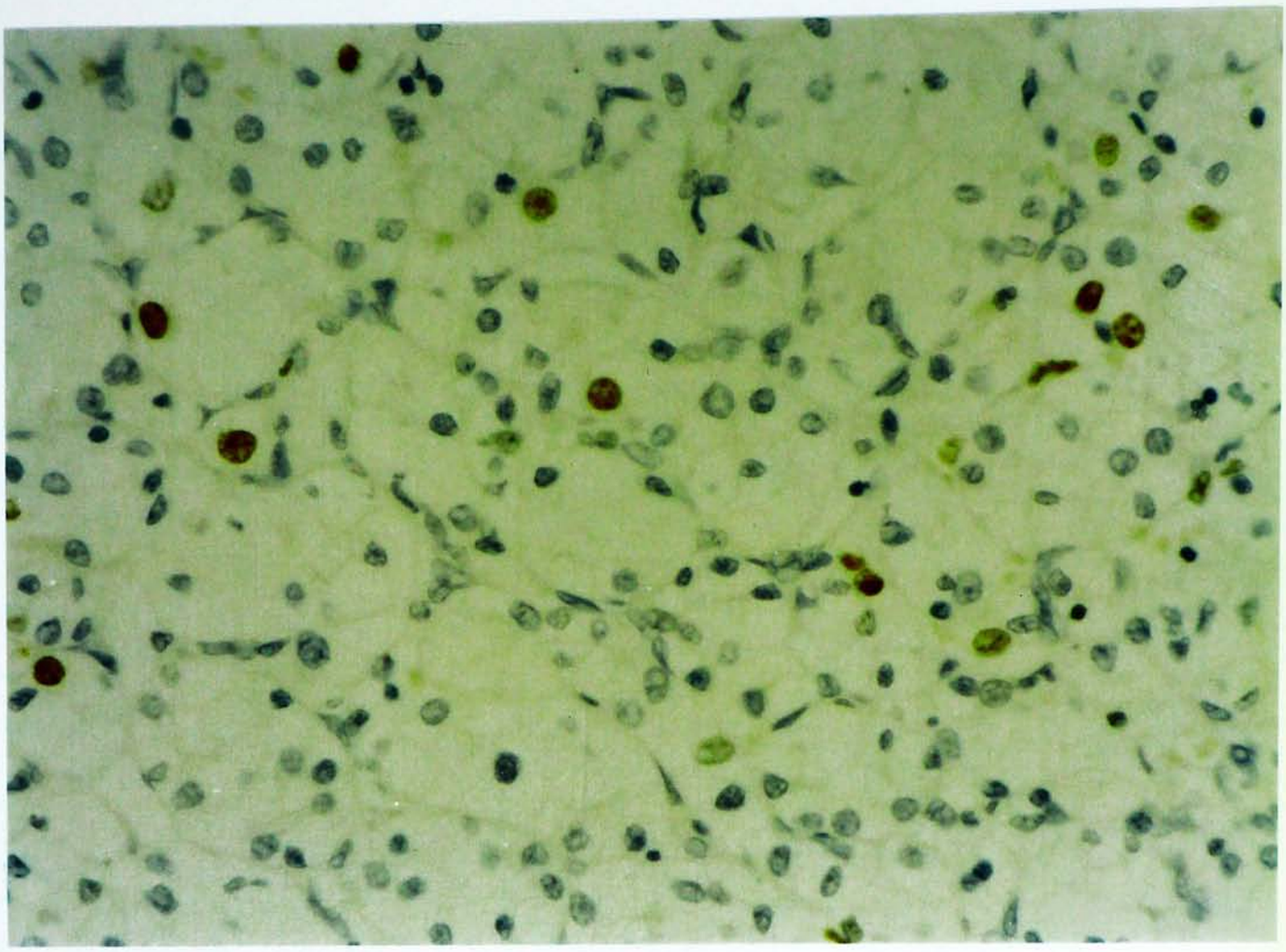

Figure 5.19 RCC with low expression of Ki 67 (MIB-1). Counterstained with Mayer's haematoxylin. Positive Ki 67 (MIB-1) staining in less than 10 percent of tumor cells (Case 3,×400).

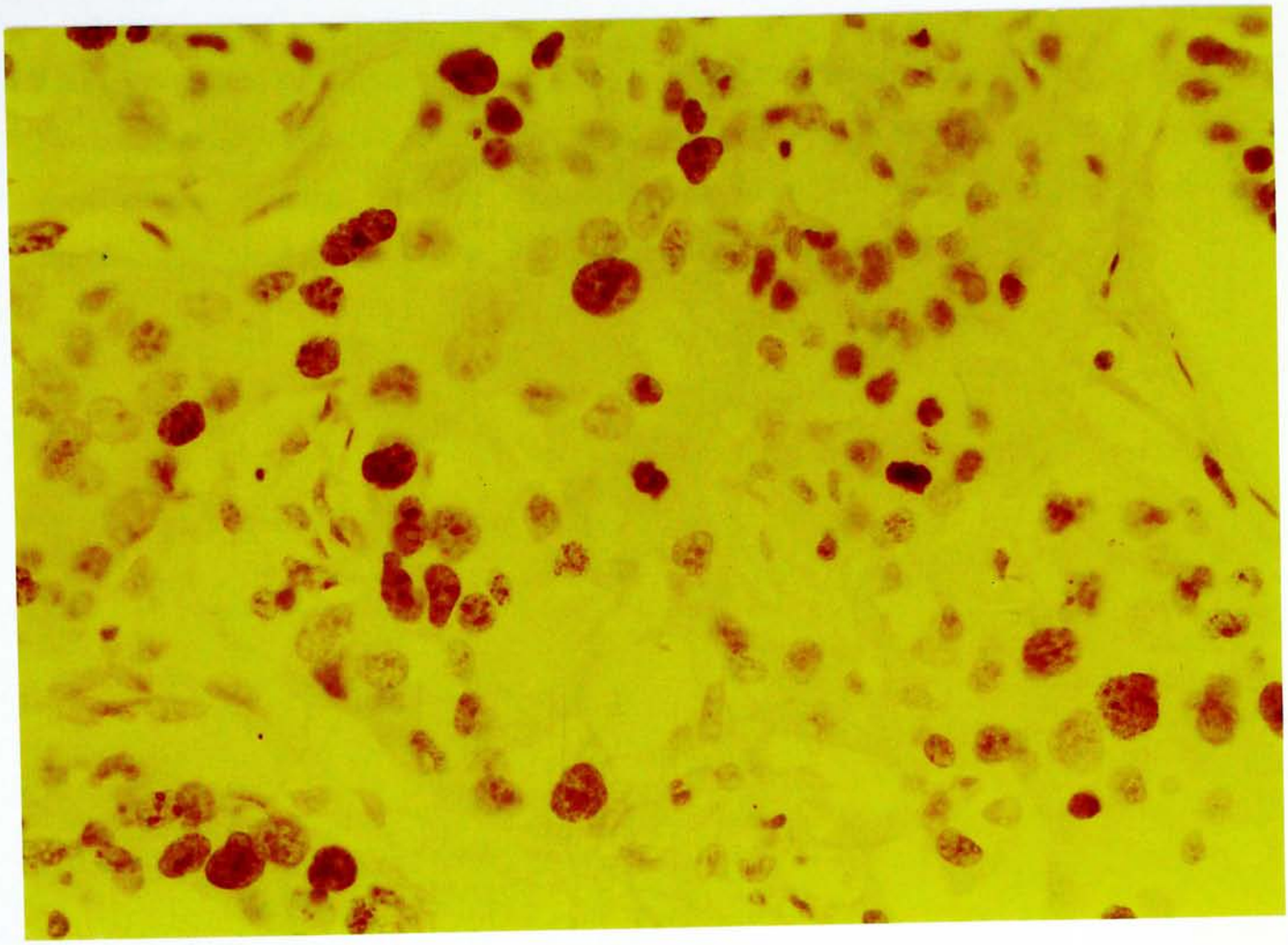

Figure 5.20 RCC with high expression of Ki 67 (MIB-1). Counterstained with Mayer's haematoxylin. Tumor cells show diffuse and intense brownish nuclear staining (Case 42, ×400).

4.2 $p27^{kip1}$

Normal ductal epithelial cells of breast were served as positive controls (Figure 5.21). Podocytes of normal glomeruli showed intense positive staining (Figure 5.22). Normal tubular epithelial cells were rarely positive, but occasional samples showed focal intense staining. Positive immunostaining for $p27^{kip1}$ in RCC is illustrated in Figure 5.23. Detailed score of $p27^{kip1}$ immunostaining is listed in Table 5.7.

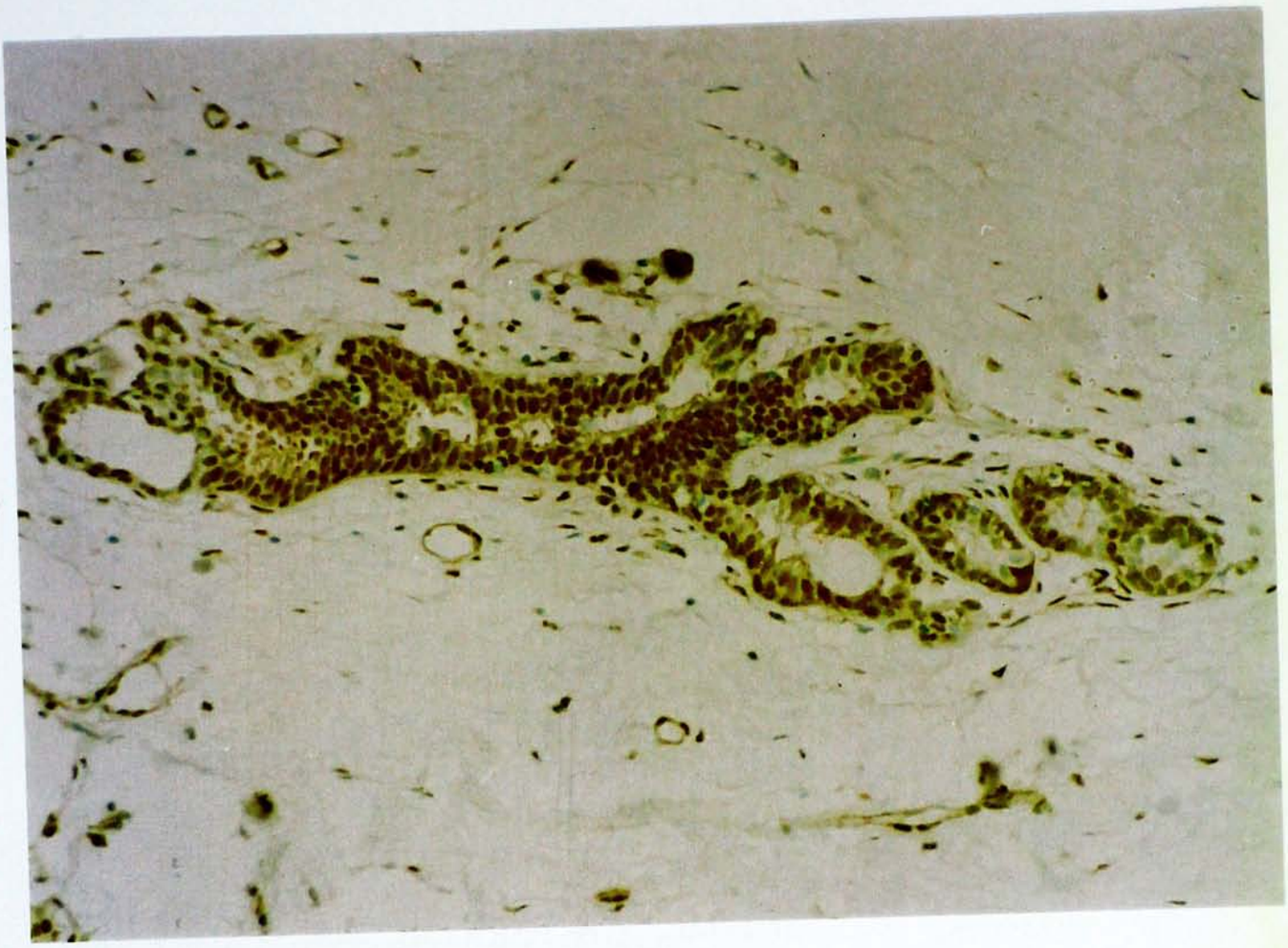

Figure 5.21 Normal ductal epithelial cells of breast (Positive control). Immunostaining for $p27^{kip1}$. Counterstained with methyl green. Intense brownish nuclear staining appreciated in the ductal epithelial cells (× 100).

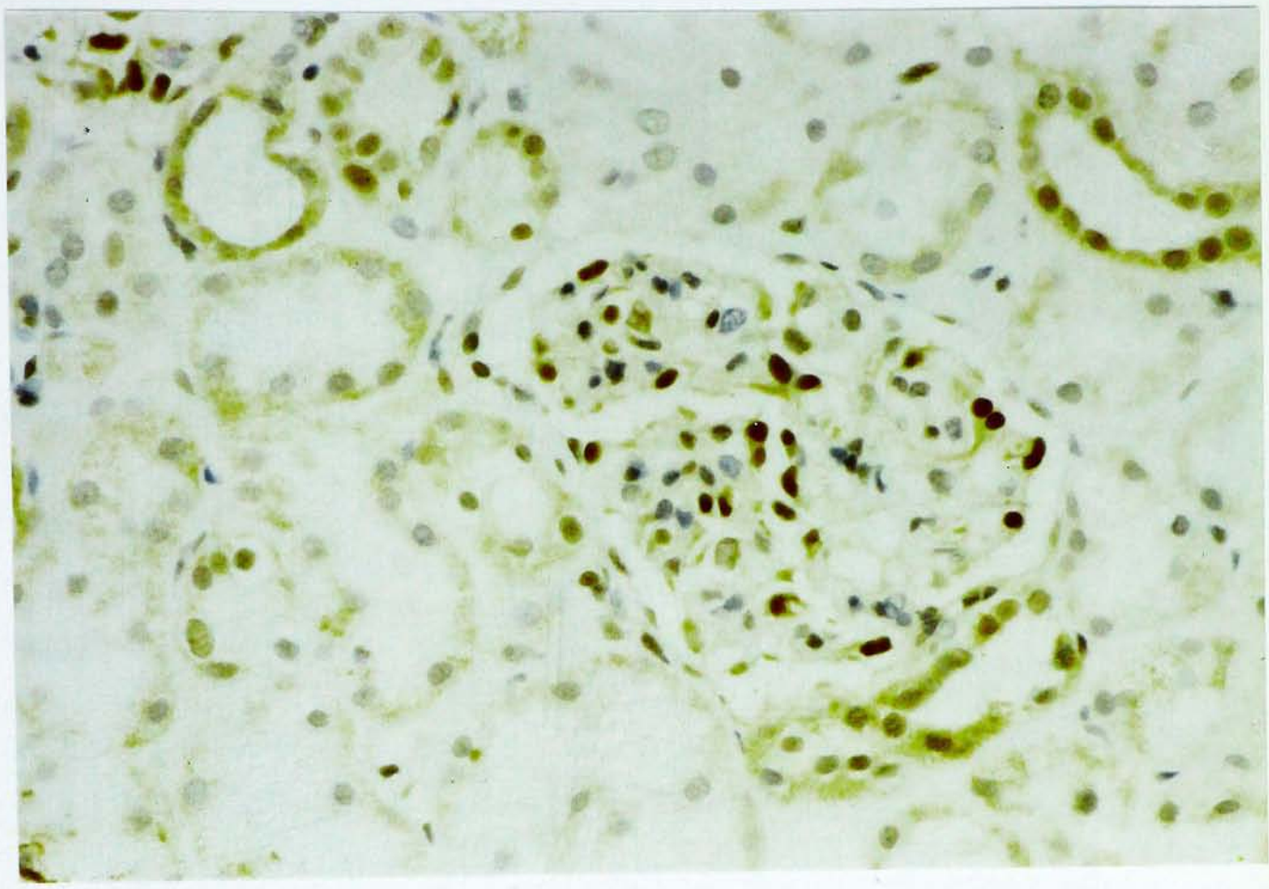

Figure 5.22 Normal kidney. Immunostaining for $p27^{kip1}$. Counterstained with Mayer's haematoxylin. Podocytes showed intense brownish nuclear staining. In this particular sample, the tubular epithelial cells also showed intense staining focally (× 400).

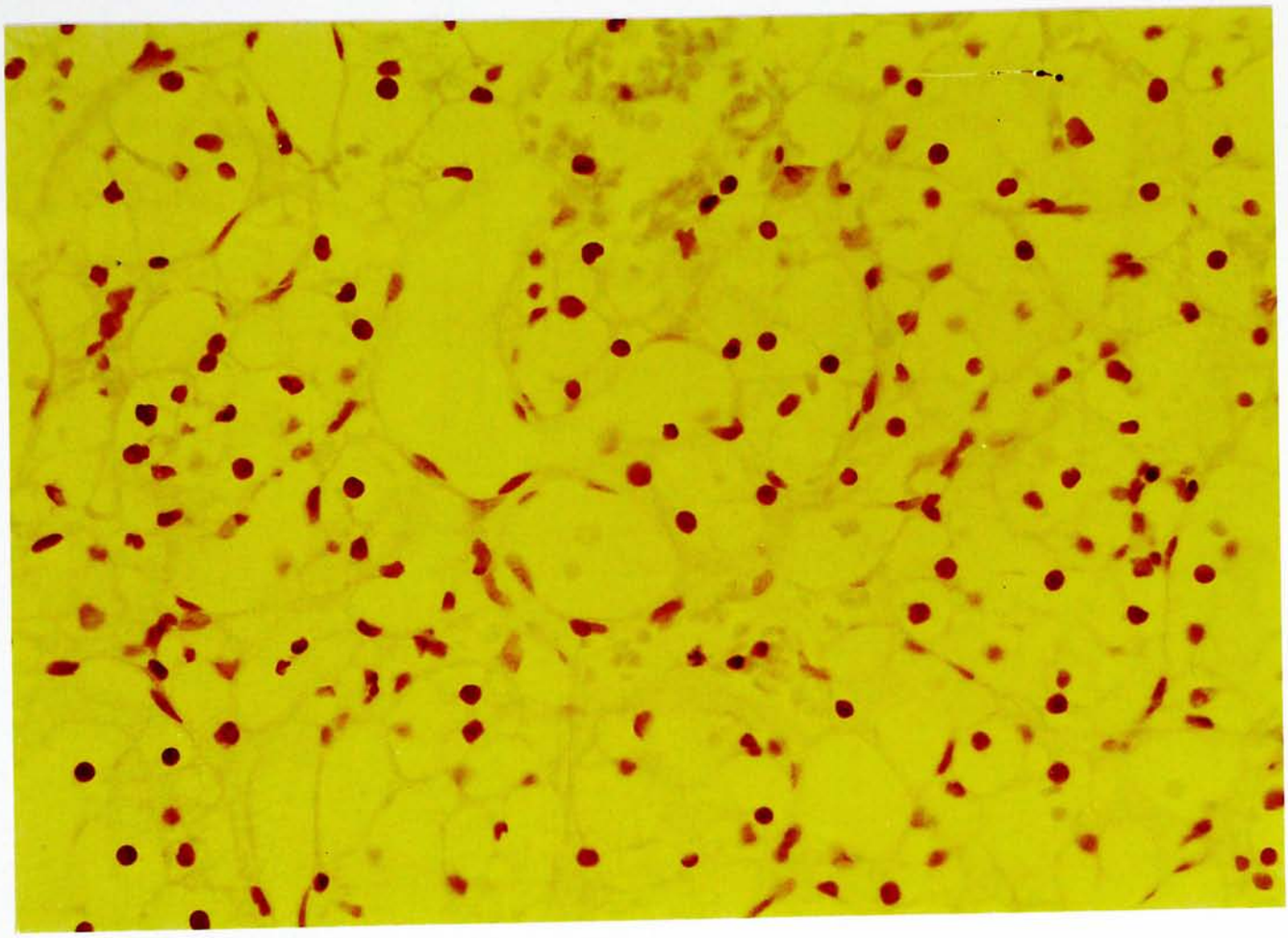

Figure 5.23 Renal cell carcinoma with high expression of $p27^{kip1}$. Counterstained with Mayer's haematoxylin. Tumor cells showed diffuse brownish nuclear staining (Case33, ×400).

Table 5.7 Expression of Ki 67 (MIB-1) and $p27^{kip1}$ in RCC by IHC (According to percentage of positive cells)

Case No.	Ki 67 (MIB-1)	$p27^{kip1}$
1	1+	4+
2	1+	6+
3	1+	7+
4	1+	4+
5	1+	1+
6	2+	1+
7	8+	1+
8	1+	8+
9	1+	1+
10	1+	1+
11	4+	1+
12	1+	8+
13	4+	5+
14	1+	4+
15	4+	1+
16	1+	1+
17	5+	2+
18	3+	1+
19	1+	1+
20	1+	1+
21	6+	1+
22	1+	1+
23	2+	5+
24	1+	1+
25	5+	1+
26	3+	2+
27	1+	5+
28	5+	1+
29	1+	2+
30	1+	1+
31	1+	1+
32	5+	1+
33	4+	9+
34	1+	1+
35	6+	7+
36	1+	9+
37	2+	3+
38	1+	1+
39	2+	7+
40	6+	7+
41	3+	1+
42	7+	2+
43	2+	7+
44	1+	7+
45	2+	4+
46	2+	1+

*The scoring criteria were described in chapter 4.

5. Statistical Analysis

Statistical analysis was performed with commercial available statistical software package SSPS (version 6.0). $p<0.05$ was regarded as statistically significance. Three cases of oncocytoma were excluded from statistical analysis.

Comparisons of data were carried out by chi-square test and Spearman's correlation coefficients were calculated. Since only two of our patients died with disease or tumor-related disease, event-free survival analysis was used. Events were defined as tumor recurrence, metastasis or disease related death. The Kaplan-Meier method was used to estimate the survival function. Patients were considered censored if they were free of diseases up to the last follow-up or had died from other causes. Differences among survival curves were tested by the log rank test. Cox regression was used for multivariate analysis.

5.1 DNA Ploidy Analysis

The results of DNA ploidy measured by FCM (ploidy F), ICM using cytospin preparations (ploidy C) and ICM using tissue sections (ploidy S) were analyzed separately.

5.1.1 DNA Ploidy Measured by Flow Cytometry (ploidy F)

Statistically significant correlation were found between ploidy F and nuclear grade ($p=0.012$), nuclear area ($p=0.0005$) and stage ($p=0.01$). A negative correlation was observed between ploidy F and $p27^{kip1}$ expression ($p=0.01$).

No significant correlation was observed between ploidy F and age, sex, histological type, and Ki 67 (MIB-1) expression.

Table 5.8 Significant correlation between ploidy F and other parameters

	$p27^{kip1}$	Nuclear grade	Stage	Nuclear area
Spearman's correlation coefficient	- 0.39	0.48	0.38	0.52
Significance	0.01	0.012	0.01	0.0005

In high stage group (stage III, IV), ploidy F was demonstrated to be of prognostic value (p=0.02) for event-free survival (Figure 5.24). As showed in Table 5.9, there were totally eight patients with high stage diseases. One out of three patients with diploid tumor was free of disease but all patients with aneuploid and tetraploid tumors had event(s).

Table 5.9 Survival distributions for ploidy F in high stage group

	Total	No. of events	No. of censored	% of censored
Diploid	3	2	1	33.33
Aneuploid	4	4	0	0
Tetraploid	1	1	0	0
Overall	8	7	1	12.5

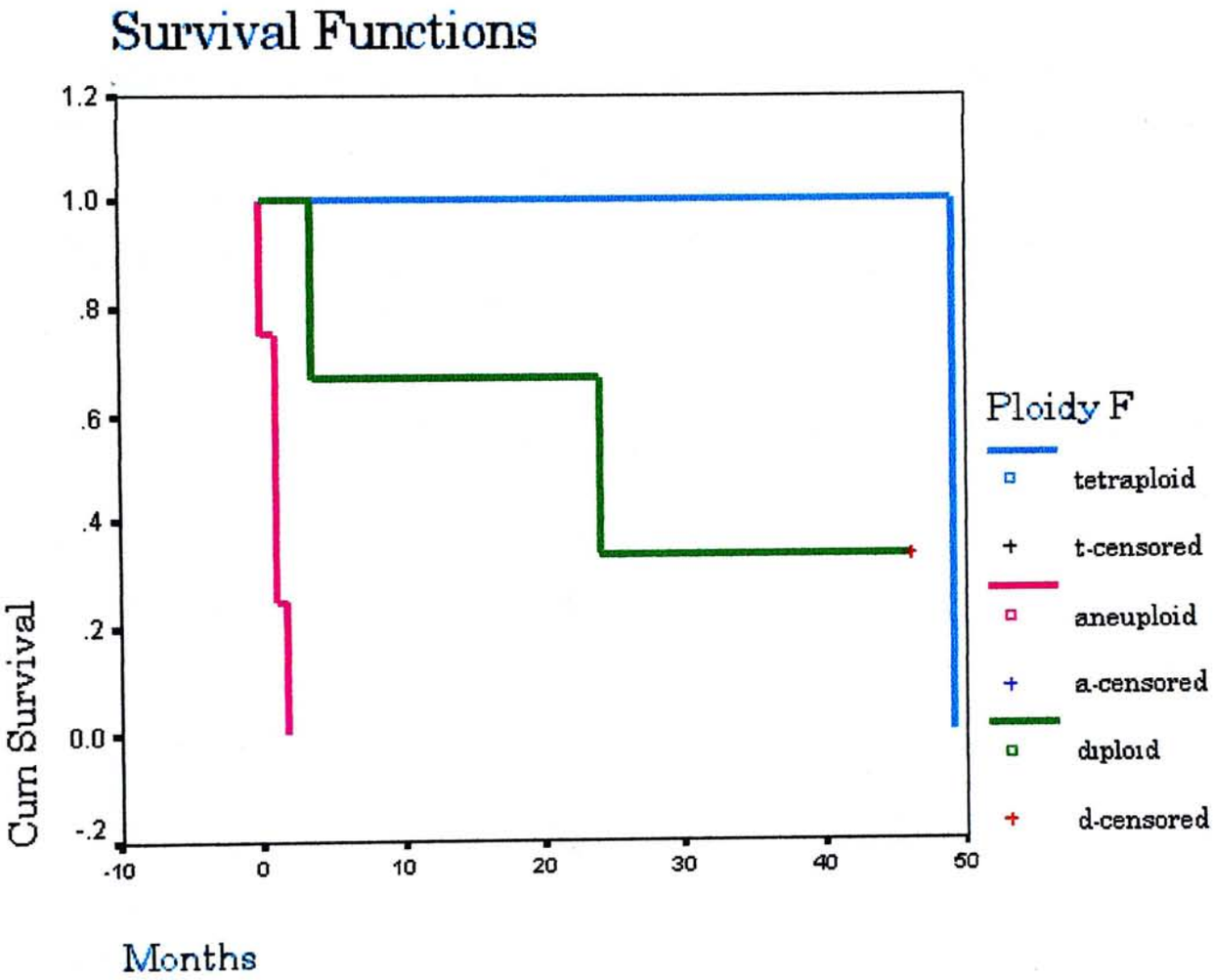

Figure 5.24 Event-free survival plotted as function of time after diagnosis for patients with high stage (III, IV) RCC grouped according to ploidy F. EFSDATEC: event-free survival date count

5.1.2 By Static Image Cytometry Using Cytospin Preparations (ploidy C)

Ploidy C correlated significantly with nuclear grade ($p<0.00001$) and nuclear area ($p<0.00001$). No significant correlation was observed between ploidy C and age, sex, histological type, stage, expression of $p27^{kip1}$ and Ki 67 (MIB-1) expression.

Table 5.10 Significant correlation between ploidy C and other parameters

	Nuclear grade	Nuclear area
Spearman's correlation coefficient	0.73	0.78
Significance	<0.00001	<0.00001

In high stage group (stage III, IV), ploidy C was shown to be a significant prognostic factor ($p=0.01$) for event-free survival (Figure 5.25). As shown in Table 5.11, Two out of three patients with diploid tumors were free of disease but all patients with aneuploid and tetraploid tumors had event(s).

Table 5.11 Survival distributions for ploidy C in high stage group

	Total	No. of events	No. of censored	% of censored
Diploid	3	1	2	66.67
Aneuploid	4	4	0	0
Tetraploid	2	2	0	0
Overall	9	7	2	22.2

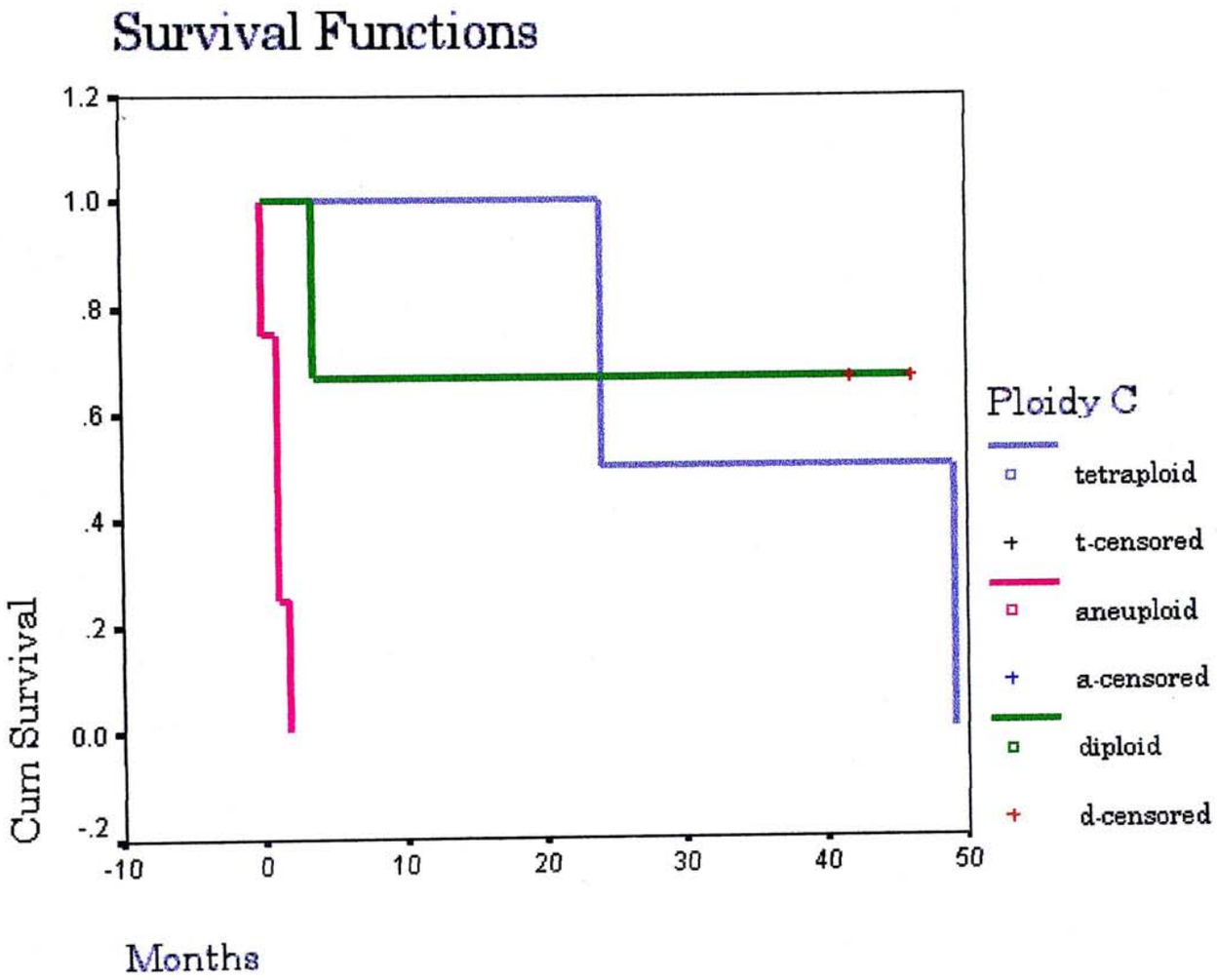

Figure 5.25 Event-free survival plotted as function of time after diagnosis for patients with high stage (III, IV) RCC grouped according to ploidy C. EFSDATEC: event-free survival date count

5.1.3 By Static Image Cytometry Using Tissue Sections (ploidy S)

Statistically significant correlation were found between ploidy S and nuclear grade ($p<0.00001$) and nuclear area ($p<0.00001$). No significant correlations were observed between ploidy S and age, sex, histological type, stage, expression of $p27^{kip1}$ and Ki 67 (MIB-1) expression.

Table 5.12 Significant correlation of ploidy S and other parameters

	Nuclear grade	Nuclear area
Spearman's correlation coefficient	0.66	0.77
Significance	<0.00001	<0.00001

In high stage group (stage III, IV), ploidy S was also demonstrated to be of prognostic value ($p=0.01$) for event-free survival (Figure 5.26). As shown in Table 5.13, Two out of three patients with diploid tumors were free of disease but all patients with aneuploid and tetraploid tumors had event(s).

Table 5.13 Survival distributions for ploidy S in high stage group

	Total	No. of events	No. of censored	% of censored
Diploid	3	1	2	66.67
Aneuploid	4	4	0	0
Tetraploid	2	2	0	0
Overall	9	7	2	22.22

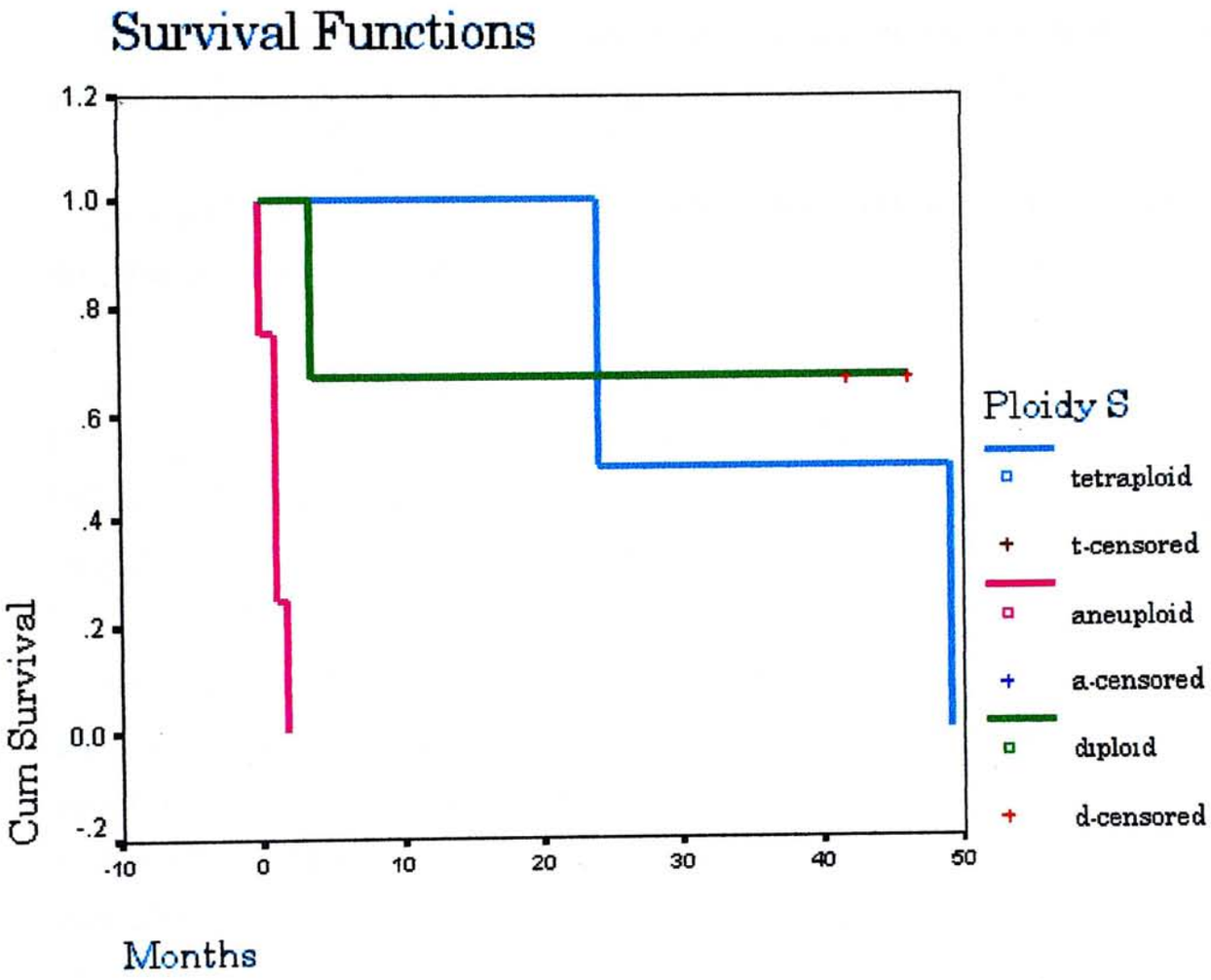

Figure 5.26 Event-free survival plotted as function of time after diagnosis for patients with high stage (III, IV) RCC grouped according to ploidy S. EFSDATEC: event-free survival date count

5.2 Ki 67 (MIB-1)

Patients were stratified into two categories according to their Ki 67 (MIB-1) expression for statistical analysis. Cases with score 1+ and 2+ were considered as low expression group. Cases with score 3+ to 10+ were grouped as high expression group.

Statistically significant correlation were found between expression of Ki 67 (MIB-1) and nuclear grade (p=0.007), nuclear area (p=0.02) and stage (p=0.004).

No significant correlation was observed between Ki 67 (MIB-1) expression and age, sex, histological type and expression of $p27^{kip1}$.

Table 5.14 Significant correlation of Ki 67 (MIB-1) and other parameters

	Nuclear grade	Nuclear area	Stage
Spearman's correlation coefficient	0.41	0.35	0.43
Significance	0.007	0.02	0.004

Expression of Ki 67 (MIB-10) was a significant prognostic parameter for event-free survival by univariate analysis (p = 0.0001) (Figure 5.27). The event-free survival distribution of Ki 67 (MIB-1) expression is shown in Table 5.15. About 91% patients with low Ki 67 (MIB-1) expression were free of event, while in high expression group, only 22%.

Table 5.15 Survival distributions for Ki 67 (MIB-1)

	Total	No. of events	No. of censored	% of censored
low expression	22	2	20	90.91
high expression	9	7	2	22.22
Overall	31	9	22	70.97

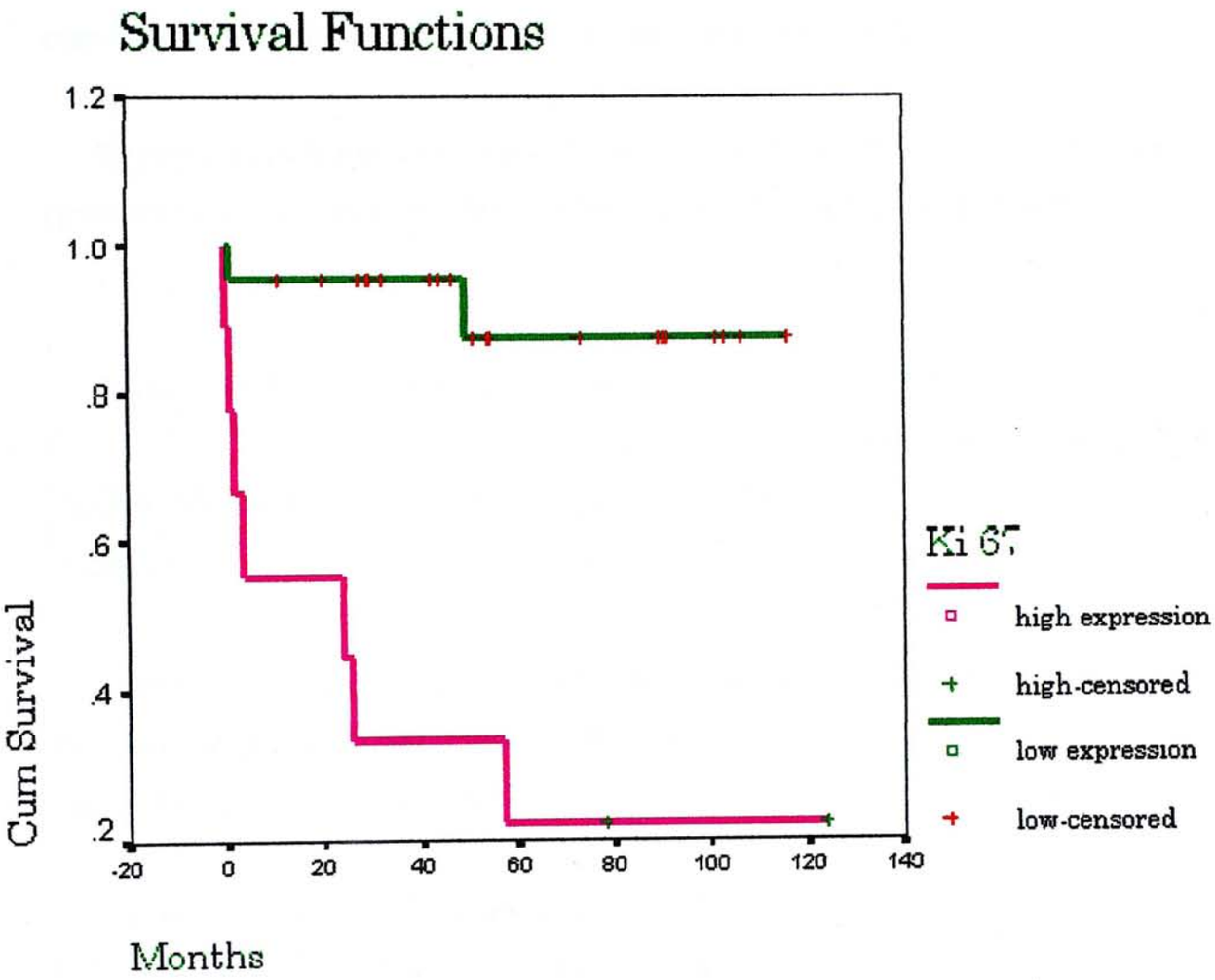

Figure 5.27 Cumulative proportion of patients with event-free survival according to Ki 67 (MIB-1) expression.
EFSDATEC: event-free survival date count

5.3 $p27^{kip1}$

Patients were stratified into two categories according to their $p27^{kip1}$ expression for statistical analysis. Cases scored 1+ to 3+ were grouped as low expression group while cases scored 4+ to 10+ were regarded as high expression group.

Negative correlation were found between expression of $p27^{kip1}$ and nuclear grade (p=0.0015), nuclear area (p=0.0005), ploidy F (p=0.01) and stage (p=0.0086).

Table 5.16 Significant correlation of $p27^{kip1}$ and other parameters

	Ploidy F	Nuclear grade	Nuclear area	Stage
Spearman's correlation coefficient	- 0.4	- 0.47	- 0.51	- 0.4
Significance	0.01	0.0015	0.0005	0.0086

Low $p27^{kip1}$ reactivity was associated with a statistically significant impaired event-free survival rate (p=0.04) (Figure 5.28). The event-free survival distribution of $p27^{kip1}$ expression is shown in Table 5.17.

Table 5.17 Survival distributions for $p27^{kip1}$

	Total	No. of events	No. of censored	% of censored
low expression	14	7	7	50
high expression	17	2	15	88.24
Overall	31	9	22	70.97

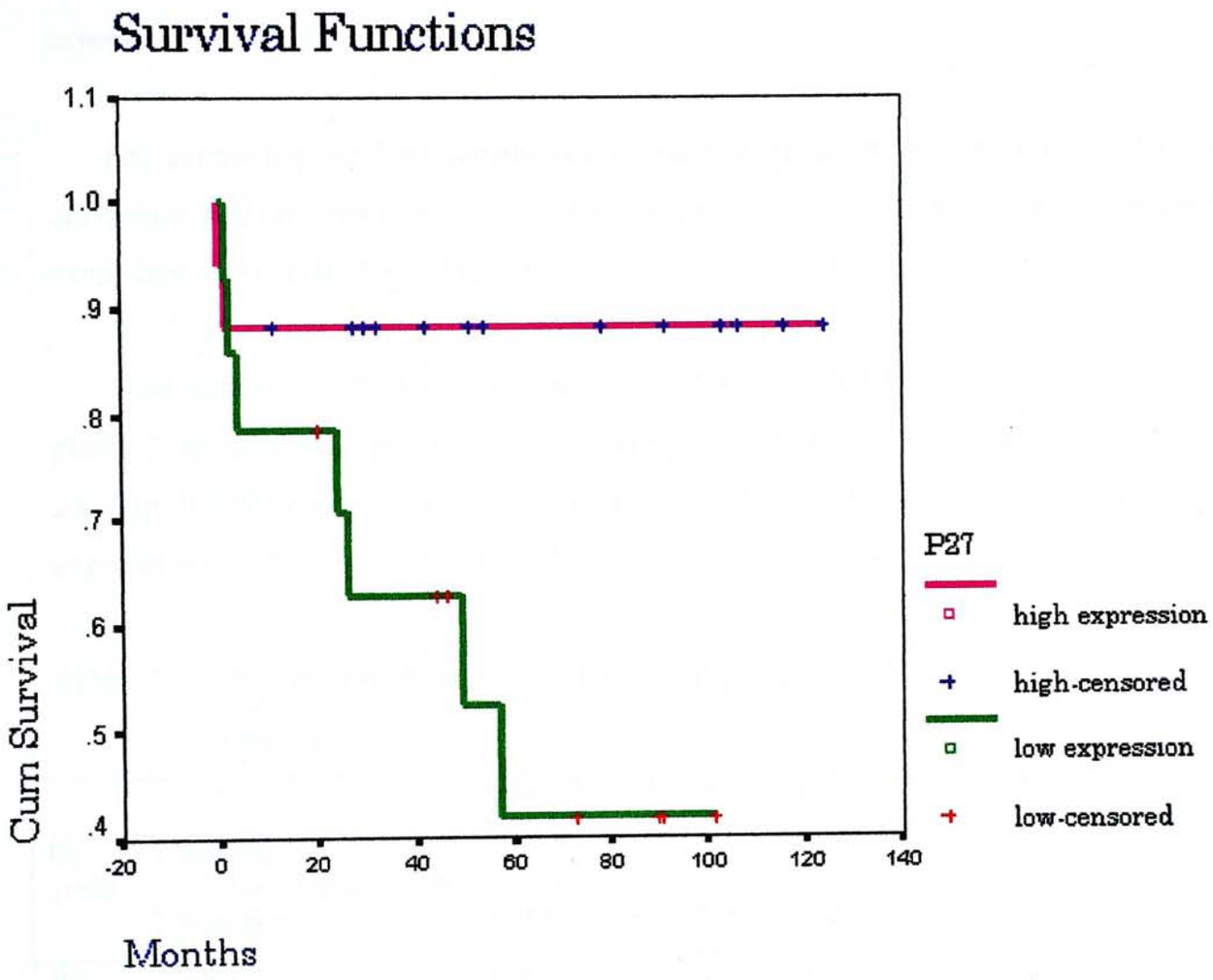

Figure 5.28 Cumulative proportion of patients with event-free survival according to $p27^{kip1}$ expression.
EFSDATEC: event-free survival date count

5.4 Nuclear Grade and Area

There was a significant correlation between nuclear grade and nuclear area ($p<0.0001$). Significant correlation were observed between grade and ploidy F ($p=0.001$), ploidy C ($p<0.00001$), ploidy S ($p<0.00001$), stage ($p=0.002$) and expression of Ki 67 ($p=0.007$). A negative correlation was observed between nuclear grade and expression of $p27^{kip1}$ ($p=0.0015$).

The event-free survival distribution of nuclear grade is shown in Table 5.19. By univariate analysis, nuclear grade was shown to be a significant prognostic factor for event-free survival ($p=0.0073$) (Figure 5.29).

Statistically significant correlation were demonstrated between nuclear area and ploidy F ($p=0.00045$), ploidy C ($p<0.0001$), ploidy S ($p<0.00001$), grade ($p<0.00001$), stage ($p=0.039$), expression of Ki 67 (MIB-1) ($p=0.02$) and a negative correlation with expression of $p27^{kip1}$ ($p=0.0005$).

Table 5.18 Significant correlation of nuclear grading and nuclear area with other parameters

		ploidyF	ploidyC	ploidyS	$p27^{kip1}$	Ki67	stage
By grade	Spearman's correlation coefficient	0.48	0.73	0.66	- 0.47	0.4	0.46
	Significance	0.001	<0.00001	<0.00001	0.0015	0.007	0.002
By nuclear area	Spearman's correlation coefficient	0.52	0.78	0.77	- 0.51	0.35	0.31
	Significance	0.00045	<0.00001	<0.00001	0.0005	0.02	0.039

Table 5.19 Survival distributions for nuclear grade

	Total	No. of events	No. of censored	% of censored
grade I	8	0	8	100
grade II	12	4	8	66.67
grade III	9	3	6	66.67
grade IV	2	2	0	0
Overall	31	9	22	70.97

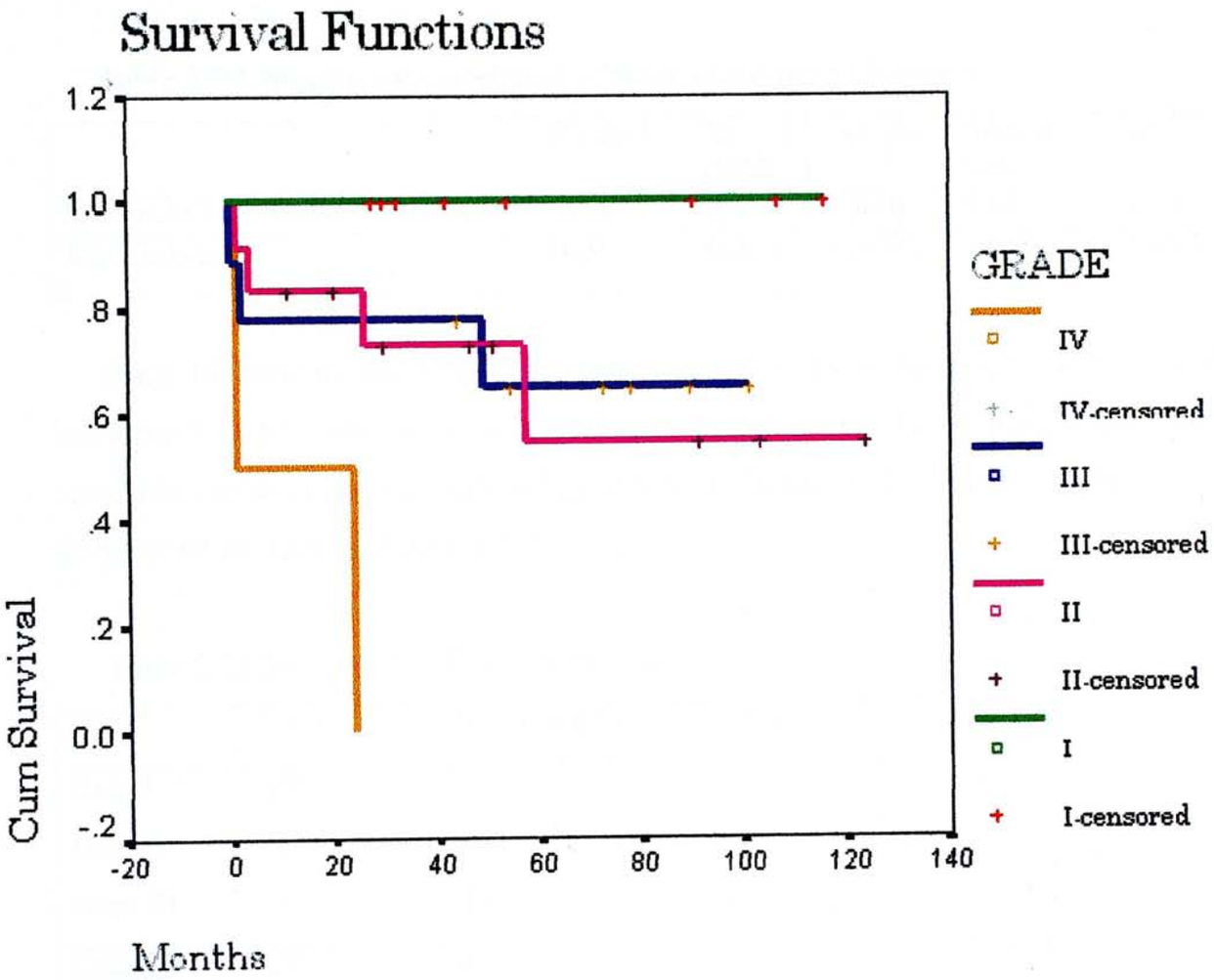

Figure 5.29 Cumulative proportion of patients with event-free survival according to Fuhrman's nuclear grade.
EFSDATEC: event-free survival date count

5.5 Stage

Statistically significant correlation were found between stage and ploidy F (p=0.01), grade (p=0.002), nuclear area (p=0.039) and expression of Ki 67 (MIB-1) (p=0.019). There was a negative correlation between stage and expression of $p27^{kip1}$ (p=0.008).

Table 5.20 Significant correlation of stage and other parameters

	Ploidy F	Ki 67 (MIB-1)	Grade	Nuclear area	$p27^{kip1}$
Spearman's correlation coefficient	0.38	0.43	0.46	0.31	- 0.4
Significance	0.01	0.004	0.002	0.039	0.008

Stage IV patients were excluded from survival analysis because by definition they had already had event(s) at the time of diagnosis. It was observed that stage had a strong correlation with event-free survival (p<0.0001) (Figure 5.30). The event-free survival distribution of stage is shown in Table 5.21.

Table 5.21 Survival distributions for stage

	Total	No. of events	No. of censored	% of censored
stage I	19	1	18	66.67
stage II	3	1	2	66.67
stage III	5	4	1	20.00
Overall	27	6	21	77.78

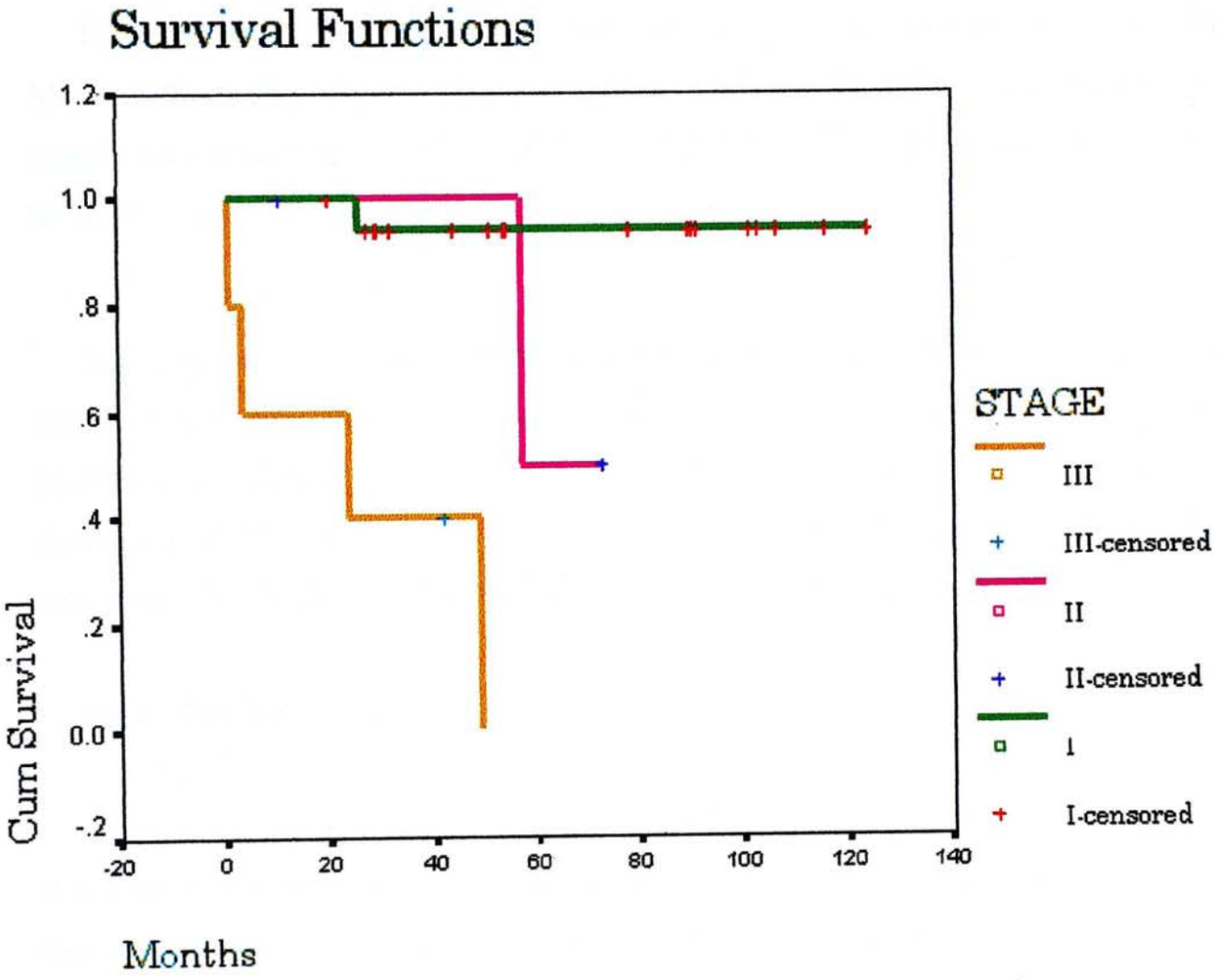

Figure 5.30 Cumulative proportion of patients with event-free survival according to stage (stage IV excluded).
EFSDATEC: event-free survival date count

5.6 Survival Analysis

5.6.1 Univariate Analysis

For event-free survival analysis, univariate analysis was carried out by Kaplan-Meier method using log rank test. In summary, variables identified as having statistical significance including Ki 67 (MIB-1) (p=0.0001), $p27^{kip1}$ (p=0.04), nuclear grade (p=0.0073) and stage (p=0.0001).

No statistical significance was demonstrated for age, sex and histological type of the tumor. Concerning the ploidy status, non-diploid cases appeared to have worse prognosis in **high stage** (stage III and IV) group: statistical significance were demonstrated for ploidy status assessed by all three methods of DNA ploidy measurement {ploidy F (p=0.02), ploidy C (p=0.01) and ploidy S (p=0.01)}.

5.6.2 Multivariate Analysis

A cox proportional hazards model (Cox, 1972) with stepwise selection of variables was used to assess the simultaneous contribution of the following baseline covariates: age, sex, clinical stage, nuclear grade, nuclear area, DNA ploidy by three different methods, Ki 67 (MIB-1) expression, $p27^{kip1}$ expression.

Only **stage** and **Ki 67 (MIB-1)** expression were retained as independent variables for event-free survival.

Chapter 6

Discussion

1. DNA Ploidy Analysis

One of the principal purposes of this study was to see whether by using three different approaches to the assessment of DNA ploidy, accurate DNA profiles of RCC could be drawn out.

1.1 Flow Cytometry

One of the primary applications of FCM was quantitative DNA analysis. It has been extensively used since it was introduced in 1960s and still, nowadays. FCM DNA content analysis offers many advantages. It is generally accepted that the method is rapid, reliable and reproducible. It can measure 10,000 to 100,000 events per second. The high-speed large-event measurement makes it possible to analysis not only the DNA ploidy status but also the distribution of cells in different cell cycle compartments. The results come out to be relatively objective because no operator interaction during the actual measurement. However, there are still many technical problems and difficult areas concerning the interpretation of the histograms.

One major limitation of FCM is the requirement that the specimen to be analyzed must be in the form of a single cell suspension. It is difficult to prepare intact nuclei from solid tumors, particularly from archival materials. Some authors have concluded from their studies that discrepant results may due to a loss of selective cell populations and have suggested that aneuploid cells may be more susceptible to cell destruction during processing and staining procedures for FCM analysis (Bauer *et al.*, 1990; Dawson *et al.*, 1990; Lee *et al.*, 1992).

In our experiments, the nuclear suspension prepared from each tissue block was subjected to both cytospin preparation for ICM and staining for FCM analysis. The cellular population subjected to FCM analysis was verified by cytological examination in the cytospin preparation. For each specimen, tumor cells were identified in varying quantities, reassuring us appropriate cells were available for FCM analysis.

Normal diploid populations within the tissue may cause a "diluting effect". They could be lymphocytes, other inflammatory cells, endothelial cells, fibroblasts, and other stromal elements, which are always present in a greater or lesser extent. As it is not possible to select target cells to be measured by FCM, overwhelming diploid populations might mask the small amount of aneuploid stemlines, thus underestimate the frequency of aneuploid tumors.

We selected tumor areas free of inflammation and necrosis in order to reduce background "noise" and normal diploid contamination. Before the preparation of nuclear suspension, unwanted portions in the sections, e.g. normal renal tissues were scrapped out.

The situation might be complicated if intratumoral heterogeneity present. The tumor possesses two or more cell clones in regarding to different DNA contents. In some of our cases, within the same tissue block (26-I, 42-II, 20-I) both diploid and aneuploid, or diploid and tetraploid were found by ICM analysis (Figure 6.1). However, all these cases showed diploid histograms in FCM. Most likely the predominant diploid tumor cell populations in FCM histograms masked the small aneuploid stemlines. But the clinical value of those small aneuploid stemlines is currently unknown.

Some authors have stated that high CV of the G_1/G_0 peak may mask aneuploid populations and it has been suggested that a high CV in itself is an indication of the presence of aneuploidy (McFadden, 1990). This may be even more difficult to interpret when using archival materials. The CVs of G_1/G_0 peaks tend to be higher (range up to 13%) (Grignon *et al.*, 1989) than the 3-5% generally achieved in studies based on fresh materials (Lanigan *et al.*, 1993).

A

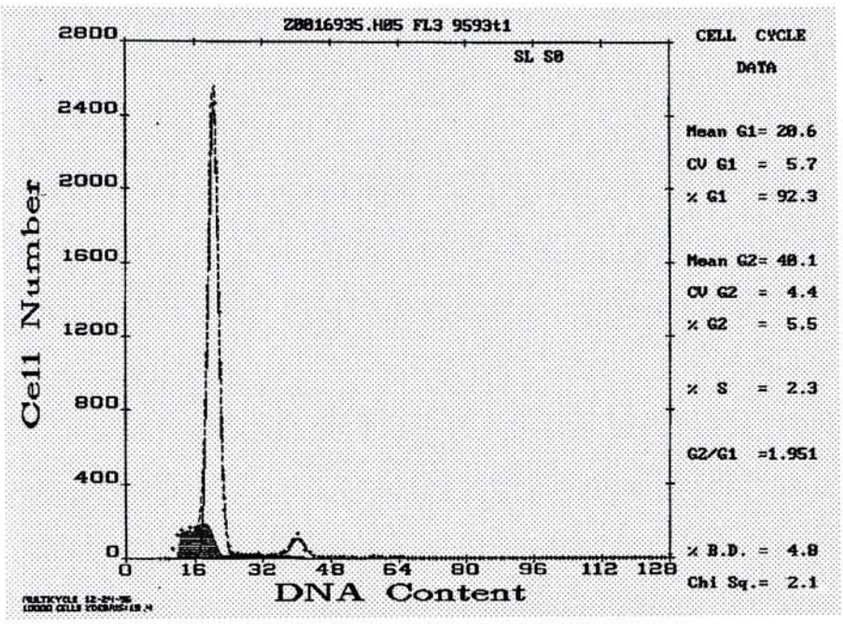

B

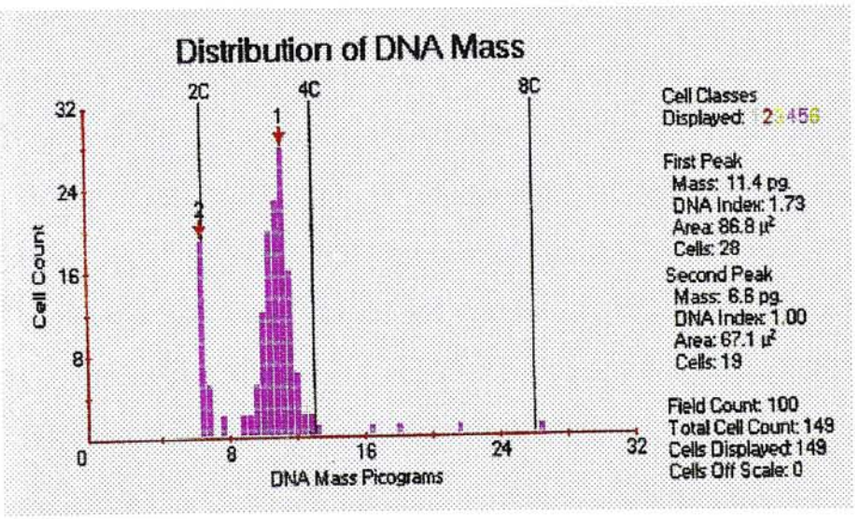

Figure 6.1 Case 26-I This case showed a diploid flow cytometric histogram (A) but both diploid and aneuploid population were detected by image analysis (cytospin) (B).

The mean of G_1/G_0 peak CVs in our study was 5.1±1.7% (range 1 - 9.1%). The results were comparable with figures quoted in other studies based on paraffin-embedded formalin-fixed materials (Currin *et al.*, 1990; Eble *et al.*, 1986; Kumar *et al.*, 1989; Roos *et al.*, 1986). Despite repeats, the CVs of the two samples of case 38 were still greater than 10%. This case was excluded from final analysis.

In our results, wide CVs appeared not interfering with DNA ploidy status assessment. Only one case's CVs were greater than 10 percent (despite repeats). This case was classified as diploid by ICM in both cytospin preparations and tissue sections.

Definition of tumor tetraploidy by FCM has always been problematic. The question of the maximum permissible count in the G_2/M phase of a cycling diploid population is controversial. Nuclear doublets (two nuclei from separate cells that are erroneously recognized as one cell) may cause elevated G_2/M peaks that are difficult to discriminate from a single tetraploid nucleus. Different cutoff points were used by different laboratories in different types of tumors (Zarbo, 1993).

In 1992, DNA cytometry consensus conference has proposed a working definition for tetraploidy which refereed to the peaks with a DI between 1.9 to 2.1, exceed the G_2/M value of similarly processed corresponding normal tissue with appropriate background debris and aggregate compensation (Shankey *et al.*, 1993). The high incidence of tetraploidy in transitional cell carcinoma reported by some authors was based on these criteria (Gustafson *et al.*, 1985). However, the prognostic significance of this FCM definition of tetraploidy is not clear in many human tumors.

In our normal renal tissue samples, the mean G_2/M region was 1.6±1.9%. Base on these data, an upper limit of 7.3% was defined as normal for the percentage of nuclei found in the G_2/M peak that would encompass 3 standard deviations above the observed mean percentage. The tetraploidy thus could be defined as DNA index between 1.8 and 2.2, and greater than 8% of nuclei in G_2/M peak. According to this definition, 16 samples could be classified as tetraploidy. However, in the literature, the upper limit of

the G_2/M normal diploid population used by most authors, varied from 10-30% in RCC (Lanigan *et al.*, 1993; Nakana *et al.*, 1993; Leslie *et al.*, 1986; William *et al.*, 1992; Ljundberg *et al.*, 1991; Jose *et al.*, 1996; Larsson *et al.*, 1993). Most of them favored 15% (Larsson *et al.*, 1993; Ljundberg *et al.*, 1991; Jose *et al.*, 1996; William *et al.*, 1992). Base on the literature, we defined tetraploidy as DNA index greater than 1.8 and less than 2.2, while the frequency of the cell population was at least 15% of the total cell number measured. According to this definition, only 1 sample (46-II) was classified as tetraploid according to these criteria.

1.2 Image Analysis Using Cytospin Preparations

During the last decade, image cytometry (ICM) has become an established technique in the field of analytical cellular pathology. The Feulgen reaction produces a specific blue staining of nuclear DNA. This reaction is said to bind stoichiometrically to nuclear DNA, so that the integrated optical density (IOD) obtained by ICM is proportional to the amount of DNA content in picogram (pg). DNA diploidy (DNA mass of normal human diploid cells) corresponds to 7.18 pg.

Calibration is essential for quantitative DNA content analysis, which corrects for differences in staining and instrumentation that occur on a day to day basis. The calibration cells of known DNA content (e.g. rat hepatocytes touch preparations) can be used to both calibrate the system and control for staining batch variation, provide for more accurate quantitation.

The CAS 200 uses a method of calibration similar to that used in chemical assays for optical density (OD) measurements, where an external standard is used to calibrate OD to mass units. This method is illustrated in figure 6.2. Since the Feulgen reaction is stoichiometric, the calibration consists of determining a linear equation relating DNA in picogram to OD as indicated in figure 6.2. Tetraploid nuclei from rat hepatocytes touch preparations are used as known standards. They represent a constant on the picogram axis of the calibration graph. The calibration procedure consists of measuring the

summed OD (∑OD) of these nuclei (Bacus and Grace, 1987), which have been in the same staining batch, preferably on the same slide, and determining the modal ∑OD from the measurements. This modal ∑OD is a variable parameter and is used with the known constant of 13.35 pg for these rat hepatocytes tetraploid nuclei to obtain a "one point" calibration (or linear equation) relating ∑OD under these staining and optical microscope operating conditions to DNA mass in picogram. The slope (k) of the calibration linear equation is determined by the intersection of the known reference nuclear DNA mass and the measured ∑OD. It is illustrated for two different calibrations in figure 6.2.

Mass in picogram for any ∑OD measurements on specimen cells can then be obtained from the linear equation during a measurement session. It is not necessary for the calibration nuclei to be equal in mass to human diploid nuclei. They simply need to be a population of objects containing a constant "packaged" amount of DNA for each object.

According to the consensus report of ESACP task force on standardization of diagnostic DNA image cytometry (Böcking *et al.*, 1994), a correction factor should be made base on the DNA measurement variations between the reference cells used and the diploid cells of the tissue under study.

In our study, normal tubular epithelial cells of the same patient served as diploid reference. The mean DNA mass of diploid control cells measured was 6.6 ± 0.44 pg. which was lower than the actual value of 7.18 pg.

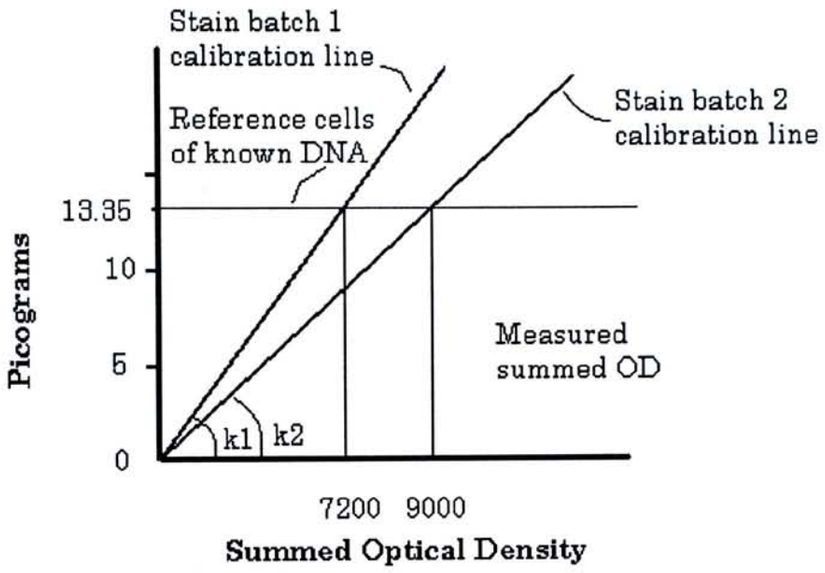

Cell Mass = k (Summed OD) for each cell measured

DNA Index = Cell Mass / Species Diploid Cell Mass

Figure 6.2 The calibration method used to obtain DNA in mass units from ΣOD measurements. Calibration cells of known DNA content are first measured to obtain a modal ΣOD values. This is used to compute the slope *k* of the linear equation relating ΣOD to mass in picograms (Bacus *et al.*, 1994).

Several factors contributed to the lower value of measured normal diploid DNA mass. First of all, the process of our specimens was different from the commercially available calibration cells, particularly in disaggregated archival tissues. Acidic solution was used during disaggregation, which prematurely started the hydrolysis and might influence the accessibility of the DNA specific dye.

Other factors include light DNA staining caused by staining error, improper calibration, false microscope and light setup etc.

DNA index (DI) was defined as the ratio of the mean values of the G_0/G_1 peak of the cells of interest (tumor cells) to certain defined standard cells (normal tubular epithelial cells of the same individual). DNA diploid was defined as DI between 0.85 to 1.15. DI fell within 1.85 to 2.15 was categorized as tetraploid. All the other DI value was termed aneuploid. Intratumoral heterogeneity was defined as two or more tumor stemlines with different DNA ploidy status present.

1.3 Image Analysis Using Tissue Sections

DNA ploidy analysis on tissue sections has been advocated in recent years. One of the distinct advantages is morphological correlation. The retention of tissue architecture in sections enables measurements performed directly on cells of interest. The potential limitation of loss of specific cell populations in disaggregation techniques for cytological preparation can be avoided (Danque *et al.*, 1993). This is also feasible to perform DNA ploidy analysis in small biopsy materials and microscopic lesions, for example in-situ lesions.

However, ICM DNA analysis performed on tissue sections presents formidable problems: cut nuclei cause a low estimate of DNA content; overlapping nuclei result in overestimation of DNA content. All these hamper the application of tissue section in DNA ploidy assessment.

Bacus *et al.* (1994) introduced a method to correct the DNA content of partially cut nuclei. The method based on the assumptions that 1. genetic materials were evenly distributed in nucleus. 2. nuclei were modeled as spheres. 3. the nuclei centered in the section would be measured even if they were cut off at the top and bottom.

The correction method used is an extension of the method first proposed by McCready and Papadimitriou (1983). The purpose is to repair the effects of sectioning a nucleus too large in diameter to be contained in the section. The equation for the volume fraction (F) of the retained sphere is

$$F = \frac{3T}{4R} - \frac{T^3}{16R^3} \qquad \text{equation(1)}$$

Where R is the radius of the nucleus, T is the section thickness. Thus the fraction of the sphere retained is only a function of the tissue thickness (T) and radius (R), which can be calculated directly from the measured nuclear area, assuming the spherical model.

Each measured nucleus with measured DNA mass (m) is then adjusted to a "corrected" DNA mass (M) according to its measured nucleus area, with thickness as constant parameter, by

$$M = \frac{m}{F} \qquad \text{equation (2)}$$

The partially cut nuclei can then be corrected to its intact volume provided that the section thickness is accurate.

Accurate section thickness is essential because of the sensibility of the correction calculation to the thickness parameter T. However, inaccuracy of microtome sectioning is well known (Allison and Vincent, 1990). Mechanical cutting errors may result in thickness deviations from the default setting (e.g. 6 μm in our study).

Uncertain section thickness can be calculated by measuring normal control cells in the section whose DNA content known to be 7.18 pg. Having known the proper T from the diploid control cells for that section, the target (tumor) cells can be corrected properly using that value of T.

Thickness correction is a defaulted function of QDA program in the CAS 200 image analyzer we used. The DNA mass in picogram of each measured nuclei can be automatically corrected for any given section thickness.

However, fragmented nuclei, overlapped nuclei, irregularly shaped or spindled nuclei, and non-uniform nuclear DNA distribution are causes of potential artifacts and wide coefficients of variation in the DNA histograms. In the QDA software program in the CAS 200 image analyzer, a filter function is installed. By selecting a proper filter, it can enable us to filter out the unwanted debris and fragmented nuclei, which were not suitable for analysis (CAS 200 user manual). Since the captured images of the nuclei were also projected in the computer screen, degenerated or fragmented cell not suitable for analysis could be rejected.

Despite the inherent limitations, ICM DNA analysis performed on tissue sections appeared to provide useful information on DNA ploidy status. In our study, a high concordant rate (89%) was found between image analysis of sections and cytospins. In one case (case 45), small cluster of high-grade nuclei can be identified in tissue section and classified as DNA aneuploid. Both samples of this case were classified as diploid by FCM and ICM cytospin measurements (Figure 6.3). We took this as evidence that the overwhelming diploid populations in FCM might mask small aneuploid stemline that was clearly identified under microscope in tissue sections and sometimes, in ICM measurement using disaggregated solid tumors samples. Our results do support the potential application of ICM on tissue section in DNA ploidy study.

A

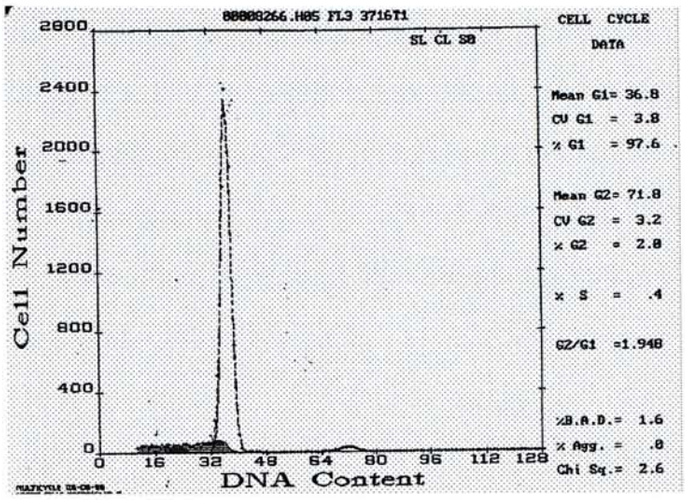

B

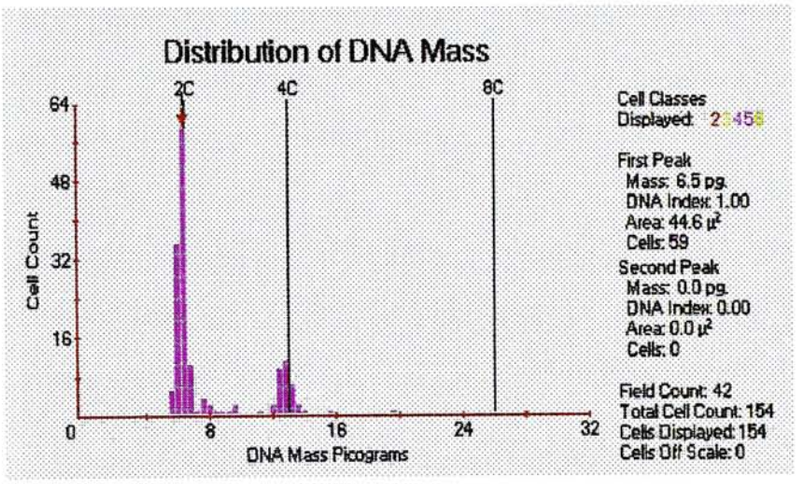

C

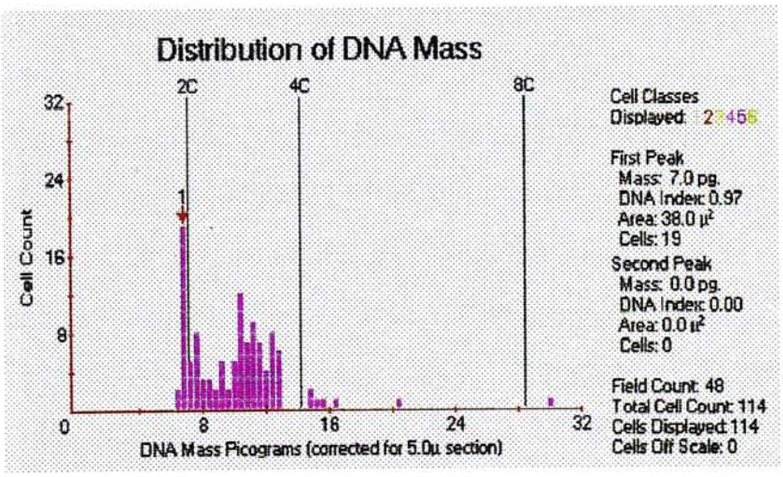

Figure 6.3 Case 45-I This case showed diploid histogram by flow cytometry (A) as well as image analysis (cytospin) (B). However, there was an aneuploid peak appeared in image analysis (section) histogram(C).

1.4 Intratumoral Heterogeneity

In the model of multistep tumor oncogenesis, multiple genetic events occur during the progression of the tumor. Each step might induce the emergence of a new subclone with a selective growth advantage (Weiss, 1985; Vogelstein *et al.*, 1989). This evolution proceeds towards increased autonomy by a temporal change in various tumor cell characteristics, where the acquisition or loss of various phenotypes can be independent of each other (Nicholson, 1987).

It is evident that malignant tumors contain a variety of subpopulations of cells with different invasive and metastatic capabilities and that increased genetic instability enhances the rate of tumor progression (Nowell, 1986). This phenomenon of "intratumoral heterogeneity" can be demonstrated on many levels including cytogenetic alteration, DNA ploidy, cell kinetic properties and etc.

Previously a considerable heterogeneity has been reported for DNA ploidy in RCC (Bringuier *et al.*, 1993; Master *et al.*, 1992; Ljundberg *et al.*, 1996). The highest frequency in RCC was reported by Ljundberg *et al.* in 1996 that is 56% of the cases.

As limited by the number of the archival paraffin blocks available and in order to standardize the number of tissue blocks taken from each tumor, two paraffin blocks were selected for each case in our study. In FCM, 4% of cases showed intratumoral heterogeneity. The percentage of heterogeneous cases in ICM (cytospins) was 19.6%, while in ICM on tissue section was 32.6%. Thus, intratumoral heterogeneity could be demonstrated by all three methods. Multiple sampling may reveal more cases having intratumoral heterogeneity. In order to properly evaluate the potential prognostic value of DNA ploidy status in RCC, multiple sampling is important. ICM detected more aneuploid and heterogeneous cases than FCM did. Even when small numbers of samples were available (2 blocks in our study), ICM detected 32.6% intratumoral heterogeneity compared with 4% by FCM. As ICM is more sensitive in detecting

aneuploidy, we can speculate that more aneuploidy can be detected by ICM using fewer samples.

On the other hand, in our study no significant difference in event-free survival time for patients with or without intratumoral heterogeneity can be demonstrated. This observation also in keeping with other study (Ljundberg *et al.*, 1996). In regarding to DNA ploidy, the prognostic significance of intratumoral heterogeneity itself is currently uncertain.

1.5 Comparison of the Results from Three Methods

In general, there were good agreements among the three methods. One case was excluded because of high CVs in FCM histograms (despite repeats). Thus, totally 90 samples from 45 cases were compared. The concordant rate between ICM using cytospin preparations and tissue sections was 89% (80 out of 90 samples). The concordant rate between ICM using cytospin preparations and FCM was 79% (71 out of 90 samples) while between ICM using tissue sections and FCM was also 79% (71 out of 90 samples).

Among those discordant cases, all were seen in cases showed diploid histograms in FCM analysis, but appeared as aneuploid or tetraploid in either ICM (cytospin) or ICM (tissue section) analysis. This observation was also in agreement with the literature and was attribute to the increased sensitivity of detecting nondiploid populations in ICM analysis (Bowman *et al.*, 1995; Lanigan *et al.*, 1993).

Image analysis offers the advantage of visual selection of target cells. Tumor cells can be identified during measurements. Thus the ICM DNA histograms contain only cells of interest. This function is important when there are only a small amount of target cells presented in the sample been measured. In flow cytometry, large numbers of cells are analyzed automatically. Detection of very small population of aneuploid or tetraploid has not always proven possible by this methods (Schmidt *et al.*, 1993;

Papadopoulos *et al.*, 1995). Selective cell loss during the processing for FCM analysis might also occurred (Bauer *et al.*, 1990; Dawson *et al.*, 1990; Lee *et al.*, 1992). High CVs, ambiguous definition of tetraploidy further hampers the accurate determination of DNA ploidy status. These are particular features when intratumoral heterogeneity appears.

ICM analysis was also advocated to clarify the difficult areas in the FCM histogram. Some of our cases may also illustrate this point. Case 7-I, 10-II were initially classified as diploid by FCM. Both of them were classified as aneuploid by ICM analysis. Re-analysis the FCM histograms found that there were small aneuploid peaks, which were ignored or regarded as S-phase fractions of the diploid populations. Comparing the results from ICM analysis, these small peaks might indicate small aneuploid populations (Figure 6.4).

Similarly, Case 11, 20 and 29 were clearly categorized as tetraploid by ICM but by definition they were diploid in FCM. In these cases the G_2/M regions were greater than the upper limit of G_2/M region of normal diploid populations (8%) but lower than our cutoff point (15%) for tetraploidy (Figure 6.5).

Regarding the discordant cases between ICM (cytospin) and ICM (tissue section), the disagreement lay mainly in the determination of tetraploid and near tetraploid aneuploid.

Both case 25-II and 35-II were classified as aneuploid by ICM cytospin but tetraploid by ICM section (Figure 6.6). Conversely, case 11-II, 19-I, 20-II and 29-II were tetraploid by ICM cytospin but aneuploid by ICM section (Figure 6.7).

A

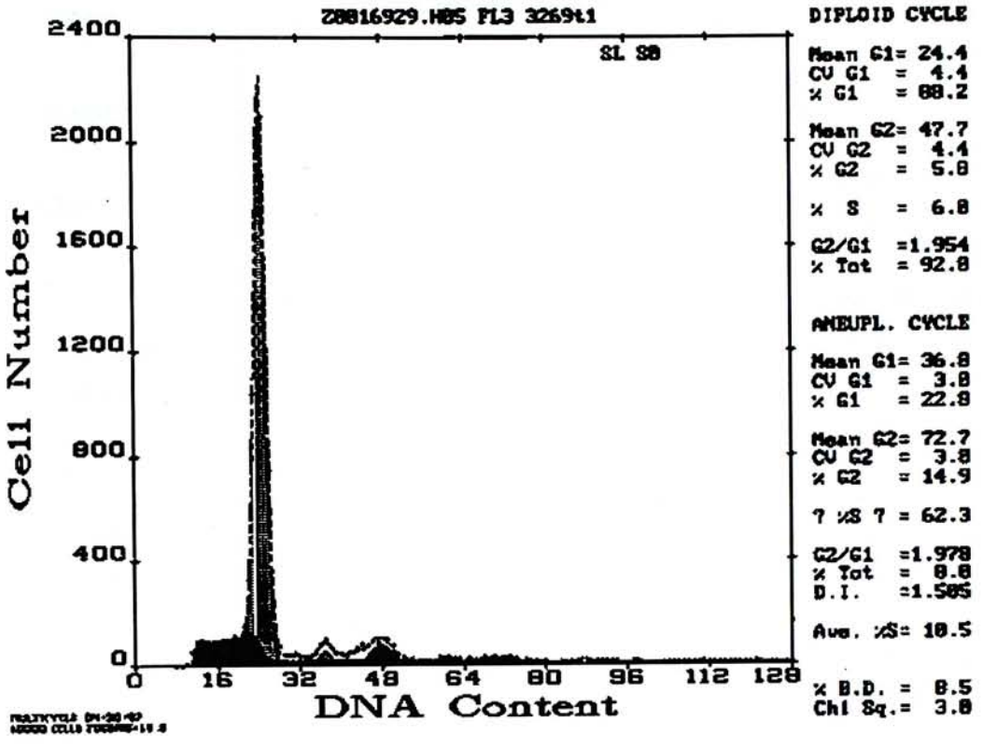

B

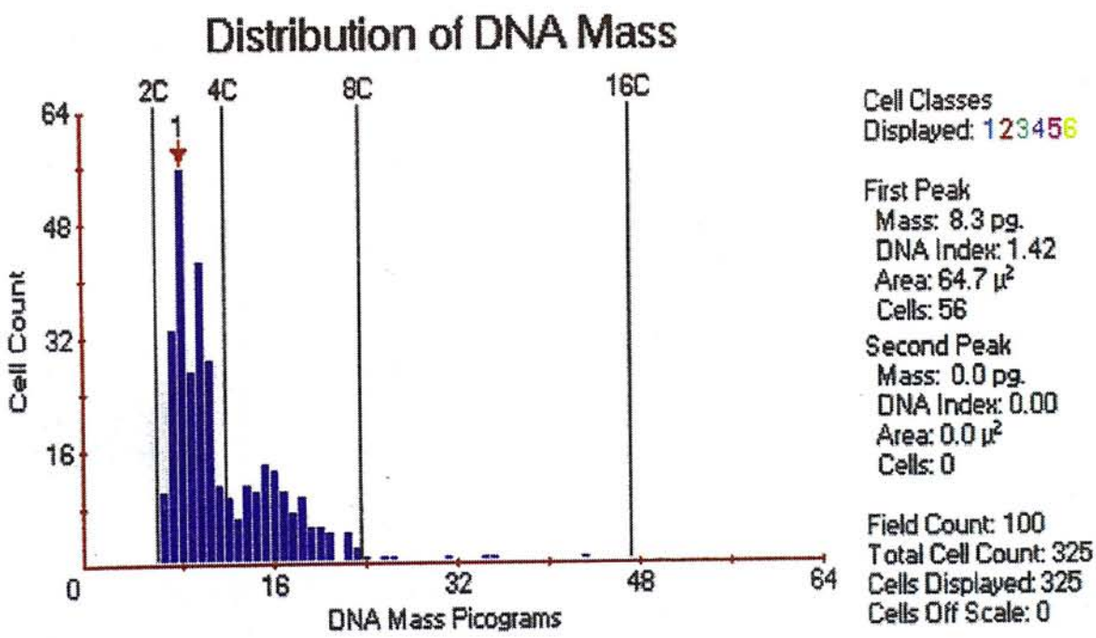

Figure 6.4 Case 7-I
This case was initially classified as diploid by flow cytometry. However, image analysis showed an aneuploid histogram (B). Re-analyzing FCM histogram found a small aneuploid peak which was first considered as the S-phase fraction of the diploid population (A).

A

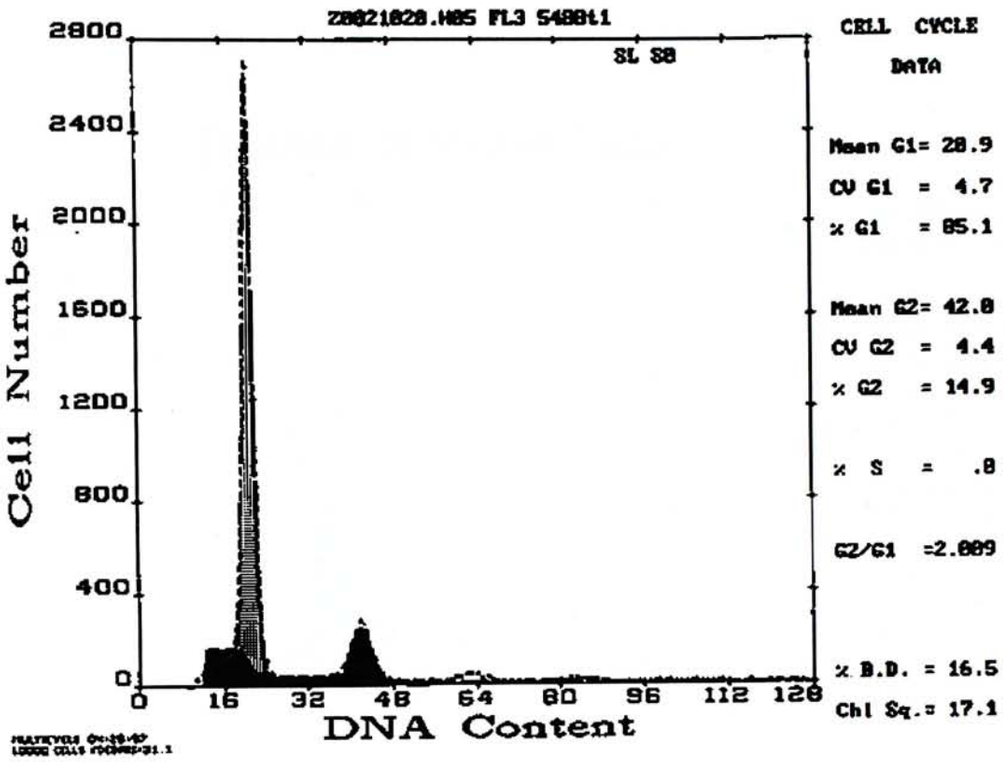

B

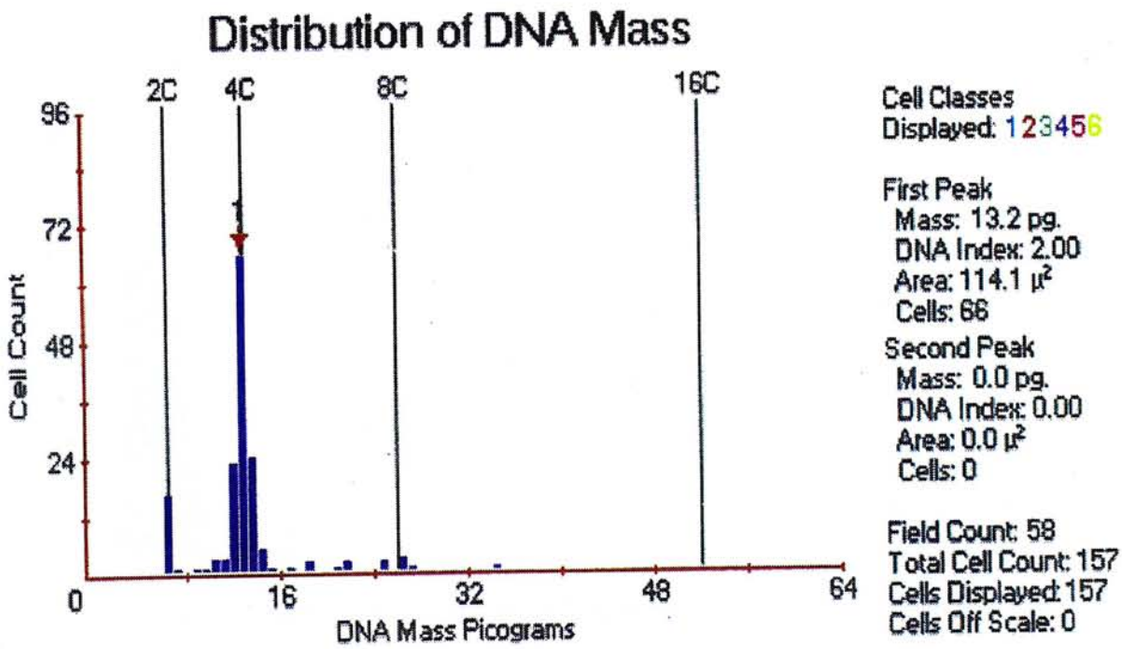

Figure 6.5 Case 29-II
Flow cytometric analysis showed a diploid histogram with relatively higher G2/M region (14.9%) (A).
Image analysis showed a tetraploid histogram (B).

A

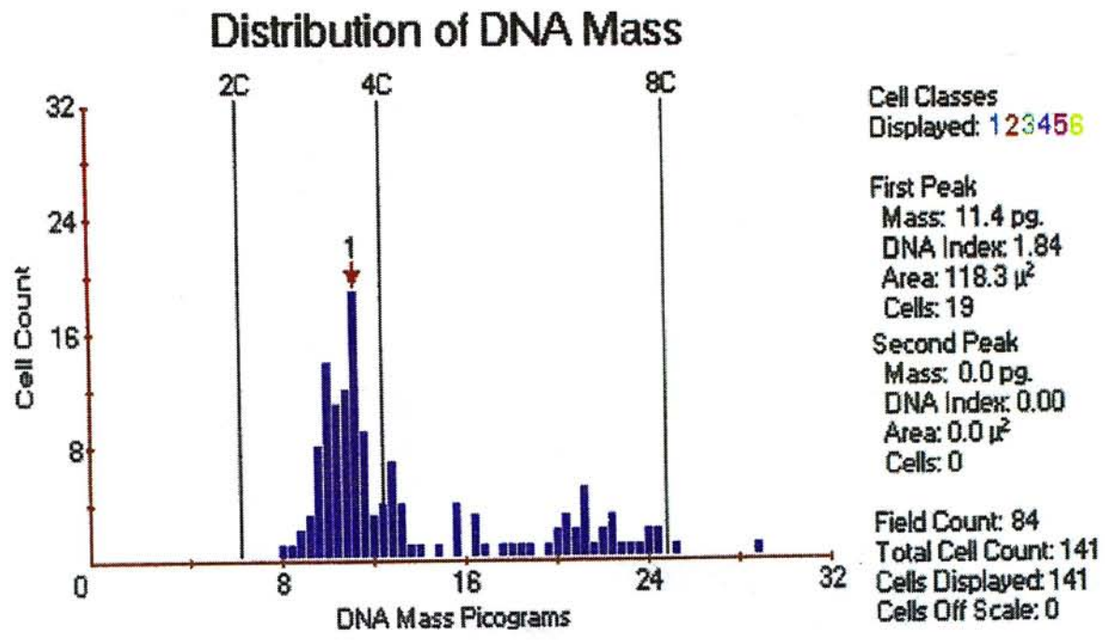

B

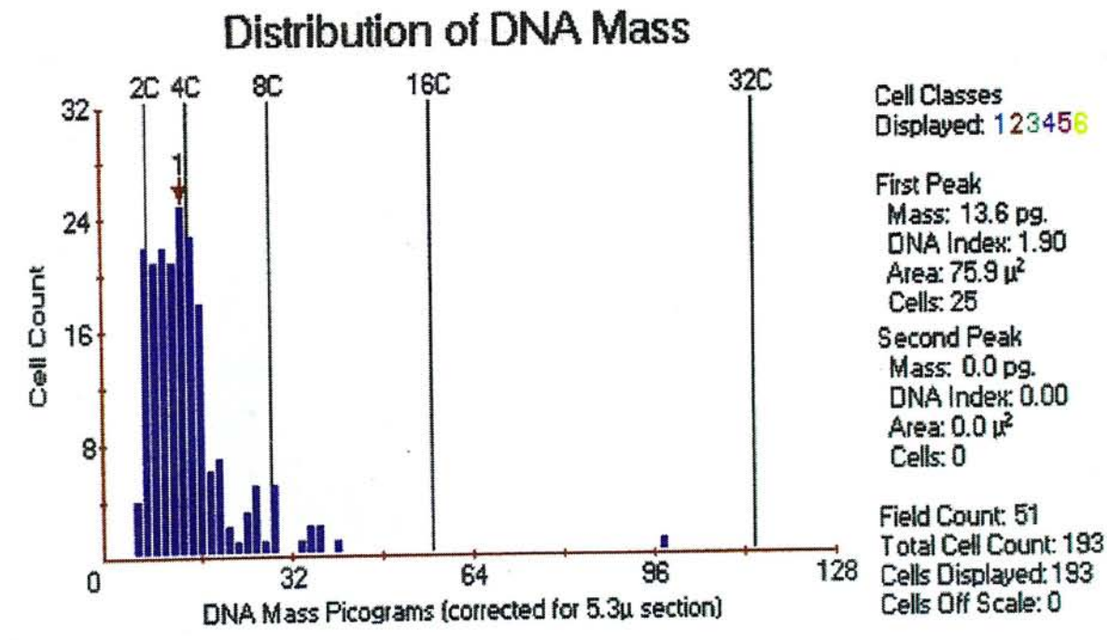

Figure 6.6 Case 25-I
This case was classified as aneuploid by image analysis (cytospin) (A) but tetraploid by image analysis (section)(B).

A

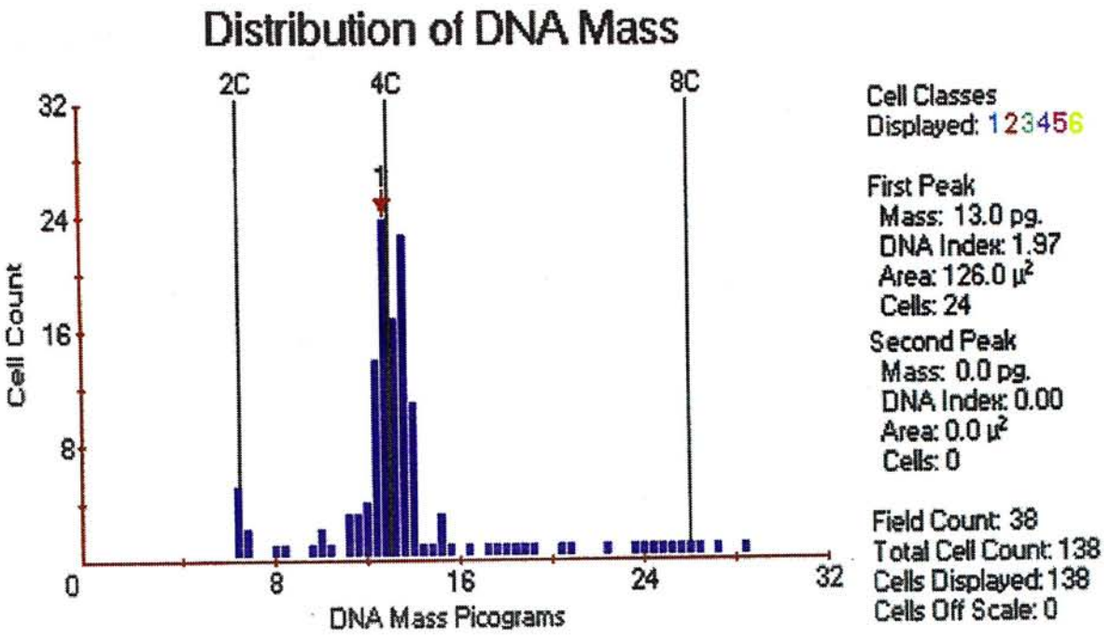

B

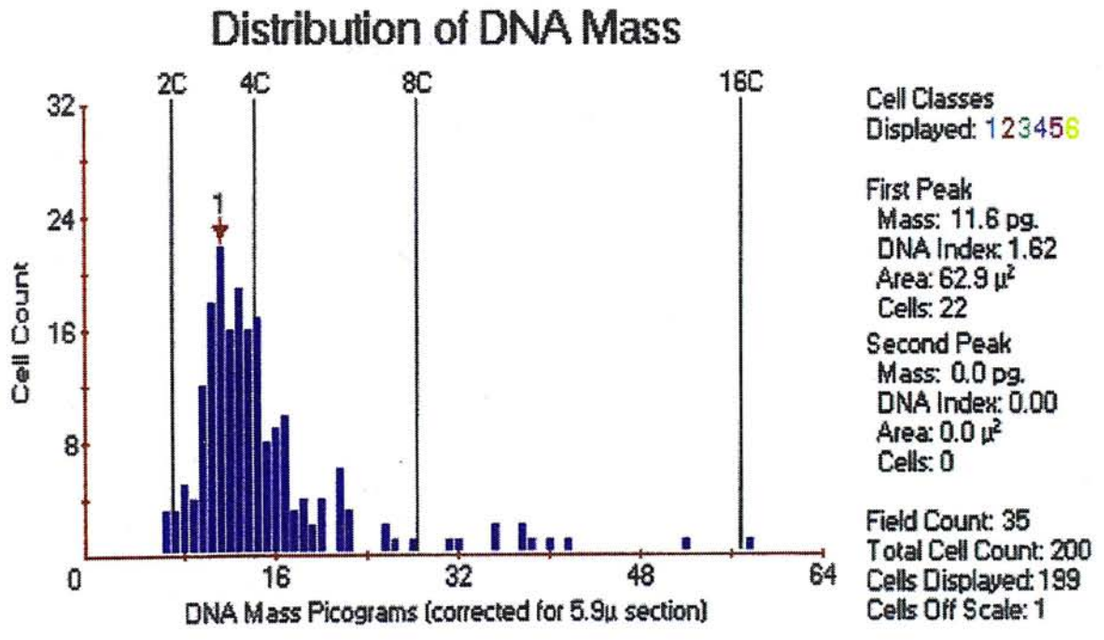

Figure 6.7 Case 11-II
Image analysis (cytospin) showed tetraploid histogram (A)
This case was classified as aneuploid by image analysis performed on tissue section (B).

A possible explanation is the limitation of thickness correction procedure. As mentioned in the previous section the thickness correction is based on the assumptions that the nuclei are perfectly spherical, the nuclear materials are uniformly distributed and the nuclei are centered in the section. Practically no nuclei can be perfectlyspherical and tumor cells will be more bizarre and pleomorphic. Nuclear materials are not uniformly distributed. In some cases that didn't have internal normal diploid cells in the same section for tissue thickness correction, this would introduce errors.

Koss (1994) has stated that tissue section can only be classified grossly as either diploid or aneuploid by ICM analysis. In regarding the detection of diploid and non-diploid samples, the concordant rate between ICM (cytospin) and ICM (tissue section) was very high in our study, i.e. 95.6% (86 out of 90 samples).

As mentioned before, in one case (case 45), small area of tumor cells with high-grade nuclei can be clearly identified in tissue section and classified as DNA aneuploid. Both samples of this case were classified as diploid by FCM and ICM cytospin measurements. This may be related to the small population of cells being masked by the diploid population or due to selective cell loss in the processing of nuclear suspension. It appears that ICM (tissue section) may be able to provide additional information in DNA ploidy analysis. Thus, our results supported the applicability of ICM on tissue section in DNA ploidy analysis.

1.6 The Potential Significance of the DNA Ploidy Status

Although the precise nature of aneuploidy as well as tetraploidy is unclear, there were numerous studies try to investigate its potential prognostic value (Russack, 1994; Ljundberg *et al.*, 1985; 1986; 1996). The prognostic value of DNA ploidy study in renal cell carcinoma has always been controversial. Although most DNA content studies in RCC have shown a significant association between tumor ploidy and patient outcome (Grignon *et al.*, 1989; Rainwater *et al.*, 1987; Raviv *et al.*, 1993; Ljundberg *et al.*, 1991), several others have not (Currin *et al.*, 1990; Lanigan *et al.*, 1993; Nakano *et al.*,

1993; Chin *et al.*, 1985). One of the possible reasons for the discrepancies can be explained by intratumoral heterogeneity. However, intratumoral heterogeneity itself has not been proven to have prognostic significance.

Other possible explanation may be related to the different measurement methods. Most studies made used of flow cytometry. However, limitations of FCM were encountered (Bauer *et al.*, 1990; Dawson *et al.*, 1990; McFadden, 1990). Several authors were also used ICM and it appeared to have a higher detection rate of non-diploid population, and might help to clarify the difficult areas in FCM histogram (Lanigan *et al.*, 1993). Our results were also in keeping with this observation. Thus, these three methods appear to be complementary and combination of different methods to the DNA ploidy assessment may be more accurate.

In our study, the ploidy status assessed by all three methods showed prognostic significance in regarding to the event-free survival in high stage patients, supporting the potential prognostic value of DNA status in those patients with renal cell carcinoma. On the other hand, the significance of detection of additional non-diploid population, presumably small population, by ICM remained uncertain. However, further studies with larger samples and longer follow up period are required addressing this issue.

Concerning with other clinical-pathological factors, positive correlation between DNA ploidy (by all 3 methods) and Fuhrman's grade as well as nuclear area have been observed. This is also in agreement with the literature (Tannapfel *et al.*, 1996; Jochum *et al.*, 1996).

It has been speculated that aneuploid may indicate increased genomic instability, increased mutability or a higher frequency of DNA rearrangements (Fallenius *et al.*, 1988). Any or all of these factors could contribute to the emergence of aggressive phenotypes. However, presence of aneuploidy implies gross genetic abnormality. Tumor cells with apparently normal DNA content (diploid) could possess chromosomal abnormalities, for example, balanced translocations, small deletions and so forth. In

addition, genetic mutations at the molecular level, which could influence the biological behavior of the tumor, would only be detected by molecular biology techniques. Nevertheless, determination of the DNA ploidy status of RCC may provide more information in the understanding of the biological behavior of this tumor. Further studies with larger numbers of cases with longer follow up may disclose additional prognostic value in DNA ploidy analysis.

2. Proliferation Activity of RCC

2.1 Ki 67

The proliferation activity of RCC was assessed by IHC using a proliferation marker: Ki 67. This antigen represents a nuclear protein that is expressed during mitosis and appears in all phase of cycling cells (G_1, S, G_2, M phase) but not in G_0 phase (Gerdes, 1983; 1984; 1991).

The initially described antibody Ki 67 required frozen tissue for IHC study. The murine antibody MIB-1, which was derived by immunization with a bacterially expressed fragment of the human Ki 67 gene (Gerdes *et al.*, 1991; Key *et al.*, 1993), recognized the "Ki 67 motif" of the human Ki 67 antigen, can apply in routine formalin-fixed paraffin-embedded tissues (Gerdes *et al.*, 1992; Schlüter *et al.*, 1993; Kubbutat *et al.*, 1994).

In our study, expression of Ki 67 detected by MIB-1 antigen showed spatial heterogeneity in most of the samples. The heterogeneous staining pattern may be related to 1. different proliferation rate in different area of the same tumor, or presence of different tumor stemlines that were functionally and kinetically distinct from each other 2. instability with time (which is the rule in tumor and as well as in normal tissues) (Brugal *et al.*, 1993). Antigen may disappear rapidly in postmitotic cells resulting in underestimation of the growth fraction (Hall and Levison, 1990). 3. Fixation,

particularly in large tissue sections. Poor penetration of fixative or over-fixed of the peripheral area may reduce the immunoreactivity. 4. Staining error caused by, for example, unevenly distributed reagents.

There is still no general consensus on whether Ki 67 positive rate should be determined in random fields or in the areas with highest expression (Linden *et al.*, 1992). However, the biological behavior of a tumor may be more related to its most rapidly proliferating region (deRiese *et al.*, 1991; 1993). Taking into account of all these factors, we scored the highest expression areas.

The diagnostic and prognostic value of Ki 67 immunoreactivity of human tumor has been widely documented and accepted (Gerdes *et al.*, 1990; Hall and Wood, 1990), for examples, in breast and bladder carcinomas (Barbareschi *et al.*, 1994; Mazerolles *et al.*, 1994). In our study, Ki 67 (MIB-1) expression was shown to be significantly associated with Fuhrman's nuclear grade ($r=0.41$, $p=0.007$), nuclear area ($r=0.35$, $p=0.02$) and Robson's stage ($r=0.43$, $p=0.004$). Multivariate analysis showed that the expression of Ki 67 (MIB-1) was an independent prognostic parameter for event-free survival in this set of patients. Our findings were in agreement with the literature of immunostaining for the Ki 67 antigen in RCC (Jochum *et al.*, 1996; deRiese *et al.*, 1993)

Immunohistochemical staining for Ki 67 (MIB-1) is a relatively simple and reliable procedure. Our results supported the prognostic value of this antigen expression and the possible role of clinical application.

2.2 $p27^{kip1}$

Recent studies of cell cycle regulation have shown that $p27^{kip1}$ protein has an important regulatory role in cell cycle progression. $p27^{kip1}$ belongs to the cip/kip family of cyclin-dependent kinase inhibitors (CKIs). It regulates progression from G_1 to S phase by binding to and inhibiting the cyclin E/Cdk2 complex, which is required for entry into S phase (Croix *et al.*, 1997). $p27^{kip1}$ is present in large amounts in quiescent

cells and declines when cells proliferate in response to mitogenic signals such as growth factors and cytokines (Nurse *et al.*, 1994; Coats *et al.*, 1996). Current theories propose $p27^{kip1}$ to be a central signal, which coordinate the varied inputs from the extracellular environment and serves as a threshold for progression to S phase or for exit from the cell cycle (Steeg *et al.*, 1997).

It was reported that expression of $p27^{kip1}$ protein was markedly decreased in benign and malignant neoplasm compared with normal tissues (Lloyd *et al.*, 1997). Some authors showed that reduced expression of $p27^{kip1}$ correlates with poor survival in breast and colorectal carcinoma patients (Loda *et al.*, 1997; Porter *et al.*, 1997). However, no studies so far have been focused on the role of this novel protein in RCC.

In our study, levels of $p27^{kip1}$ protein were evaluated by IHC. Some of the tumor samples showed heterogeneous staining. In these cases, the tumors were scored according to the areas of the highest expression.

Intense positive staining was observed in Podocytes of the glomeruli in normal renal tissues. Unexpectedly, normal tubular epithelial cells had a low positive expression rate. Negative correlation were found between $p27^{kip1}$ and Fuhrman's grade ($r=-0.47$, $p=0.0015$), Robson's stage ($r=-0.4$, $p=0.0086$) and DNA ploidy measured by FCM ($r=-0.47$, $p=0.01$). Reduced expression also correlated with poor event-free survival by univariate analysis ($p=0.04$).

The exact role of $p27^{kip1}$ abnormalities in tumor development is uncertain. As mutations are relative rare in $p27^{kip1}$ gene, other mechanisms, such as translational control with decreased $p27^{kip1}$ protein (Hengst *et al.*, 1996) or down-regulation of $p27^{kip1}$ by specific mitogens (Coats *et al.*, 1996) or possibly by brain-specific activators such as the noncyclin activator p35 (Lee *et al.*, 1996) may occur during tumor development. Increased proteasome-mediated degradation may also contribute to the low expression of $p27^{kip1}$ (Loda *et al.*, 1997).

Interestingly, three cases of oncocytoma had a negative $p27^{kip1}$ immunostaining. Two of them had follow-up data and both were remain free of disease at the time of last follow up. The implication and significance of this observation remained unclear.

Nevertheless, the current findings suggested a potential prognostic value of this recently described antigen expression in renal cell carcinoma patients. Further studies are required confirming these findings.

3. Nuclear Grade

The histological grade of the tumor has been found to be an independent prognostic factor on patients with RCC (Fuhrman *et al.*, 1982; Nurmi, 1984; Thoenes *et al.*, 1986; Syrjanen *et al.*, 1978). Although many grading systems have been described, none can be said to have achieved universal acceptance. One possible reason is the inherent subjectivity of histological grading criteria and poor reproducibility. Consequently, a high rate of intraobserver and interobserver variation has been reported (Lanigan *et al.*, 1994).

Nevertheless, significant correlations were observed in our study between grade and DNA ploidy measured by all three methods. The finding was in agreement with previous studies (Baish *et al.*, 1982; Ljundberg *et al.*, 1986., Oosterwijk *et al.*, 1988). DNA ploidy may provides us useful information in discriminating between low and high-grade tumors.

Correlation between grade and nuclear area was expected. It also correlates with expression of Ki 67 (MIB-1), stage, and a negative correlation with expression of $p27^{kip1}$. It was also shown to be a significant prognostic factor for event-free survival ($p=0.0073$) by univariate analysis but not an independent prognostic factor in multivariate analysis.

Nuclear grading can be performed on routinely examination of tissue section. It appears that it still remains a useful and easily applicable prognostic factor.

4. Stage

Stage of patients with renal cell carcinoma has been the most consistent predictor of outcome (Fuhrman *et al.*, 1982; Skinner *et al.*, 1971; Nurmi, 1984; Medeiros *et al.*, 1988). The staging system proposed by Robson *et al.* has achieved widespread acceptance. Many studies have supported the prognostic value of Robson staging system (Nurmi, 1984; Medeiros *et al.*, 1988; Sogani *et al.*, 1983), although others have refuted this point (Skinner *et al.*, 1971; Libertino *et al.*, 1987; Medeiros *et al.*, 1988).

In the current study, Robson stage has been demonstrated to be a strong predictor of event-free survival ($p<0.0001$). It was also an independent prognostic parameter by multivariate analysis.

Regarding the relationship between the ploidy status and tumor stage, Tribukait *et al.* (1987) reported that the correlation is unclear. However, Currin *et al.* (1990) indicated that the incidence of aneuploid tumors was higher on patients with N1 or M1 disease than on patients with $T_{1\text{-}2}N_0M_0$ tumors.

The current study showed a trend for more aneuploid tumors among patients with high-stage disease, which is consistent with the report of Currin *et al.* However, statistical significance can not be demonstrated.

Chapter 7

Conclusion

Our studies supported that all three methods, namely FCM, ICM (cytospin) and ICM (tissue section), are applicable in DNA ploidy analysis in routine formalin fixed, paraffin embedded tissue.

There was a high concordant rate among the different methods. Despite the inherent limitations, the findings supported the applicability of DNA ploidy study by ICM analysis in tissue section. Thus, small biopsy samples and microscopic lesion may be also feasible for analysis.

Each methods have it's own advantages and disadvantages. The results can be complementary and help to clarify the DNA ploidy status. Although ICM analysis appeared more sensitive in detecting non-diploid population, the significance remained to be elucidated.

In this study, intratumoral heterogeneity of DNA ploidy was found up to 32.6% of cases. This implies that multiple sampling is important in properly evaluation of the ploidy status of RCC.

Significant differences in event-free survival were found between diploid and non-diploid tumors in high stage patients no matter what methods used. These findings supported the potential prognostic value of DNA ploidy analysis.

Nuclear grading remained to be an easily applied prognostic parameter. It also correlated with event-free survival by univariate analysis. Our study also confirmed the independent prognostic value of staging.

Evaluation of Ki 67 immunoreactivity is relatively objective and easy to perform in formalin-fixed paraffin-embedded specimens using MIB-1 antibody. Our study showed that expression of Ki 67 not only significantly correlated with nuclear grade and tumor stage, but also to the clinical course of RCC. It was an independent prognostic parameter for event-free survival by multivariate analysis.

In agreement with the literature, our results suggested that Ki 67 (MIB-1) expression is an independent prognostic factor in RCC patients. The potential clinical implications need to be addressed.

$p27^{kip1}$ protein also suggested being a potential prognostic marker. Its expression is associated with a better outcome on patients with renal cell carcinoma. It has significant correlation with event-free survival by univariate analysis. Negative correlation were found between $p27^{kip1}$ expression and nuclear grade ($r = -0.47$, $p=0.0015$), tumor stage ($r=-0.4$, $p=0.0086$) and DNA ploidy status measured by FCM ($r=-0.4$, $p=0.01$).

Chapter 8

Further studies

Comprehensive and comparative studies of DNA ploidy studies by three available methods, namely FCM, ICM (cytospin) and ICM (tissue section) are largely lacking. Our study represents an attempt to correlate the results of the three methods. Our findings supported the complementary role of these methods and the applicability of ICM on tissue sections. Further studies of similar kinds are required to confirm the findings.

Our results suggested the prognostic value of DNA ploidy status in high stage patients. The prognostic value of $p27^{kip1}$ as demonstrated in our study represented a de novo finding. However, further studies with larger cases and longer follow up period may require confirming these observations. Further attempts or studies in other cell cycle-related antigens may help to understand the biological behavior of RCC and the possible interrelationship with other clinical-pathological parameters.

Our data confirmed the independent prognostic value of expression of Ki 67 (MIB-1) in RCC patients. The potential clinical implications on management need to be investigated.

By univariate survival analysis, DNA ploidy, expression of cell cycle-related antigen (Ki 67 and $p27^{kip1}$), nuclear grade and clinical stage carried prognostic information. Stage and Ki 67 expression were the most powerful independent parameters for event-free survival by multivariate analysis. It is likely that no single parameter will serve as a complete accurate prognostic indicator when applied to individual case of RCC. Combinations of parameters may be more accurate in predicting the prognosis. Given the observation that the biological behavior of RCC patients is notoriously unpredictable, further studies in these areas remain challenging.

References

1. Alberts B, Bray D, Lewis J, Raff M, Robert K and Watson JD. Molecular biology of the cell. 2nd edtion, New York, Garland Publishing Inc., 1989.

2. Allison RT and Vincent JF. Measuring the forces acting during microtomy by the use of load cell. J Microsc 1990;159:203.

3. Asal NR, Risser DR, Kadamani S *et al.* Risk factors in renal cell carcinoma, I. Methodology, demographics, tobacco, beverage use, and obesity. Cancer Detect Prev 1988;11:359-77.

4. Askensten U, Moberger B, Auer G. Methodological aspects of cytochemical DNA assessment of adenocarcinoma of the endometrium by means of image and flow cytometry using conventionally formalin-fixed and paraffin-embedded specimens. Arch Geschwulstforsch 1990;60:209-16.

5. Auer GU, Steinberg RS and Zetterberg AD. Molecular makers in diagnostic pathology. In: The computerized cytology and histology laboratory.

6. BÜchner TH, GÖhde W, Schneider R, Hiddemann W, Kamanabroo D. Zellsynchronisation und cytocide effekte durch chemotherapie der leukämie in der klinik anhand der impulszytophotometrie. In: Impulscytophotometrie. Andreeff M (ed), Springr-Verlag, Berlin-Heidelberg-New York, 1975, pp77-86.

7. Bacus JW, Bacus JV. A method correcting DNA ploidy measurements in tissue sections. Mod Pathol 1994;7:652-64.

8. Bacus JW, Grace LJ. Optical microscope system for standardized cell measurements and analysis. Appl Optics 1987;26:3280.

9. Baisch H, KlÖppel G, Otto U. DNA analysis in renal neoplasia. In: Tumors and tumor-like conditions of the kidneys and ureters. Eble JN (ed), Churchill Livingstone, New York, 1990, pp249-260.

10. Baisch H, Otto U, KÖuig K, KlÖppel G, KÖllermann M, Linden WA. DNA content of human kidney carcinoma cells in relation of histological grading. Br J Cancer 1982;45:878-86.

11. Baisch H. Durchflubzytometrische untersuchungen des DNS-gehaltes und der proliferationskinetik menschlicher tumoren. Strahlentherapie 1984;160:431-5.

12. Banner BF *et al.* Multiparameter flow cytometric analysis of colon polyps. Am J Clin Pathol 1987;87:313.

13. Barbareschi M, Girlando S, Mauri FM, Forti S, Eccher C, Mauri FA *et al.* Quantitative growth fraction evaluation with MIB1 and Ki 67 antibodies in breast carcinomas. Am J Clin Pathol 1994;102:171-175.

14. Bard RH, Lord B, Fromowitz F. Papillary adenocarcinoma of kidney, II. Radiographic and biologic characteristics. Urology 1982;19:16-20.

15. Bauer KD, Duque RE, Shankey TV. Clinical flow cytometry: Principles and applications. Bauer KD, Duque RE and Shankey TV (eds), Baltimore, Williams and Wilkins, 1993, pp1.

16. Bauer KD, Merkel DE, Winter JN *et al.* Prognostic implication of ploidy and proliferative activity in diffuse large cell lymphoma. Cancer Res 1986;46:3173-8.

17. Bauer TW, Tubbs RR, Edinger MD, Suit PF, Gephardt GN, Levin HS. A prospective comparison of DNA quantitation by image and flow cytometry. Am J Clin Pathol 1990;93:322-6.

18. Beesley JE. Immunocytochemical avenues. In: Immunocytochemistry. A practical approach. Beesley JE (ed), The practical approach series. Oxford University press, Oxford, 1993.

19. Beltz BS and Burd GD. Immunocytochemical techniques, principles and practice. Blackwell Scientific, Massachusetts, 1989.

20. Bennington JL, Mayall BH. DNA cytometry on four-micrometer sections of paraffin-embedded human renal adenocarcinomas and adenomas. Cytometry 1983;4:31-9.

21. Benson MC *et al.* The application of perpendicular and forward light scatter to assess nuclear and cellular morphology. Cytometry 1984;5:515.

22. Bernstein J, Robbins TO. Renal involvement in tuberous sclerosis. Ann N Y Acad Sci 1991;615:36-49.

23. Berryman I, Sterrett GF, Papadimitriou JM. Feulgen DNA cytophotometry in histologic sections of mammary neoplasms. Anal Quant Cytol Histol 1984:6:19-23.

24. Bertoni F, Ferri C, Benati A, Bacchini P, Corrado F. Sarcomatoid carcinoma of the kidney. J Urol 1987;137:25-28.

25. Blute ML, Tsushima K, Farrow GM, Thernean TM, Lieber MM. Transitional cell carcinoma of the renal pelvis: Nuclear deoxyribonucleic acid ploidy studied by flow cytometry. J Urol 1988;140:944.

26. Böcking A, Giroud F, Reith A. Consensus report of the ESACP task force on standardization of diagnostic DNA image cytometry. Analy Cellular Pathol 1995;8:67-74.

27. Bowman R, Kanacki ZA, Garberolio C and Chase DR. Comparison between image and flow cytometry. A priori factors that influence technique. Anal Quant Cytol Histol 1995; 17:276-83.

28. Breeden L. Cell-cycle regulated promoters in budding yeast. Trends in Genetics 1988;4:249-253.

29. Brenner BM and Rector FC, Jr. (eds). The Kidney. 4th edtion, W. B. Saunders, Philadelphia, 1991.

30. Bretheau D *et al.* Prognostic value of nuclear grade of renal cell carcinoma. Cancer 1995;76:2543-9.

31. Bringuier PP, Bouvier R, Berger N, Piaton E, Revillard JP, Perrin P, Devoner M. DNA ploidy status and DNA content instability within single tumors in renal cell carcinoma. Cytometry 1992;14:559-64.

32. Brodsky GL and Garnick MB. Renal tumors in the adult patients. In: Renal Pathology: With Clinical and Functional Correlations. Tisher CC and Brenner BM (eds), 2nd edtion, J.B. Lippincott Company, Philadelphia, 1994.

33. Brown DC, Cole D, Gatter KC, Mason DY. Carcinoma of the cervix uteri: an assessment of tumor proliferation using the monoclonal antibody Ki 67. Br J Cancer 1988;57:178-81.

34. Brugal G. Interpretation of proliferation markers. The Computerized Cytology and Histology Laboratory. pp234-240.

35. Bubendorf L, Sauter G, Moch H, Schmid HP, Gasser TC, Jordan P and Mihatsch MJ. Ki 67 labeling index: an independent predictor of progression in prostate cancer treated by radical prostatectomy. J Pathol 1996;178:437-441.

36. Burholt DR, Shackney SE, Ketterer DM, Pollice AA, Schepart BS. Karyotypic evolution of a human undifferentiated large cell carcinoma of the lung in tissue culture. Cancer Res 1989;49:3355-61.

37. Cattoretti G, Pileri S, Pataavicini C, Becker MHG, Pgooi S. Antigen unmasking on formalin-fixed paraffin-embedded tissue sections. J Pathol 1992;168:357-63.

38. Catty D (ed). Antibodies: A practical approach, Vol. I, IRL Press, Oxford, 1988.

39. Catzavelos C, Bhattacharya N, Ung YC, Wilson JA, Roncari L, Sandhu C, Shaw P, Yeger H, Morava-Protzner I, Kapusta L, Franssen E, Pritchard KI and Slingerland JM. Decreased levels of the cell-cycle inhibitor $p27^{Kip1}$ protein: prognostic implications in primary breast cancer. Nature Med 1997;3:227-230.

40. Chieco P, van Noorden C. Mod Pathol 1996;9(1):84-6 (Letter).

41. Chin JL, Pontes JE, Frankfurt OS. Flow cytometric deoxyribonucleic acid analysis of primary and metastatic human renal cell carcinoma. J Urol 1985;133:582-5.

42. Chisholm GD. Nephrogenic ridge tumors and their syndromes. Ann NY Acad Sci 1974;230:403-23.

43. Claud III D, Weinstein RS, Howeedy A, Straus AK, Coon JS. Comparison of image analysis of imprints with flow cytometry for DNA analysis of solid tumors. Mod Pathol 1989;2:463-7.

44. Coats S, Flannagan W, Nourse J and Roberts J. Requirement of $p27^{Kip1}$ for restriction point control of the fibroblast cell cycle. Science 1996;272:877-880.

45. Cohen C, DeRose PB. Mod Pathol 1996;9:85-9 (Letter)

46. Cohen C. Image cytometric analysis in pathology. Hum Pathol 1996;27:482-93.

47. Colvin RH and Dickersin GR. Pathology of renal tumors. In: Genitourinary Cancer. Skinner DG and DeKernion JB (eds), W. B. Saunders, Philadelphia, 1978, pp84.

48. Coon JS, Scheartz D, Summers JL, Miller AW, Weistein RS. Flow cytometry of deparaffinized nuclei in urinary bladder carcinoma. Compare with cytogenetic analysis. Cancer 1986;57:1549-99.

49. Cox D. Regression models and life tables (with discussion) J.R. Statist. Soc. 1972;B34:187-220.

50. Currin SM, Lee SE, Walther PJ. Flow cytometric assessment of deoxyribonucleic acid content in renal adenocarcinoma: does ploidy status enhance prognostic stratification over stage alone? J Urol 1990;143:458-63.

51. Danque POV, Chen HB, Patic J, Jagirdar J, Orsatti G, Paronetto F. Image analysis versus flow cytometry for DNA ploidy quantitation of solid tumors: a comparison of six methods of sample preparation. Mod Pathol 1993;6:270.

52. Darzynkiewicz Z, Traganos F, Kapuscinski J, Staiano-Cuico L, Melamed MR. Accessibility of DNA in situ to various fluorochromes: relationship to chromatin

changes during erythroid differentiation of Friend Leukiemia cells. Cytometry 1984;5:355-63.

53. Davis CJ, Jr., Mostofi FK, Sesterhenn IA. Renal medullary carcinoma: the seventh sickle cell nephropathy. Am J Surg Pathol 1995;19:1-11.

54. Dawson AE, Austin RE, Weinberg DS. Nuclear grading of breast carcinoma by image analysis: classification by multivariate and neural network analysis. Am J Clin Pathol 1991;95:suppl1:s29-s37.

55. Dawson AE, Norton JA, Weinberg DS. Comparative assessment of proliferation and DNA content in breast carcinoma by image and flow cytometry. Am J Clin Pathol 1990;136:1115-123.

56. De Jong ASH, Van Kessel-Van Mark and Raap AK. Sensitivity of various visualization methods for peroxidase and alkaline phosphatase activity in immunoenzyme histochemistry. J Histochem 1985;17:1119-30.

57. deKernion JB and Belldegrun A. Renal tumors. In: Campbell's Urology. Walsh PC *et al.* (eds), 6th edtion, Philadelphia, WB Saunders Co., 1992, pp1053-1093.

58. deRiese W, Allhoff E, Werner M, Stief CG, Atzpodien J and Kirchner H. Proliferation kinetics and prognosis of renal cell carcinoma. Onkologie 1991;14:297-302.

59. deRiese WT, Crabtree WN, Allhoff E, Werner M, Liedke S, Lenis G *et al.* Prognostic significance of Ki-67 immunostaining in nonmetastatic renal cell carcinoma. J Clin Oncol 1993;11(9):1804-1808.

60. Devonec M, Hijazi A, Bringuier PP, Dutrieux-Berger N, Perrin P, Revillard JP. Flow cytometric demonstration of shared antigens between human bladder cancer cells and normal host macrophages. Eur Urol 1989;16:57-62.

61. Devonec M, Hijazi A. A new concept in the natural history of human bladder cancer based on genetic instability of tumors as evidenced by flow cytometric DNA analysis. In: Clinical cytometry and histometry. Burger G, Plooem JS and Goerttler K (eds), Academic Press, London, 1987, pp441-6.

62. Di Silverio F, Gallucci M, Flammia GP, De Vico A, Caponera M, Eleuteri P, Forte D, Cavallo D, De Vita R. Biological and clinical implication of cellular DNA content in renal cell carcinomas. Eur Urol 1992;21 Suppl 1:43-7.

63. Dierendonck JH van, Keijeaer R, van de Velde CJH, Cornelisse CJ. Nuclear distribution of the Ki 67 antigen during the cell cycle: comparison with growth fraction in human breast cancer cells. Cancer Res 1989;49:2999-3006.

64. Dunphy WG and Newport JW. Unravelling of mitotic control mechanisms. Cell 1988;55:925-928.

65. Eble JN, Sledge G. Cellular deoxyribonucleic acid content of renal oncocytomas: flow cytometric analysis of paraffin-embedded tissues from eight tumors. J Urol 1986;136:522-4.

66. Eble JN. Neoplasms of the kidney. In: Urologic surgical pathology. Bostwick DG and Eble JN (eds). Mosby, 1997, pp84.

67. Ei-Deiry WS, Tokino T, Velculescu VE, Levy DB, Parsons R, Trent JM, Lin D, Mercer WE, Kinzler KW, Vogelstein B. WAF1, a potential mediator of p53 tumor suppression. Cell 1993;75:817-825.

68. Ekfors TO, Lipasti J, Narmi MJ, Eerola E. Flow cytometric analysis of the DNA profile of renal cell carcinoma. Pathol Res Pract 1987:182:58-62.

69. Ellis WJ, Bauer KD, Oyasu R and McVary KT. Flow cytometric analysis of small renal tumors. J Urol 1992;148:1774-1777.

70. El-Naggar AK, Ro JY and Ensign LG. Papillary renal cell carcinoma: clinical implication of DNA content analysis. Hum Pathol 1993;24:316-321.

71. Epstein JI, Christensen WN, Steinberg GD *et al.* Comparison of DNA ploidy and nuclear size, shape and chromatin irregularity in tissue section and smears of prostate carcinoma. Anal Quant Cytol Histol 1990;12:352-8.

72. Erhardt K, Auer G, Bjorkholm E *et al.* Prognostic significance of nuclear DNA content in serous ovarian tumors. Cancer Res 1984;44:2198-202.

73. Erler BS, Chein K, Marchevsky AM. Method in pathology. An image analysis workstation for the pathology laboratory. Mod Pathol 1993;6:612-8.

74. Evans MP, Podratz KC. Endometrial neoplasia: prognostic significance of ploidy status. Clin Obstet Gynecol 1996;39:696-706.

75. Evenson D, Darzynkiewicz Z, Jost L, Ballachey B. Changes in accessibility of DNA to various fluorochromes during spermatogenesis. Cytometry 1986;7:45-53.

76. Ewers SB, Langström E, Baldetrop B, Killander D. Flow cytometric DNA analysis in primary breast carcinoma and clinicopathological correlations. Cytometry 1984;5:408-19.

77. Falker UG. Image DNA cytometry: Diagnostic prognostic applications in clinical tumor pathology. Cell vision 1994;1:79-83.

78. Falkmer UG. Methodological aspects on the value of flow and image cytometric nuclear DNA assessments of neoplastic cells of prostate adenocarcinoma. Acta Oncol 1991;30:201-3.

79. Fallenius AG, Auer GU and Cartensen JM. Prognostic significance of DNA measurements in 409 consecutive breast cancer patients. Cancer 1988;62:331-41.

80. Fallon B, Williams RD. Renal cancer associated with acquired cystic disease of the kidney and chronic renal failure. Semin Urol 1989;7:228-36.

81. Farnsworth WV, DeRose PB, Cohen C. DNA image cytometric analysis of paraffin-embedded sections of small renal cortical neoplasms. Cytometry (Communications in clinical cytometry) 1994;18:223-7.

82. Farrow, Lieber and Tomera. Well differentiated (grade 1) clear cell renal carcinoma. J Urol 1983;129:933-937.

83. FarrowGM, Lieber MM and Tomera KM. Sarcomatoid renal cell carcinoma. J Urol 1983; 130:657-659.

84. Fausel RE, Burleigh W, Kaminsky DB. DNA quantification in colorectal carcinoma using flow and image analysis cytometry. Anal Quant Cytol Histol 1990;12:21-7.

85. Fero ML, Rivkin M, Tasch M, Porter P, Carow CE, Firpo E, Polyak K, Tsui LH, Broudy V, Perlmutter RM, Kaushansky K, Roberts JM. A syndrome of multiorgan hyperplasia with features of gigantism, tumor genesis and female sterility in $p27^{kip1}$-deficient mice. Cell 1996;85:733-744.

86. Ferrando AA *et al.* Mutational analysis of the human cyclin-dependent kinase inhibitor p27kip1 in primary breast carcinomas. Hum Genet 1996;97:91-94.

87. Fidler IJ, Hart IR. Biological diversity in metastatic neoplasms: Origins and implications. Science 1982;217:998-1003.

88. Frankfurt OS, Slocum HK, Rustum YM, Arbuck SG, Pavelic ZP, Petrelli N, Huben RP, Pontes EJ, Greco WR. Flow cyotmetric analysis of DNA aneuploidy in primary and metastatic human solid tumors. Cytometry 1984;5:71-80.

89. Franklin WA, Bibbo M, Doria MI *et al.* Quantitation of estrogen receptor and Ki 67 staining in breast carcinoma by the micro TICAS image analysis system. Analyt Quant Cytol Histol 1987:9:279-86.

90. Franzen G, Olafsson J, Risberg B, Klintenberg C, Nordenskjöld. DNA measurements on formalin-fixed, paraffin-embedded squamous cell carcinomas from different ENT regions. Path Res Pract 1986;181:230-235.

91. Fu YS, Cheng L, Huang I *et al.* DNA ploidy analysis of cervical condyloma and intraepithelial neoplasia in specimens obtained by punch biopsy. Anal Quant Cytol Histol 1989;11:187-95.

92. Fuhrman SA, Lasky LC, Limas C. Prognostic significance of morphologic parameters in renal cell carcinoma. Am J Surg Pathol 6:655-663,1982.

93. Gerdes J, Becker MHG, Key G and Cattoretti G. Immunohistochemical detection of tumor growth fraction (Ki-67 antigen) in formalin-fixed and routinely processed tissues. J Pathol 1992;168:85-87.

94. Gerdes J, Lemke H, Baisch H, Wacher H-H, Schwab U, Stein H. Cell cycle analysis of a cell proliferation - associated human nuclear antigen defined by monoclonal antibody Ki-67. J Immunol 1984;133:1710-1715.

95. Gerdes J, Li L, SchlÜter C *et al.* Immunobiochemical and molecular biologic characterization of the cell proliferation-associated nuclear antigen that is defined by monoclonal antibody Ki-67. Am J Pathol 1991;138:867-873.

96. Gerdes J, Schwab U, Lemke H, Stein H. Production of a mouse monoclonal antibody reactive with a human nuclear antigen associated with cell proliferation. Int I Cancer 1983;31:13-20.

97. Gilchrist KW, Hagan TF, Harberg J, Sonneland PRL. Prognostic significance of nuclear sizing in renal cell carcinoma. Urology 1984;24:122-124.

98. Graham RC, Ludholm U, Kamovsky MJ. Cytochemical demonstration of peroxidase activity with 3-amino-9-ethylcarbazole. J Histochem and Cytochem 1965;13:150-2.

99. Gregoire JR, Torres VE, Holley KE *et al.* Renal epithelial hyperplastic and neoplastic proliferation in autosomal dominant polycystic kidney disease. Am J Kidney Dis 1987;9:27-38.

100. Grignon DJ, Ayala AG, EL-Nagger A, Wishnow KI, Ro JY, Swanson DA *et al.* Renal cell carcinoma: a clinicopathological and DNA flow cytometric analysis of 103 cases. Cancer 1989;64:2133-40.

101. Grignon DJ, el-Naggar A, Green LK, Ayala AG, Ro JY, Swanson DA, Troncoso P, Mclemore D, Giacco GG, Guinee VF. DNA flow cytometry as a predictor of outcome of stage I renal cell carcinoma. Cancer 1989;63:1161-1165.

102. Gutierrez JL, Val BJ, Garijo MF, Buelta L, Portillo JA. Nuclear morphometry in prognosis of renal adenocarcinoma. Urology 1992;39:130-134.

103. Hall PA and Levison DA. Review: assessment of cell proliferation in histological material. J Clin Pathol 1990;43:184-192.

104. Hall PA, Richard MA, Gregory WM, d'Adenne Aj, Lister TA, Stansfeld AG. The prognostic significance of Ki 67 immunostaining in non-Hodgkin's lymphomas. J Pathol 1988;154:223-35.

105. Hanker JS, Yates PE, Matz CB. A new, specific, sensitive and non-carcinogenic reagent for the demonstration of horseradish peroxidase. J Histochem 1977;9:789-92.

106. Hedley DW *et al.* Application of DNA flow cytometry to paraffin-embedded archival material for the study of aneuploidy and its clinical significance. Cytometry 1985;6:327.

107. Hedley DW *et al.* Method for analysis of cellular DNA content of paraffin-embedded pathological material using flow cytometry. J Histochem Cytochem 1983;31:1333-5.

108. Hedley DW, Rugg CA, Gelber RD. Association of DNA index and S-phase fraction with prognosis of nodes positive early breast cancer. Cancer Res 1987;47:4729-35.

109. Heim S, Mitelman F. Cancer Cytogenetics. Alan R Liss Inc., New York, 1987.

110. Hengst L and Reed SI. Translational control of $p27^{Kip1}$ accumulation during the cell cycle. Science 1996;271:1861-1864.

111. Hiddemann W *et al.* Convention on nomenclature for DNA cytometry. Committee on nomenclature, society for analytical cytology. Cancer Genet Cytogenet 1984;13:181.

112. Hofmockel G *et al.* Significance of conventional and new prognostic factors for locally confined renal cell carcinoma. Cancer 1995;76:296-306.

113. Ichikawa T, Kyprianou N, Isaacs JT. Genetic instability and the acquisition of metastatic ability by rat mammary cancer cells following V-H-ras oncogene transfection. Cancer Res 1990;50:6349-57.

114. Inomiya H *et al.* Prognostic factors in patients with non-metastatic renal cell carcinoma. Nippon Hinyokika Gakkai Zasshi (JAPAN)1996;87:1099-104.

115. Jackson P and Blythe D. Immunolabelling techniques for light microscopy. In: Immunocytochemistry. A practical approach. Beesley JE (ed), The practical approach series. Oxford University press, Oxford, 1993.

116. Jochum W, Schröder S, Al-Taha R, August C, Gross AJ, Berger J and Padberg BC. Prognostic significance of nuclear DNA content and proliferative activity in renal cell carcinomas. Cancer 1996;77:514-521.

117. Johnson TS, Williamson KD, Cramer MM, Peters LJ. Flow cytometric analysis of head and neck carcinoma DNA index and S-fraction from paraffin-embedded sections, Comparison with malignancy grading. Cytometry 1985;6:461-70.

118. Kamb A. Cell-cycle regulators and cancer. Trends in Genetics 1995;11:136-140.

119. Kamel OW, Franklin WA, Ringus JC, Meyer JS. Thymidine labeling index and Ki 67 growth fraction in lesions of the breast. Am J Pathol 1989;134:107-13.

120. Kanamaru H *et al.* Analysis of histological heterogeneity in renal cell carcinoma: tumor size-related histological change and its prognostic significance. Int J Urol 1996;3:256-60.

121. Kennedy SM, Merino MJ, Linehan WM, Roberts JR, Robertson CN, Neumann RD. Collecting duct carcinoma of the kidney. Hum Pathol 1990;21:449-456.

122. Key G, Becker MHG, Baron B, Duchrow M, Schluter C, Flad HD, Gerdes J. New Ki 67 equivalent murine monoclonal antibodies (MIB 1-3) generated against bacterially expressed parts of the Ki 67 c-DNA containing 362 base pair repetitive elements encoding for the Ki 67 epitope. Lab Invest 1993;68:629-36.

123. Kiesewetter F, Hornstein OP, Hermauek P, Herrlinger A, Eberhard S. MÖglichkeiten der DNS-impullszytometrie bei nierenkarzinomen. Urologe (A) 1987;26:126-167.

124. Kimler BF, O'Connor E and Jiménez-Cruz F. Value of deoxyribonucleic acid ploidy and nuclear morphometry for prediction of disease progression in renal cell carcinoma. J Urol 1996;155:459-465.

125. Kiyokawa H, Kinerman RD, Manova-Todorova M, Soares VC, Hoffman ES, Ono M, Khanam D, Hayday AC, Frohman LA, Koff A. Enhanced growth of mice lacking the cyclin-dependent kinase inhibitor function of $p27^{kip1}$. Cell 1996;85:721-732.

126. KlÖppel G, KnÖfel WT, Baisch H, Otto U. Prognosis of renal cell carcinoma related to nuclear grade, DNA content and Robson stage. Eur Urol 1986;12:426-431.

127. Klein MJ, Valensi QJ. Proximal tubular adenomas of kidney with so-called oncocytic features, a clinicopathologic study of 13 cases of a rarely reported neoplasm. Cancer 1976;38:9096-914.

128. Kleinhans G, Langer EM, Pohl J, Leusmann DB. Aneuploidie und prognoses beim nierenzellkarzinom. Tumordiag Ther 1987;8:97-101.

129. Kohler G and Milstein C. Nature 1975;256:495.

130. Koss LG. Quantitative and analytical cytology in historical perspective. J Cellular Biochem 1994;19:23-7.

131. Kovacs G, Erlandsson R, Boldog F *et al.* Consistent chromosome 3p deletion and loss of heterozygosity in renal cell carcinoma. Proc Natl Acad Sci USA 1988;85:1517-75.

132. Kovacs G, fuzesi L, Emanual A, Kung HF. Cytogenetic of papillary renal cell tumors. Genes Chromosom Cancer 1991;3:249-55.

133. Kubbies M, Friedl R, Betterken T, Hpehn H. The fate of the primary diploid population during spontaneous transformation of growth factor supplemented murine cell cultures. Cytometry 1986;7:551-7.

134. Kubbutat MHG, Key G, Duchrow M, Schlüter C, Flad HD, Gerdes J. Epitope analysis of antibodies recognizing the cell proliferation associated nuclear antigen previously defined by the antibody Ki-67 (Ki-67 protein). J Clin Pathol 1994;47:524-528.

135. Kumar S, Marsden HB, Cowan RA, Barnes JM. Prognostic relevance of DNA content in childhood tumors. Br J Cancer 1989;59:291-5.

136. Kvaloy S, Morton PF, Kaalhus O, Hoie J, Foss-Abrahamsen A, Godal T. 3H thymidine uptake in B cell lymphomas. Relationship to treatment response and survival. Scand J Haematol 1985;34:429-35.

137. La Vecchia C, Negri E, D'Avanzo B *et al.* Smoking and renal cell carcinoma. Cancer Res 1990;50:5231-3.

138. Laffin J, Fogleman D, Lehman JM. Correlation of DNA content, p53, T antigen and V antigen in simian virus 40-infected human diploid cells. Cytometry 1989;10:205-13.

139. Lajtha LG. On the concept of the cell cycle. J Cell Comp Physiol 1963;62(Suppl 1):143-5.

140. Lanigan D, Conroy R, Barry-Walsh C, Loftus B, Royston D, Leader M. A comparative analysis of grading systems in renal adenocarcinoma. Histopathology 1994;24:473-6.

141. Lanigan D, Mc Lean, Curran B, and Leader M. Comparison of flow and static image cytometry in the determination of ploidy. J Clin Pathol 1993;46:135-9.

142. Lanigan D, McLean PA, Murphy DM, Donovan MG, Curran B and Leader M. Ploidy and prognosis in renal carcinoma. J Urol 1993;71:21-24.

143. Larsson P, Roos G, Steinling R and Ljungberg B. Tumor-cell proliferation and prognosis in renal-cell carcinoma. Int J Cancer 1993;55:566-570.

144. Layfield LJ, Ritchie AWS, Ehrlich R. The relationship of deoxyribonucleic acid content to conventional prognostic factors in Wilms tumor. J Urol 1989;142:1040-3.

145. Lee AKC, Wiley B, Dugen JM, Hamilton WH, Loda M, Heatley GJ, Cook L, Silverman ML. Quantitative DNA analysis and proliferation in breast carcinoma. Pathol Res Pract 1992;188:428-32.

146. Lee M and Nurse P. Cell cycle control genes in fission yeast and mammalian cells. Trends in Genetics 1988;4:287-290.

147. Lee MH, Nikolic M, Baptista CA, Lai E, Tsai LH and Massagué J. The brain specific activator p35 allows CDK 5 to escape inhibition by $p27^{Kip1}$ in neurons. Proc Natl Acad Sci USA 1996;93:3259-3263.

148. Lee MH, Reynisdottir L, Massague J. Cloning of $p57^{kip2}$, a cyclin-dependent kinase inhibitor with unique domain structure and tissue distribution. Genes Dev 1995;9:639-649.

149. Libertino JA, Zinman L, Watkins E. Long-term results of resection of renal cell carcinoma with extension into inferior vana cava. J Urol 1987;137:21-4.

150. Linden MD, Torres FX, Kubus J and Zarbo RJ. Clinical application of morphologic and immunocytochemical assessments of cell proliferation. AJCP 1992;5 (Suppl 1):S4-S13.

151. Linehan WM, Shipley WU, Longo DL. Cancer of the kidney and ureter. In: Principles and Practice of Oncology. Devlta VT, Hellman S and Rosenberg SA (eds), Philadelphia, JB Lippincott, 1993, pp1023-51.

152. Ljundberg B, Larsson P, Stenling R, Roos G. Flow cytometric deoxyribonucleic acid analysis in stage I renal cell carcinoma. J Urol 1991;146:697-9.

153. Ljundberg B, Mehle C, Stenling R and Roos G. Heterogeneity in renal cell carcinoma and its impact on prognosis - a flow cytometric study. British J Cancer 1996;74:123-7.

154. Ljundberg B, Stenling R, Roos G. DNA content in renal call carcinoma with reference to tumor heterogeneity. Cancer 1985;56:503.

155. Ljundberg B, Stenling R, Roos G. Prognostic value of deoxyribonucleic acid content in metastatic renal cell carcinoma. J Urol 1986;136:801.

156. Ljundberg S, Carstensen J, Rundquist I. DNA flow cytometry and histopathological grading of paraffin-embedded prostate biopsy specimens in a survival study. Cancer Res 1987;47:1973-7.

157. Lloyd RV, Jin L, Qian X and Kulig E. Aberrant $p27^{Kip1}$ expression in endocrine and other tumors. Am J Pathol 1997;150:401-407.

158. Lloyd RV, Jin L, Qian X, Kulig E. Aberrant $p27^{kip1}$ expression in endocrine and other tumors. Am J Pathol 1997;150(2):401-407.

159. Loda M, Cukor B, Tam SW, Lavin P, Fiorentino M, Draetta GF, Jessup M and Pagano M. Increased proteasome-dependent degradation of the cyclin-dependent kinase inhibitor p27 in aggressive colorectal carcinomas. Nature Med 1997;3:231-234.

160. Macartney C and Camplejohn RS. DNA ploidy analysis by flow cytometry. In: Quantitative clinical pathology. Hamilton PW and Allen DC (eds), Blackwell Science Ltd., 1995.

161. Mancilla-Jimenzez R, Stanley RJ, and Blath RA. Papillary renal cell carcinoma: A clinical radiological and pathologic study of 34 cases. Cancer 1976;38:2469.

162. Marcollet M, Morin J, Lecher P. Comparison between two chromogenic substrates for revealing an immunoperoxidase reaction of human metaphase chromosomes. Stain Technology 1980;55:35-39.

163. Masters JRW, Camplejohn RS, Constance Parkinsson M, Woodhouse CRJ and O'Reilly SM. Does DNA flow cytometry give useful prognostic information in renal parenchymal adenocarcinoma? Br J Urol 1992;70:364-9.

164. Matsuoka S, Edwards MC, Bai C, Parker S, Zhang P, Baldini A, Harper JW, Elledge SJ. P57/kip2, a structurally distinct member of the p21/CIP1 Cdk inhibitor family, is a candidate tumor suppressor gene. Genes Dev 1995;15:650-662.

165. Mazerolles C, Rishmann P, Chopin D, Popov Z, Malavaud B, Selves J, *et al.* Usefulness of MIB1 monoclonal antibody in assessing the proliferative index in human bladder carcinoma comparison with Ki-67 antibody. Histopathology 1994;25:563-568.

166. McCready RW, Papadimitriou JM. An analysis of DNA cytophotometry on tissue sections in a rat liver model. Anal Quant Cytol Histol 1983;5:117.

167. McFadden PW, Clowry LJ, Daehnert K, Hause LL, Koethe SM. Image analysis confirmation of DNA aneuploidy in flow cytometric DNA distributions having a wide coefficient of variation of the G_0/G_1 peak. Am J Clin Pathol 1990;93:637-42.

168. McLaughlin JK, Blot WJ, Mehl ES *et al.* Relation of analgesic use to renal cancer: population-based findings. NCI Monogr 1985;69:217-22.

169. Medeiros LJ, Gelb AB, Weiss LM. Renal cell carcinoma: Prognostic significance of morphologic parameters in 121 cases. Cancer 1988;61:1639-1651.

170. Mellin W. Cytophotometry in tumor pathology. A critical review of methods and applications, and some results of DNA analysis. Path Res Pract 1990;186:37-62.

171. Michael M Lieber. Renal oncocytoma. In: Cancer of the kidney. Nasser J (ed), Thieme-Stratton Inc., New York, 1984.

172. Mikel UV. Absolute DNA values from Feulgen microspectrophotometric measurements and quantitative electron microscopy. Anal Quant Cytol Histol 1987;9:13.

173. Montie JE and Levin HS. Detection and diagnosis of renal cell carcinoma. In: Clinical management of renal cell cancer. Montie JE *et al.* (eds), Year book medical publishers Inc., 1990, pp6-90.

174. Montie JE. Follow-up after partial or total nephrectomy for renal cell carcinoma. Urol Clin North Am 1994;21:589-92.

175. Morgan DO. Principles of CDK regulation. Nature 1995;374:131-134.

176. Mostofi FK, Davis Col CJ, Jr. Pathology of tumors of the kidney.

177. Mostofi FK. Pathology and spread of renal cell carcinoma. In: Renal neoplasia. King JS Jr. (ed), Little Brown & Co., Boston, 1967, pp41-85.

178. Murad T, Komaiko W, Oyasu R, Bauer K. Multilocular cystic renal cell carcinoma. Am J Clin Pathol 1991;95:633-637.

179. Murphy GF, Partin AW, Maygarden SJ, Mohler JL. Nuclear shape analysis for assessment of prognosis in renal cell carcinoma. J Urol 1990;143:1103-1107.

180. Nakano E, Kondoh M, Okatani K, Seguchi T and Sugao H. Flow cytometric analysis of nuclear DNA content of renal cell carcinoma correlated with histology and clinical features. Cancer 1993;72:1319-1323.

181. Nakayama K, Ishida N, Shirane M, Inomata A, Inoue T, Shishidu N, Horii I, Loh DY, Nakayama KI. Mice lacking $p27^{kip1}$ display increased body size, multiple organ hyperplasia, retinal dysplasia, and pituitary tumors. Cell 1996;85:707-720.

182. Nasser J. Natural history, diagnosis, and staging of renal cancer. In: Cancer of the kidney. Nasser J (ed), Thieme-Stratton Inc., New York, 1984.

183. Nativ O, Sabo E, Bejar J, Halachmi S, Moskovitz B, Miselevich I. A comparison between histological grade and nuclear morphometry for predicting the clinical outcome of localized renal cell carcinoma. Br J Urol 1996;78(1):33-8.

184. Nicolson GL. Tumor cell instability, diversification, and progression to the metastatic phenotype: from oncogene to oncofetal expression. Cancer Res 1987;47:1473-87.

185. Norming U, Nyman CR, Tribukait B. Comparative flow cytometric deoxyribonucleic acid studies on exophytic tumor and random mucosal biopsies in untreated carcinoma of the bladder. J Urol 1989;142:1442-7.

186. Norris HJ, Bahr GF, Mikel UV. A comparative morphometric and cytophotometric study of intraductal hyperplasia and intraductal carcinoma of the breast. Anal Quant Cytol Histol 1988;10:1-9.

187. Nourse J *et al.* Interleukin-2-mediated elimination of $p27^{kip1}$ cyclin-dependent kinase inhibitor prevented by rapamycin. Nature 1994;372:570-573.

188. Nowell PC. Mechanisms of tumor progression. Cancer Res 1986;46:2203-7.

189. Nurmi MJ. Prognostic factors in renal cell carcinoma. An evaluation of operative findings. Br J Urol 1984;56:270-5.

190. O'Brien CJ, Holgate C, Quirke P *et al.* Correlation of morphology, immunophenotype and flow cytometry with remission induction and survival in high grade non-Hodgkin's lymphoma. J Pathol 1989;158:31-9.

191. O'Leary TJ, Mikel UV, Becker RL. Computer-assisted image interpretation: Use of a neural network to differentiate tubular carcinoma from sclerosing adenosis. Mod Pathol 1992;5:402-5.

192. Oberholzer M, Ostreicher M, Christen H, Bruhlmann M. Methods in quantitative image analysis in pathology. Histochem cell Biol 1996;105:333-55.

193. Oosterwijk E, Warnaar SO, Zwartendijk J, van der Velde EA, Fleuren GJ, Cornelisse CJ. Relationship between DNA ploidy, antigen expression and survival in renal cell carcinoma. Int J Cancer 1988;42:703-8.

194. Otto U, Baisch H, Huland H, KlÖppel G. Tumor cell deoxyribonucleic acid content and prognosis in human renal cell carcinoma. J Urol 1994;132:237.

195. Oud PS, Pahlplatz MMM, Beck JLM, Wiersma-Van Tilburg A, Wagenaar SJ, Vooijs GP. Image and flow cytometry of small cell carcinoma of the lung. Cancer 1989;64:1304-9.

196. Papadopoulos I, Weichert-Jacobsen K *et al.* Quantitative DNA analysis in renal cell carcinoma. Comparison of flow and image cytometry. Anal Quant Cytol Histol 1995;17:272-5.

197. Perter PL, Malone KE, Heagerty PJ, Alexander GM, Gatti LA, Firpo EJ, Daling JR and Roberts JM. Expression of cell-cycle regulators $p27^{Kip1}$ and cyclin E, alone and in combination, correlate with survival in young breast cancer patients. Nature Med 1997;3:222-225.

198. Piffko J, Bankfalvi A, Ofner D, Kusch F, Bocker W, Joos U and Schmid KW. In situ assessment of cell proliferation at the invasive front of oral squamous cell carcinomas. Virchow Arch 1996;429:229-34.

199. Polyak K, Kato JY, Solomon MJ, Sherr CJ, Massague J, Roberts JM, Koff A. $p27^{kip1}$, a cyclin-Cdk inhibitor, links transforming growth factor-β and contact inhibition to cell cycle arrest. Genes Dev 1994;8:9-22.

200. Polyak K, Lee MH, Erdjument-Bromage H, Koff A, Roberts JM, Tempst P, Massague J. Cloning of $p27^{kip1}$, a cyclin-dependent kinase inhibitor and a potential mediator of extracellular antimitogenic signal. Cell 1994;78:59-66.

201. Quastler H and Sherman FG. Cell population kinetics in the intestinal epithelium of the mouse. Exp Cell Res 1959;17:420-438.

202. Querzoli P, Albonico G, Ferretti S, Rinaldi R, Magri E, Indelli M and Nenci I. MIB-1 proliferative activity in invasive breast cancer measured by image analysis. J Clin Pathol 1996;49:926-30.

203. Rabinovitch PS. Multicycle: A program for DNA content and cell cycle analysis. Phoenix flow systems,1991.

204. Rabinovitch PS. Practical considerations for DNA content and cell cycle analysis. In: Principles of clinical flow cytometry. 1992, pp58-83.

205. Rabinovitch RA *et al.* Patterns of failure following surgical resection of renal cell carcinoma: Implications for adjuvant local and systemic therapy. J Clin Oncol 1994;12:206-12.

206. Rainwater LM, Hoaska Y, Farrow GM, Lieber MM. Well-differentiated clear cell renal cell carcinoma. Significance of human deoxyribonucleic acid pattern studied by flow cytometry. J Urol 1987;137:15-20.

207. Raviv G, Leibovich I, Mor Y, Nass D, Medalia O, Goldwasser B, Nativ O. Localized renal cell carcinoma treated by radical nephrectomy. Influence of pathologic data and the importance of DNA ploidy pattern on disease outcome. Cancer 1993;72(7):2207-12.

208. Raymond WA, Leong AS-Y. The relationship between growth fractions and oestrogen receptors in human breast carcinoma, as determined by immunohistochemical staining. J Pathol 1989;158:203-11.

209. Reznicek SB, Narayana AS, Culp DA. Cystadenocarcinoma of the kidney: a profile of 13 cases. J Urol 1985;134:256-9.

210. Riches E. On carcinoma of the kidney. Ann R Coll Surg Engl 1963;32:201-208.

211. Ritchie AW and deKernion JB. The natural history and clinical features of renal cell carcinoma. Semin Nephrol 1987;7:131-139.

212. Ro JY, Ayala AG, Sella A, Samuels ML, Swanson DA. Sarcomatoid renal cell carcinoma: A clinicopathologic study of 42 cases. Cancer 1987;59:516-526.

213. Robson CJ, Churchill BM, and Anderson W. The results of radical nephrectomy for renal cell carcinoma. Trans Am Assoc Genitourin Surg 1968;60:122.

214. Rooney DE and Czepulkowski BH (eds). Human cytogenetics. A practical approach. IRL Press, Oxford-Washinton, 1986.

215. Roos G, Stenling R, Ljundberg B. DNA content in renal cell carcinoma: a comparison between flow and static cytometric methods. Scand J Urol Nephrol 1986;20:295-300.

216. Rosen FS, Steiner LA, Unanue ER. Dictionary of immunology. Macmillan, London, 1989.

217. Russack V. Image cytometry: current applications and future trends. Crit Rev Clin Lab Sci 1994;31:1-34.

218. Sahih AA, Ro JY. Ki 67 immunostaining in node negative stage I/II breast carcinoma. Significant correlation with prognosis. Cancer 991;68:549-57.

219. Sandberg AA. The chromosomes in human cancer and leukemia. Elsevier, New York-Amsterdam, 1980.

220. Sapi Z, Hendricks JB, Pharis PG *et al.* Tissue section image analysis of breast neoplasm: Evidence of false aneuploidy. Am J Clin Pathol 1993;99:714-20.

221. Sasaki K, Matsumura K, Tsuji T, Shinozaki F, Takahasha M. Relationship between labeling indices of Ki 67 and BrdUrd in human malignant tumours. Cancer 1988;62:989-93.

222. Schefft P *et al.* Surgical for renal cell carcinoma extending into inferior vena cava. J Urol 1978;120:28.

223. Schlüter C, Duchrow M, Wohlenberg C, Becker MHG, Key G, Flad HD *et al.* The cell proliferation-associated antigen of antibody Ki-67: a very large, ubiquitous nuclear protein with numerous repeated elements, representing a new kind of cell cycle-maintaining proteins. J Cell Biol 1993;123:513-522.

224. Schmidt D, Wischmeier P, Lenschner I, Sprenger E, Langenau E, von Schweinitz D, Harms D. DNA analysis in hepatoblastoma by flow and image cytometry. Cancer 1993;72:2914-9.

225. Schneller J, Eppich E, Greenebaum E *et al.* Flow cytometry and Feulgen cytophotometry in evaluation of effusions. Cancer 1987;59:1307-13.

226. Schrape S, Jones DB, Wright DH. A comparison of three methods for the determination of the growth fraction in non-Hodgkin's lymphomas. Br J Cancer 1987;55-283-6.

227. Schulte *et al.* DNA densitometry. In: Quantitative clinical pathology. Hamilton PW and Allen DC (eds), Blackwell Science Ltd., 1995.

228. Schumperli D. Cell-cycle regulation of histone gene expression. Cell 1986;45:471-472.

229. Schwabe HW, Adolphs HD, Vogel J. Flow cytometric studies in renal cell carcinoma. Urol Res 1983;11:121-6.

230. Schwarting R, Gerdes J, Niehus J, Jaesche L, Stein H. Determination of the growth fraction in cell suspensions by flow cytometry using the monoclonal antibody Ki 67. J Immunol Methods 1986;90:365-71.

231. Scopsi L, Larsson LI. Increased sensitivity in peroxidase immunohistochemistry: A comparative study of a number of peroxidase visualization methods employing a model system. J Histochemistry 1986;84:221-30.

232. Seckinger D, Sugarbaker E, Frankfurt O. DNA content in human cancer. Application in pathology and clinical medicine. Arch Pathol Lab Med 1989;113:619-26.

233. Selli C, Hinshaw WM, Woodard BH, Pzaulson DF. Stratification of risk factors in renal cell carcinoma. Cancer 1983;52:899-903.

234. Shackney SE, Smith CA, Miller BW, Burholt DR, Murtha K, Giles HR, Ketterer DM, Pollice AA. Model for the genetic evolution of human solid tumors. Cancer 1989;49:3344-54.

235. Shankey TV, Rabinovitch PS, Bagwell B, Bauer KD *et al.* Guidelines for implementation of clinical DNA cytometry. Cytometry 1993;14:472-7.

236. Shankey TV. Urology cancers. In: Clinical flow cytometry: Principles and applications. Bauer KD, Duque RE and Shankey TV (eds), Baltimore, Williams and Wilkins, 1993, pp271-305.

237. Sheibani K and Tubbs RR. Enzyme immunohistochemistry: Technical aspects. Semin in Diagnostic Pathol 1984;1:235-50.

238. Sherr CJ, Roberts JM. Inhibitors of mammalian G1 cyclin-dependent kinases. Genes Dev 1995;9:1149-1163.

239. Silvestrini R, Costa A, Vereroni S, Del Bino G, Persici P. Comparative analysis of different approaches to investigate cell kinetics. Cell Tissue Res 1988;21:123-31.

240. Simanis V and Nurse P. Characterization of the fission yeast cdc10^{+} protein that is required for commitment to the cell cycle. J Cell Sci 1989;92:51-56.

241. Skinner DG *et al.* Diagnosis and management of renal cell carcinoma. A clinical and pathologic study of 309 cases. Cancer 1971;28:1165.

242. Sogani PC, Herr HW, Bains MS, Whitmore WF. Renal cell carcinoma extending into inferior vena cava. J Urol 1983;130:660-3.

243. Sokoloff, Mitchell H *et al.* Current management of renal cell carcinoma. CA Cancer Clin 1996;46:284-302.

244. Spirin KS *et al.* $p27^{kip1}$ mutation found in breast cancer. Cancer Res 1996;56:2400-2404.

245. Srigley J, Barlogie B, Butler JJ *et al.* Heterogeneity of non-Hodgkin's lymphoma probed by nucleic acid cytometry. Blood 1985;65:1090-6.

246. Störkel SF. Classification of renal cell carcinoma based on morphologic and cytogenetic correaltions. In: Biology of renal cell carcinoma. Bukowski RM, Finke JH and Klein EA (eds), Springer-Verlag New York Inc., 1995, pp3-12.

247. St. Croix B, Florenes VA, Rak JW, Flanagan M, Bhattacharya N, Slingerland JM and Roberts SK. Impact of the cyclin-dependent kinase inhibitor $p27^{Kip1}$ on resistance of tumor cells to anticancer agents. Nature Med 1996;2:1204-1210.

248. Steeg PS and Abrams JS. Cancer prognostic: past, present and p27. Nature Med 1997;3:152-154.

249. Striepecke E, Handt S, Weis J, Koch A, Cremerius U, Reinike T, Bull U, Schroder JM, Zang KD and Bocking A. Correlation of histology, cytogenetics and proliferation fraction (Ki-67 and PCNA) quantitated by image analysis in meningiomas. Path Res Pract 1996;192:816-24.

250. Sufrin G *et al.* Paraneoplastic and serologic syndromes of renal adenocarcinoma. Semin Urol 1989;7:158-71.

251. Suit PF and Bauer TW. DNA quantitation by image cytometry of touch preparations from fresh and frozen tissue. Am J Clin Pathol 1990;94:49.

252. Syrjanen K, Hjelt L. Grading of human renal adenocarcinoma. Scand J Urol Nephrol 1978;12:49-55.

253. Tannapfel A, Hahn HA, Katalinic A, Fietkau RJ, Kühn R and Wittekind CW. Prognostic value of ploidy and proliferation markers in renal cell carcinoma. Cancer 1996;77:164-171.

254. Tannock IF. Cell proliferation. In: The basic science of oncology. Tannock IF and Hill RP (eds), McGraw-Hill, 1992, pp154.

255. Thoenes W, Storkel S, Rumpelt HJ, Moll R, Baum HP, Werner S. Chromophobe cell renal cell carcinoma and its variants - a report on 32 cases. J Pathol 1988;155:277-287.

256. Thoenes W, Storkel ST, Rumpelt HJ *et al.* Cytomorphological typing of renal cell carcinoma - a new approach. Eur Urol 1990;18 (suppl):6-9.

257. Thoenes W, Storkel ST, Rumpelt HJ. Histopathology and classification of renal cell tumors (adenomas, oncocytomas, and carcinomas). The basic cytological and histopathological elements and their use for diagnostics. Pathol Res Pract 1986;181:125-43.

258. Thomas M, Andreas G, Gregor M *et al.* Tissue section image analysis comparison of different software releases. Am J Clin Pathol 1994;11:673-4.

259. Thompson IM and Peek M. Improvement in survival of patients with renal cell carcinoma: The role of the serendipitously detected tumor. J Urol 1988;140:487-90.

260. Tisher CC and Brenner BM. Renal Pathology: With Clinical and Functional Correlations. 2nd edtion, J.B. Lippincott Company, Philadelphia, 1994.

261. Tomera KM, Farrow GM, Lieber MM. Sarcomatoid renal cell carcinoma. J Urol 1983;130:657-659.

262. Trerè D. Critical analysis of the methods commonly employed in the assessment of cell proliferation: advantages of the NOR silver-staining technique in routine cyto-histopathology. Analyt Cell Pathol 1993;5:191-201.

263. Trojanowski JQ, Obrocka MA, Lee VM. A comparison of eight different chromogen protocols for the demonstration of immunoreactivity neurofilaments or glial filaments in rat cerebellum using the peroxidase-antiperoxidase method and monoclonal antibodies. J Histochem Cytochem 1983;31:1217-22.

264. Tubbs RR and Sheibani K. Chromogen for immunohistochemistry. J Histochem cytochem 1981;29:684.

265. Tubbs RR, Velasco ME, and Benjamin SP. Immunocytochemical identification of human chorionic gonadotrophin. Comparative study of diaminobenzidine and 3-amino-9-ethylcarbazole, a non-hazardous chromogen. Archives Pathol Lab Med 1979;103:534-8.

266. Tytor M, Franzen G, Olofsson J. DNA pattern in oral cavity carcinomas in relation to clinical stage and histological grading. Path Res Pract 1987;182:202-6.

267. Uwatoko N *et al.* Histological prognostic factors in 146 patients with renal cell carcinoma: comparison between incidental and non-incidental cases. Hinyokika Kiyo (JAPAN) 1996;42:341-5.

268. Van de Werf-Messing B. Carcinoma of the kidney. Cancer 1973;32:1056-1061.

269. Veloso JD, Solis OG, Barada JH, Fisher HAG and Ross JS. DNA ploidy of oncocytic-granular renal cell carcinoma by image analysis. Arch Pathol Lab Med 1992;116:154-8.

270. Verhuijen R, Kuijpers HJH, Schlingemann RO *et al.* Ki 67 detects a nuclear matrix-associated proliferation-related antigen. I Intracellular localization during interphase. J Cell Sci 1989;92:123-30.

271. Verhuijen R, Kuijpers HJH, VanDriel R *et al.* Ki 67 detects a nuclear matrix-associated proliferation-related antigen. II Localization in mitotic cells and associated with chromosomes. J Cell Sci 1989;92:531-41.

272. Veroni S, Costa A, Motta R, Giardini R, Rilke F, Silvestrini R. Comparative analysis of [^{3}H]-thymidine labeling index and monoclonal antibody Ki 67 in non-Hodgkin's lymphoma. Haematol Oncol 1988;6:21-8.

273. Vieillefond A, paradis V, Gros P *et al.* Est-il utile d'isoler parmi les carcinomes du rein, une variante a cellules chromophobes? Arch Anat Cytol Pathol 1992;40:250-4.

274. Vindelov LL *et al.* Long-term storage of samples for flow cytometric DNA analysis. Cytometry 1982;3:317.

275. Vindelov LL, Hansen HH, Gersel A, Hirsch FR, Nissen NI. Treatment of small cell carcinoma of the lung monitored by sequential flow cytometric DNA analysis. Cancer Res 1982;42:2499-502.

276. Vogelstein B, Fearon ER, Kern SE, Hamilton SR, Preisinger AC, Nakamura Y and Whiter. Allelotype of colorectal carcinomas. Science 1989;244:207-11.

277. Wake N, Isaace J, Sandberg AA. Chromosomal changes associated with progression of the Dunning R-3327 rat prostate adenocarcinoma system. Cancer Res 1989;49:3713-21.

278. Waters WB and Richie JP. Aggressive surgical approach to renal cell carcinoma: Review of 130 cases. J Urol 1979;122:306.

279. Weiberg RA. Oncogenes, antioncogenes, and the molecular bases of multistep carcinogenesis. Cancer Res 1989;49:3713-21.

280. Weiss L. Principles of metastasis. Academic Press, Orlando,1985.

281. Wied GL, Bartles PH, Bibbo M *et al.* Image analysis in quantitative cytopathology and histology. Hum Pathol 1989;20:549-71.

282. Wilbur DC, Zakowski MF, Kosciol CM, Sojda DF, Pastuszak WT. DNA ploidy in breast lesions: a comparative study using two commercial image analysis systems and flow cytometry. Anal Quant Cytol Histol 1990;12:28-34.

283. Williams RA, Charlton IG and Rode J. Comparative ploidy stidies using cytological and paraffin section preparations. Cytopathology 1991;2:29-37.

284. Xiong Y, Hannon GJ, Zhang H, Casso D, Kobayashi R, Beach D. p21 is a universal inhibitor of cyclin kinases. Nature 1993;366:701-704.

285. Yagoda A. Chemotherapy of renal cell carcinoma: 1983-1989. Semin Urol 1989;7:199-206.

286. Zarbo RJ. Quality control issues and technical considerations in flow cytometric DNA and cell cycle analysis of solid tumors. In: Flow cytometry. Analysis of solid tumors. 1993, pp425-469.